HUMAN DERMAL FIBROBLAST ACTIVATION UNDER PULSED ELECTRICAL STIMULATION VIA CONDUCTIVE FABRICS: SIGNALLING PATHWAYS AND POTENTIAL BENEFIT FOR WOUND HEALING

Thèse

Yongliang Wang

Doctorat en Médecine Expérimentale
Philosophiae Doctor (Ph.D.)

Québec, Canada

HUMAN DERMAL FIBROBLAST ACTIVATION UNDER PULSED ELECTRICAL STIMULATION VIA CONDUCTIVE FABRICS: SIGNALLING PATHWAYS AND POTENTIAL BENEFIT FOR WOUND HEALING

Thèse

Yongliang Wang

Sous la direction de :

Ze Zhang, directeur de recherche

Mahmoud Rouabhia, codirecteur de recherche

Résumé

Lors de la cicatrisation, plusieurs types cellulaires dont les kératinocytes et les fibroblastes ainsi que plusieurs facteurs de croissance jouent d'importants rôles. La cicatrisation cutanée peut aussi être activée par des facteurs exogènes, dont la stimulation électrique (SE). La SE peut moduler les fonctions fibroblastiques durant la cicatrisation. Le fibroblaste contribue de façon active à la cicatrisation en sécrétant différentes protéines (collagène, fibronectine, élastine) pour favoriser le comblement tissulaire. Les fibroblastes adoptent aussi un phénotype contractile en exprimant l'α-actine contribuant à la fermeture de la plaie. Notre hypothèse est que certaines de ces fonctions fibroblastiques pourraient être modulées par une stimulation électrique. Pour vérifier cette hypothèse nous avons utilisé une membrane biocompatible et conductrice à base de polyethylene terephthalate (PET) recouvert de polypyrrole (PPy). Les fibroblastes dermiques humains ont été cultivés sur ces membranes conducteurs, puis exposés ou non à un courant pulsé (PES) selon deux régimes : soit 10s PES suivi de 1200s de repos, ou 300s PES suivi de 600s de repos, durant 24 h. Deux intensités électriques ont été étudiées, 50 et 100 mV/mm. Nos travaux démontrent que la SE favorise l'adhésion, la prolifération et la migration des fibroblastes dermiques. Ces activités cellulaires sont consolidées par une sécrétion importante de FGF2 et d'α-SMA. Il est important de noter que l'effet de la SE favorise le changement phénotypique des fibroblastes en myo-fibroblastes grâce à la voie des Smad et de TGFβ/ERK. Nous avons aussi démontré que l'effet de la SE est maintenue à long terme et est transférable de la cellule mère vers les cellules filles. En effet après sous-culture les cellules expriment toujours de façon importante l'α-SMA. En conclusion, nous avons démontré que la stimulation électrique pulsée module positivement les fonctions cicatricielles des fibroblastes humains. Ces travaux démontrent pour la première fois les voies de signalisation (Smad et TGFβ/ERK) sollicitées par la SE pour activer les fibroblastes lors de la cicatrisation. Ces travaux suggèrent l'utilisation de la SE pour favoriser la guérison/cicatrisation des plaies.

Summary

During skin wound healing, cutaneous cells particularly fibroblasts and keratinocytes as well as several growth factors play important roles. Wound healing can be activated by exogenous factors, including electrical stimulation (ES). ES can also modulate fibroblast functions. Fibroblasts contribute to healing by secreting structural proteins (collagen, fibronectin, elastin) to repair the wound area. Fibroblasts also adopt a contractile phenotype expressing α-actin contributing to wound closure. The hypothesis of the thesis is that fibroblasts proliferate and transdifferentiate into myofibroblasts by sensing pulsed electrical signals and adjusting relevant signalling pathways. To test this hypothesis we used biocompatible polyethylene terephthalate (PET) fabrics coated with electrically conductive polypyrrole (PPy). Human dermal fibroblasts were cultured on these conductive fabrics and exposed to the optimized pulsed ES: either 10s PES in a period of 1200s, or 300s PES in 600s period, for a total of 24 hours. Two electric intensities were studied, 50 and 100 mV/ mm. Our work showed that the PES promoted the adhesion, proliferation and migration of dermal fibroblasts. These cellular activities were consolidated by an elevated level of fibroblast growth factor 2 (FGF2) and the high expression of α-smooth muscle actin (α-SMA). Important findings were that PES promoted the phenotypic change of fibroblasts to myofibroblasts, and such change was coordinated through the Smad and TGFβ/ERK pathways. It also demonstrated that the effect of PES was able to maintain for a long period of time after the end of stimulation, and was transferable from the mother cells to the daughter cells. Following subculture, the electrically stimulated fibroblasts still expressed significant amount of α-SMA. In conclusion, this thesis demonstrates that PES through conductive fabrics can activate the wound healing functions in human dermal fibroblasts. This work revealed for the first time that Smad and TGFβ/ERK pathways are required by the PES-induced fibroblasts-to-myofibroblasts differentiation. This work also demonstrated that the PES activated cells can survive *in vivo*. These studies suggest the application of the PES in promoting tissue regeneration and wound healing.

Foreword

This thesis is composed of five chapters. The first chapter introduces the background knowledge related to the research project, which includes the relationship of EF and life science, wound healing, and conductive materials. Also, it describes the motivation, hypothesis and objectives.

The chapters II, III, IV represent the principal research as mentioned in "Summary"， in form of published or submitted articles. Chapter II discusses the preparation and characterization of the PPy-PET fabrics and the culture of fibroblasts under selective PES, which iss published in "Journal of Material Chemistry B". Chapter III reveals that PES can modulate fibroblast behaviors through Smad signalling pathway, which is published in "Journal of Tissue Engineering and Regenerative Medicine". Chapter IV further shows that the ES triggered fibroblast differentiation is mediated by TGFβ1/ERK signalling pathway, and that the PES effect can be memorized by descendent cells *in vitro* and *in vivo*, which has been submitted to "Journal of Acta Biomaterialia". All these three articles were designed with the help of the thesis supervisors and completed 90% by the author of this thesis.

Chapter V summarizes the general conclusions and discussed the perspectives.

Acknowledgements

The reasons why I can finish my research and complete the final thesis should be explained in several aspects. There are the helps from my two supervisors and the helps and technical assistances from my colleagues.

Above all, I feel grateful to my two supervisors, Drs. Ze Zhang and Mahmoud Rouabhia, for their attractive research project and rich experience. To find out how and why cells response to electrical stimulation is a cutting-edge research that is vital prior to applying electrical stimulation (ES) in clinic. Their whole views regarding the project guided me to avoid getting lost in research and their suggestions in research guaranteed my effective study in short time. The regular meetings allowed me to tell them the progress of my experiment and solve the problems in research as quickly as possible. Furthermore, the step-by-step method gives me a deep impression and will influence my career in future.

The technical assistances from Mr. Eric Jacques and postdoctoral fellow Ms. Hyunjin Park helped me to solve the difficulties encourntered in my research. Eric tought me how to perform qPCR and Western blot, and Hyunjin showed me how to do immunohisochemistry. Mr. Stéphane Turgeon, Madame Pascale Chevallier, and Mr. Sébastien Meghezi helped me to do material characterizations. Herein, I feel deeply thankful to their assistance. I also feel grateful to the generous discussions about my research with Mr. Jifu Mao, Mr. Zhiyong Du, Madam Dingkun Wang, Dr. Adil Akkouch, Dr. Shiyun Meng, Dr. Zhenkun Sun, and Dr. Huan Liang.

I very appreciate the financial support from the Canadian Institutes of Health Research (CIHR) and the partial financial aid from the Center for Applied Research on Polymers and Composites (CREPEC) and Desjardins Bank. They assure me to focus on my study and to enjoy an easy life at Laval University.

My hearty thanks go to my parents and relatives and friends, for their understanding and support for my study abroad. Our talks by phone and through internet made me feel warm and not lonely.

I dedicate this thesis to my lovely parents, Fengling Wang and Xiujie Ni!

Education bestows the skills on us, to make our society better!

CONTENTS

List of Tables

List of Figures

List of Abbreviations

BAFFR	B-cell activation factor receptor
BDNF	Brain-derived neurotrophic factor
bFGF, or FGF2	Basic fibroblast growth factor
BMP	Bone morphogenetic protein
CaMK	Ca^{2+}/calmodulin-dependent protein kinase
CB	Conduction band
CBP	C/EBP-binding protein
CP	Conductive polymer
CRET	Capacitive-resistive electric transfer
CTGF or CCN2	Connective tissue growth factor
DAG	Diacylglycerol
DC	Direct current
DRG	Dorsal root ganglia
DSC	Differential scanning calorimetry
ECG	Electrocardiogram
ECM	Extracellular matrix
EF	Electrical field
EGF	Epidermal growth factor
ENC	Extracellular negative-charge cluster
EO	Ethylene oxide
ERK	Extracellular-signal-regulated kinase
ES	Electrical stimulation
FGF1	Fibroblast growth factor 1

FGFRs	FGF receptors
FREMS	Frequency rhythmic electrical modulation system
FRS2	FGFR substrate 2
FTIR	Fourier transform infrared spectroscopy
GM-CSF	Granulocyte-macrophage colony-stimulating factor
GRB2	Growth factor bound-2
HB-EGF	Heparin-binding EGF-like growth factor
HF	Hair follicle
HFSCs	Hair follicles stem cells
HMW	High molecular weight
HSCs	Hepatic stellate cells
HSPG	Heparan sulphate proteoglycan
ICC	Immunocytohistology
IGF-1	Insulin growth factor-1
IHC	Immunohistochemistry
IKK	IκB kinase
IL-1R	Interleukin-1 receptor
IL-6	Interleukin-6
INC	Intracellular negative-charge cluster
IRAK	Interleukin-1 receptor-associated kinase
JAK	Janus kinases
KCNK9	Potassium channel, subfamily K, member 9
KGF	Keratinocyte growth factor
KIM	Kinase interaction motif

Kir channels	Inwardly rectifying K^+ channels
LAP	Latency-associated peptide
LIDC	Low-intensity direct current
LLC	Large latent complex
LMW	Low molecular weight
LTBP	Latent TGFβ–binding protein
LTβR	Lymphotoxin β-receptor
LVPC	Low voltage pulse current
MAPK	Mitogen activated protein kinase
MKPs	MAP kinase phosphatases
MLTK	MLK-like mitogen activated protein triple kinase
MMPs	Matrix metalloproteinases
nAChR	Nicotinic acetylcholine receptor
NFAT3	Nuclear factor of activated T cells
NF-κB	Nuclear factor-κB
NGF	Nerve growth factor
NLS	Nuclear localization sequences
NO	Nitric oxide
P/CAF	p300/CBP-associated factor
PANI	Polyaniline
PCD	Programmed cell death
PDGF	Platelet-derived growth factor
PEDOT	Poly(3,4-ethylenedioxythiophene)
PES	Pulsed electrical stimulation

PET	Polyethylene terephthalate
PI3K	Phosphoinositide 3-kinase
PKC	Protein kinase C
PLA	Polylactide
PLCγ	Phospholipase Cγ
PPy	Polypyrrole
qPCR	Quantitative PCR
RANK	Receptor activator for nuclear factor κB
RER	Rough endoplasmic reticulum
RSK	Ribosomal S6 kinase
SEM	Scanning electron microscopy
SH2	Src homology 2
Shh	Sonic hedgehog
SHP-2	SH2 domain-containing tyrosine phosphatase
SLC	Small latent complex
SMCs	Smooth muscle cells
SOS	The son of sevenless
SRF	Serum response factor
STAT	Signal transducer and activator of transcription
TEP	Transepithelial potential
TGA	Thermalgravametric analysis
TGF	Transforming growth factor
TIMPs	Tissue inhibitor of metalloproteinases
TLR	Toll-like receptor

TM	Transmembrane
TNFR	Tumor necrosis factor receptor
TNF-α	Tumor necrosis factor-α
TRPM7	Transient receptor potential melastatin 7; Transient receptor potential cation channel subfamily M member 7
TRPV6	Transient receptor potential vanilloid 6
TSP	Thrombospondin
TβRI	TGFβ receptor I
UTR	Untranslated region
VB	Valence band
VEGFA	Vascular endothelial growth factor A
VGCC	Voltage-gated calcium channel
VGSCs	Voltage-gated sodium channels
XPS	X-ray photoelectron spectroscopy
YAP	Yes kinase-associated protein
α-SMA	α-smooth muscle actin

CHAPTER I

INTRODUCTION

1. 1 Bioelectrical field

The existence of bioelectricity is due to the movement or build-up of ions (e.g., free ions such as sodium or calcium ions or immobilized ionic groups such as functional groups in proteins) that are rich in biosystem such as human. The flow of such free ions (negatively charged anions or positively charged cations) forms current and the concentration difference of the ions generates electrical potential.

1.1.1 Formation of transmembrane potential and transepithelial eletrical potential

Animal cells have a lipid bilayer plasma membrane and membrane proteins including ion transporter/pumps embedded in it. The plasma membrane has an intrinsically high electrical resistivity, that is, a low permeability to ions. However, the ion transporter/pumps are able to actively transporting ions from one side of the membrane to the other, which keeps the different ion concentrations inside and outside of cells, normally $[K^+]_{cyto}>[K^+]_{out}$, $[Na^+]_{cyto}<[Na^+]_{out}$, $[Cl^-]_{cyto}<[Cl^-]_{out}$ (Fig. 1). Ion pumps transport the ions against their concentration gradient with consumption of ATP, in a low speed [1]. A major contributor, sodium-potassium pump, establishes the membrane potential. On each cycle, Na^+/K^+ pump swaps three intracellular Na^+ ions with two K^+ ions from the extracellular space, which makes a net movement of one positive charge from intracellular to extracellular space. Finally, this process gives the intracellular space a negative voltage with respect to the extracellular space, namely, membrane potential. Although sodium-calcium exchanger is also involved in sodium transport, this effect is less important with respect to the high sodium and potassium concentrations.

Another type of ion channel is permeable only to specific types of ions, depending on the transmembrane concentration gradient of that particular ion, in a high speed. The channels are subtly controlled by voltage, transmitter, and other stimuli such as light and pressure. Ion channel usually fulfills open-close process in a fraction of millisecond and could transport ions with very high efficiency (10^6-10^8 ions/s) [2], which meets the fast regulation criteria. In an individual cell, the difference in net charge across plasma membrane caused by ion concentration gradient generates the transmembrane potential in a range of 30-100 mV, inside positive [3]. When these cellular membrane potentials are

combined in a multicellular architecture, e.g., epithelial layer, due to the cell communication through gap jucntions, they collectively created the so-called transepithelial electrical potential (TEP), which has a regulatory effect in wound healing.

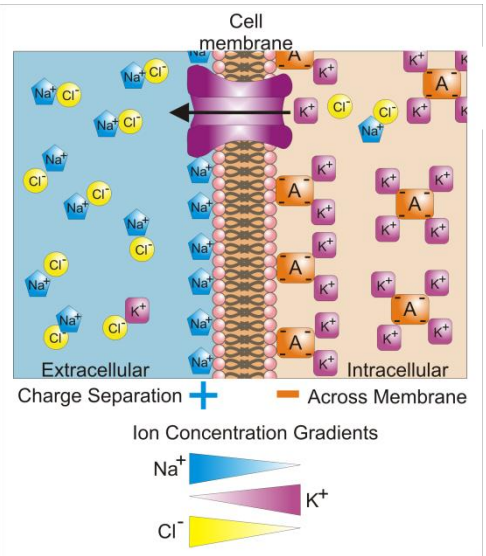

Fig. 1 Ion distribution and membrane potential. It shows the asymmetric distribution of ions and the consequent positive extracellular environment and the negative intracellular potential. http://en.wikipedia.org/wiki/Membrane_potential.

1.1.2 Important ion channels

1.1.2.1 Sodium ion channels

Sodium channels modulate fast depolarization and mediate electrical impulses conduction throughout nerve, heart and muscle. Sodium ion channel consists of a complex of α subunit (α1-10) and one/more β subunits (β1-3), with each α subunit containing 4 domains which have six transmembrane segments. Segment 4 (S4) has two conserved positively charged amino acids as voltage sensor [4]. A re-entrant loop between S5 and S6 determines the selectivity. The outer funnel-like vestibule, central cavity and intracellular activation gate form the basis of selectivity and high conductance of Na_vAb channel (a member of the NaChBac family and a voltage-gated sodium-selective ion channel, Figure 2), in which Glu 177 alignment with Glu determines ion selectivity [5]. Hille's single-ion pore model and Eisenman's theory describes the permeation and selection. After escaping

the high-field-strength site, the hydrated Na^+ ions enter the central cavity by diffusion and go across the open activation gate into the cytoplasm. There are some other important amino acids in specific site exerting key functions. For instance, R2 (R, arginine) and R3 'gating charges' in Na_vAb interact with a conserved extracellular negative-charge cluster (ENC), whereas the R4 gating charge interacts with a conserved intracellular negative-charge cluster (INC). S4 movement in the membrane electric field is thought to be stabilized and catalysed by these ion-pair interactions [6]. Met 221 could block the ion conduction pathway. In addition, membrane lipids also participate in the regulation of sodium ion channel because that lipid can penetrate and lie deep within the central cavity. Sodium ion channels are expressed in different tissues, e.g., $Na_v1.1$, $Na_v1.2$ and $Na_v1.6$ in central nervous system, and $Na_v1.4$ and $Na_v1.5$ in skeletal and cardiac myocytes [7, 8]. Their behaviours follow three rules: voltage-dependent activation (except ion dependent activation channel), rapid inactivation, and selective ion conductance.

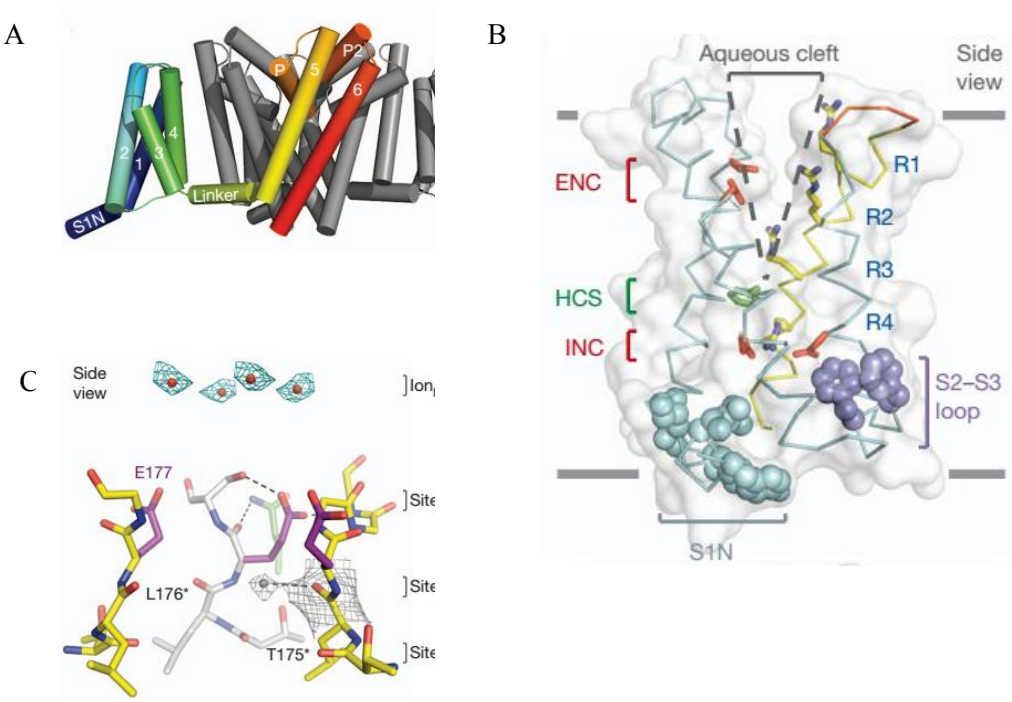

Figure 2. Structure of NavAb and the activated voltage-sensing domain (VSD) [5]. A. Structural elements in NavAb. **B**. Side and top views of the VSD illustrating the ENC (red), INC (red), HCS (green), residues of the S1N helix (cyan) and phenylalanines of the S2–S3 loop (purple). S4 segment and gating charges (R1–R4) are in yellow. **C**. Side view of the selectivity filter. Glu 177 (purple) interactions with Gln 172, Ser 178 and the backbone of Ser 180 are shown in the far subunit.

1.1.2.2 Potassium channels

K^+ channels enjoy an important role in retaining the normal physiology of cellular repolarization, smooth muscle relaxation, cardiac action potential repolarization, immune function, neurotransmitter release, and insulin secretion. As another type of important ion channel, potassium channels have two major classes defined by the transmembrane (TM) structure, i.e., 2TM inwardly rectifying K^+ channels (Kir channels) and 6TM voltage-gated K^+ channels (Kv channels) [9]. Kir family is composed of 15 members divided into four groups: K^+ transport channels, classical K_{ir} channels, G-protein gated K^+ channels, and ATP sensitive K^+ channels. Kv channels, the biggest K^+ channels family, are encoded by 40 genes and constitute of 12 subfamilies. In electrically excitable cells such as nerve, muscle and pancreatic β cells, the cytoplasmic higher K^+ concentration assigns the Kv channels to terminate action potential through extracellular 'leak' of K^+ [10]. Kir1.1, expressed in renal epithelial cells plays an important role in the homeostasis of K^+ in urine and blood [11]. Kir channels are affected by Mg^{2+}, polyamine, extracellular K^+ concentration, phosphatidylinositol 4,5-bisphosphate, phosphorylation, and protein-protein interaction [12].

1.1.2.3 Other channels

Ca^{2+} and Cl^- channels also have a widespread expression profile in a variety of tissues and cells including heart, nerve, renal, etc and extensively regulate life activities such as cell volume, cell organelle acidification, impulse, etc [13-15]. Ca^{2+} channels trigger membrane depolarization in many different cell types and introduce Ca^{2+} influx in response to action potentials and subthreshold depolarizing signals. They have four major TM domains, each of which consists of six TM helices [15]. Three processes, namely, VDI (voltage-dependent inactivation), CDI (calcium-dependent inactivation) and CDF (calcium-dependent facilitation) regulate channels flux. Cytosolic Ca^{2+} increase is due to the entering through voltage-gated calcium channels (VGCCs) or stretch-activated cation channels (SACCs), and the release through the inositol 1, 4, 5 triphosphate receptor (InsP3R) on endoplasmic reticulum (ER). Ca^{2+} extrudes across the plasma membrane by the plasma membrane calcium-ATPase (PMCA) pump and sodium-calcium exchanger (NCX) and, especially, ER Ca^{2+} re-uptakes through sacro/endoplasmic reticulum ATPase (SERCA) [14].

1.1.3 Endogenous EF participates in physiological regulations

1.1.3.1 EF in development and regeneration

Growing from a single cell to multi-cellular organism, how is this process controlled precisely and how does the loss of tissue in an organism get regenerated after wounding? It is undoubted that the biological factors such as growth factors, signalling pathways, take a pivotal part; however cell communications depend not only on the protein- and peptide-based talkings but also on the physical cues such as mechanical forces and endogenous EF. To be noted, there are a large number of archived articles and reports regarding endogenous EF directives in embryonic development, vertebrate limb regeneration, and wound healing [16-18]. Both in mouse and chick embryo, Na^+ uptake by ectoderm introduces inward flux ofs current. And also, an outwardly directed ionic current, ranged from 0.04–10.8 $\mu A/cm^2$, accompanies the development of the mouse limb bud [19]. Abnormal limb formation in chick embryo was recorded by reversely applying electrical field. In addition, the development of left-right patterning of non-mammalian vertebrates in embryos was reported requiring a potential variance between blastomeres at a very early developmental stage, which was affirmed by the regulation of early, H^+-V-ATPase-dependent proton flux [20]. Recent studies confirmed the asymmetrical localization of maternal H^+/K^+-ATPase subunits along the three axes (e.g. left-right, dorso-ventral, and animal-vegetal axes) during the first cleavage stages [21]. Not only in animals but also in plants, the endogenous electrical field also has its functions such as in vascular pattern formation in leaves [22].

1.1.3.2 EF in nervous system

The rapid transmission of information from sensory organs to central nervous system and the delivery of commands from center nervous system to muscles depend on the transmission of electrical pulse along axons. At resting state, cell membrane is depolarized with high concentration of sodium ions in extracellular space. Stimuli (heat, mechanical pressure, light, chemicals, etc) induce sodium influx and the reach of threshold potential leads to a sudden change of membrane EF or membrane depolarization [23]. Nerve pulse or “fire” is in fact the travel of alternatively changing membrane EF alone axon to or from neuron cell body (soma). Action potentials can travel

along axons at speeds of 0.1 to 120 m/s. The speed is affected by 3 factors: temperature, axon diameter and myelin sheath.

1.1.3.3 EF in heart rhythm: automaticity and pacemaking

Another electrophysiological regulation is heart rate. A type of specialized cardiac cells, called pacemaker cells, are able to generate and transmit electrical impulse in response to body's need. These cells usually are located at sinoatrial (SA) node, atrioventricular (AV) node, the bundle of His and Purkinje fibre. SA node normally generates the action potential, and excites the right atrium (RA). From the AV node, the impulse then travels through the bundle of His and down the bundle branches which terminates in Purkinje fibres [24]. The general measurement of cardiac electrophysiology is electrocardiogram (ECG), which turns out to be a very important parameter in diagnosis.

1.1.4 Reactions of different types of cells to ES

Electrical or electromagnetic field (EMF) has been widely reported to affect a variety of activities of many types of cells, to ameliorate the healing of traumatic or degenerative tissue lesions, and has been used in aesthetic medicine as well [25, 26]. Among other things, ES is capable of affecting the adhesion, orientation, migration, differentiation and proliferation of stem cells, fibroblasts and endothelial cells, to name but a few. Some of the important studies about the effects of EF on different type of cells are summarized in Table 1.

Table 1 Studies of the ES induced cell reactions

Cells	**Mode of ES**	**Effects**	***In vitro/ vivo***	**Signalling**	**Ref.**
nerve stem cells	biphasic pulse	proliferation, differentiation	*In vitro*	-	27
	pulsed DC	differentiation	*In vitro*	-	28
	constant DC	proliferation, neurite growth	*In vitro*	-	29
	transcranial DC	migration	*In vivo*	-	30

Table1

(continued)

Cells	**Mode of ES**	**Effects**	***In vitro/ vivo***	**Signalling**	**Ref.**
embryonic stem cells	pulse	cardiac differentiation, maturation	*In vitro*	ROS signalling	31
human mesenchymal stem cells	pulse	proliferation	*In vitro*	ERK1/2	32
fish keratocytes	pulse	intracellular calcium waves	*In vitro*	-	33
keratinocytes	low frequency pulse; pulse	differentiation	*In vitro*	-	34 ,38
	DC	proliferation, migration, CCL20		p53/HDM2/SIV A1 axis;	35-37
human epithelial cells	pulse	activated p53 function	*In vitro*	p38-p53 signalling	39
Xenopus epithelial cells	DC	change cell shape, actin distribution	*In vitro*	-	40
microvascular endothelial cells	pulse	increase in blood flow; capillary morphogenesis	*In vitro*	NO; MAPK/ERK pathway	41, 42
endothelial cells	DC	Angiogenesis, proliferation	*In vitro*	VEGFR+	43, 44
retinal progenitor cell	pulse	differentiation, pronounced neuronal morphologies	*In vitro*	PKC	45
adult neural stem progenitor cell	DC	neurite outgrowth and maturation	*In vitro*	-	46
peripheral nerves	pulse	nerve regeneration	*In vitro*	Neuronal neurotrophin	47, 48
Schwann cells	DC; sine wave	morphological change; improve the neurotrophic ability	*In vitro*	brain-derived neurotrophic factor, Ca	49, 50
PC-12 cells	DC; pulse	neurite outgrowth, differentiation, increased FN adsorption	*In vitro*	-	51-53
SaOS-2	pulse	Biomineralization, differentiation	*In vitro*	-	54, 55

Table1

(continued)

Cells	**Mode of ES**	**Effects**	***In vitro/ vivo***	**Signalling**	**Ref.**
osteoblasts	pulse; DC	proliferation, differentiation, maturation, alkaline phosphatase	*In vitro*	-	56-60
MC3T3	pulse	TGFβ1 mRNA upregulation	*In vitro*	Ca^{2+}/calmodulin pathway	61
bone marrow stromal cells	DC	osteogenesis	*In vitro*	-	62
skin fibroblasts	pulse	collagen I downregulation, Ca^{2+} uptake; insulin receptors+,TGFβ1	*In vitro*	-	63, 64,65
foreskin fibroblasts	pulse	Ca^{2+} entry	*In vitro*	-	66
corneal stromal	DC	directed migration	*In vitro*	-	67
heart fibroblasts	pulse	polarity and adhesion, proliferation	*In vitro*	CaN–NFAT pathway	68, 69
lung fibroblasts	pulsed galvanic stimuli	protein and DNA synthesis	*In vitro*	-	70
NIH-3T3 (mouse)	pulse	orientation	*In vitro*	-	71
COS5-7	pulse	enhances adsorption and uptake of macromolecules	*In vitro*	-	72
human fibro-scarcomar HT1080 cells	DC	migrates in 3D collagen gel	*In vitro*	calcium, PLC	73
C3H/10T1/2 mouse embryo fibroblasts	DC	morphology change, skeleton	*In vitro*	-	74
U937 cell	pulse	TGFβ1 secretion	*In vitro*	-	65
skeletal muscle cell	pulse	Decreased TβRI levels	*In vitro*	TGFβ signalling	75
Etc					

1.1.5 ES and cell signalling

EF mediated biological response has already been investigated for many years. However, most of these studies are about phenomena. The mechanisms at molecular levels are still to be understood. The following part will review the ES activated cell signalling pathways and the important signalling molecules including calcium channels, tranforming growth factor β (TGFβ) and extracellular signal-regulated kinase (ERK).

1.1.5.1 Calcium signal

Calcium ions act as important second messenger participating in the regulation of cell division, proliferation, differentiation, and apoptosis. Since most calcium channels are known being sensitive to membrane potential, calcium signal transduction has become the center of the mechanistic studies related to EF exposure. It was reported that both inductive coupling and EMF initiated the release of Ca^{2+} from intracellular stores and so influenced cytoskeletal calmodulin [76]. Similarly, the ES induced-secretion of nerve growth factors and brain-derived neurotrophic factor (BDNF) in Schwann cells was found dependent on the calcium influx through the T-type voltage-gated calcium channel (VGCC) [50, 77]. So does articular chondrocytes signal transduction under ES [78].

1.1.5.2 TGFβ

TGFβ is the member of TGFs family. TGFβ plays important roles in regulating cell proliferation, differentiation and other cellular responses. TGFβ and TGFβ receptors (TGFβRs) are expressed by a variety of cell types including fibroblasts, platelets, keratinocytes, macrophages, etc. The research about TGFβ signalling caused by ES is just at the beginning. Literally, current literatures merely reported the elevated expression of TGFβ and TGFβ type I receptor under ES. The type of cells showing this behaviour includes osteoblasts, human dermal fibroblasts, U937 human monocytic cell line, and skeletal muscle cells [61, 65, 75]. However, none of these studies dealt with the downstream signalling pathways in dermal fibroblasts in the context of ES.

1.1.5.3 ERK signalling

ERK signalling is widely studied in biological research because it is so important in cell life in terms of growth, ageing, dysfunction and apoptosis. The ES-cell reaction has also been thought involving ERK activation. In human mesenchymal stem cells, capacitive-resistive electric transfer (CRET) was reported to introduce PCNA and ERK1/2 upregulation [32]. Neurite outgrowth is enhanced by NGF-induced ERK1/2 activation [79]. Besides, dorsal horn neurons embrace more pERK as a result of ES administration [80]. Also, the high-frequency ES-promoted capillary morphogenesis *in vitro* was accompanied by ERK pathway activation in endothelial cells [42].

1.1.5.4 Other signalling molecules and pathways

In addition to the aforementioned signal pathways involved in the ES mediated cell response, other pathways have also been studied. For example, superoxide is considered as a 'bridge' to translate ES from outside to inside of cells [81]. Notch and Wnt signalling was suggested playing a potential role in the ES-induced increase in the mass of paralyzed muscle [82]. Mild ES was reported to exert its function via signalling pathways of liver kinase B1 (LKB1)-5', AMP-activated protein kinase (AMPK), tumor suppressor p53, phosphoinositide 3-kinase (PI3K)-Akt, and p38 mitogen activated protein kinase (MAPK) [83-86]. Apparently, a number of signalling pathways could be affected by stimulations. However, mechanistic study about ES to human dermal fibroblasts is rare [87] and none of such studies was oriented to wound healing.

1.2 Wound physiology

1.2.1 An overview of human skin

Human skin can be divided into two major layers: epidermis and dermis. Epidermis is measured with a thickness of 0.04-1.6 mm depending on the sites. Epidermis consists of 5 distinct strata of cells (stratum corneum, stratum lecidum, stratum granulosum, stratum spinosum, and stratum basale) but contains no blood vessels. Four types of cells settle at epidermis including keratinocytes, melanocytes, Langerhans cells as well as Merkel cells. Keratinocytes are stratified from basale to corneum and these cells gradually lose their proliferation ability, and thus need to be replaced by new keratinocytes. Melanocytes

determine the pigmentation. Langerhans cells function as resident immune cells and Merkel cells is reportedly responsible for mechanosense. Dermis has a thickness in the range of 0.3-3.0 mm, which is a connective tissue composed by a large quantity of extracellular matrix and various cellular populations, e.g., fibroblasts, endothelial cells, immune cells, nerve cells and fat cells. It also contains hair follicles, glands, and blood vessels. Epidermis and dermis have a crosstalk. For instance, the nutrients supplied by capillaries in dermis will naturally feed the epidermis cells, and the metabolic wastes will be removed through circulation. Their interactions were also witnessed in the wound healing process.

Human skin has a well-architected structure. Functionally, human skin prevents water loss from inner tissue attributed to the stratum corneum made up of keratins, and protects the inside against bacterial infection and against ultraviolet irritation due to pigment in it.

1.2.2 Wound healing process

1.2.2.1 Overview of healing process

In general, the healing process of a full thickness wound is divided into four phases: hemostasis, inflammation, proliferation and maturation/remodeling [88]. In the hemostasis phase, the disruption of blood vessels exposes the subendothelial collagen to platelets, triggering platelet activation and the formation of platelet plug, followed by the formation of blood clot sealing the disrupted vessels so that bleeding is controlled. The clot is rich in platelets and polymorphous nuclear cells trapped in a fibrin network, also serving as a temporary bacterial barrier, a reservoir of growth factors/cytokines, and a scaffold for migrating cells. The next task is to clean the wound bed, which happens in the inflammation phase. Wound "cleanup" refers to the breakdown and elimination of any devitalized tissue and bacteria by a group of white blood cells such as neutrophils, T lymphocytes and macrophages. The inflammation phase normally lasts approximately 3 days. The intensity and duration of inflammation phase depends on local factors such as bacterial infection, the extent of devitalized tissue, as well as the adequate build-up and maintenance of extracellular matrix (ECM) containing pro-inflammatory cytokines and anti-inflammatory factors [89]. The third phase of wound healing is proliferation, which includes three key components: epithelialization, neoangiogenesis and collagen deposition. A hallmark of this phase is the formation of granulation tissue, which begins

as the inflammatory phase subsides. Granulation tissue is a mixture of a large quantity of ECM (collagen, fibrin, fibronectin, etc.) and several cell populations, e.g., fibroblasts, immune cells and endothelial cells. Endothelial cells mainly restore blood vessels, namely, angiogenesis that supply oxygen and nutrients to the wound bed and meanwhile, take away the metabolic wastes. When the newly synthesized connective tissue fills wound defect activated epithelial cells migrate from the edge of the wound to reconstruct epithelium layer. After the wound site is covered by new epithelium, maturation/remodeling begins and is characterized by a dual processes of synthesis and degradation of the ECM, where new collagen (collagen type I) with more ordered structures and higher tensile strength will gradually replace the temporary scaffold mainly composed by collagen type III. This process relies on fibroblasts and ECM proteins (e.g. matrix metalloproteinases, MMPs) [90].

1.2.2.2 Involved cells and their functions

Various cell populations play their roles in the wound repair process, including platelets, macrophages, T cells, fibroblasts, epithelial cells/keratinocyptes, to name but a few. They produce many cytokines/chemokines and growth factors to coordinate their interactions temporally and spatially. The followings will review the cells firstly and then relevant cytokines/growth factors. The comprehensive list regarding their functions and origins will be presented in Table 2.

Platelets: As the first player in wound healing when bleeding is involved, platelets go through the routine "adhesion-activation-aggregation-platelet plug-clot" to avoid blood loss. They also secrete chemotactic factors to attract and activate inflammatory cells. The chemotactic factors include fibroblast growth factor 1 (FGF1), FGF2, platelet-derivated growth factor (PDGF), transforming growth factor α (TGFα), TGFβs, insulin growth factor 1 (IGF-1), epidermal growth factor (EGF), etc. Also, the clot becomes a scaffold for cell infiltration.

Inflammatory cells: Neutrophils infiltrate into the site of injury in response to the degranulation of platelets and the products of bacterial degradation [91]. Later, monocytes appear and differentiate into macrophages. It is reported that macrophage coordinates the later events of injury. These inflammatory cells are capable of fabricating growth factors and cytokines which affect other cells via autocrine and/or paracrine effect.

Keratinocytes: Keratinocytes exert their functions at the beginning of wound healing within hours. The well-organized epithelium commences phenotypic alternation in order to allow keratinocytes move with the dissolution of demosomes and hemidemosomes. They migrate between collagenous dermis and the fibrin eschar in concert with the degradation of ECM by collagenase such as MMP1 [92]. Keratinocytes could create keratinocyte growth factor (KGF), PDGF, vascular growth factors (VEGFs), TGFs, interleukin-6 (IL-6), etc.

Endothelial cells (ECs): New tissue formation can not happen without blood supply. The formation of new capillaries from existing vasculature, i.e., angiogenesis, depends on the migration and proliferation of endothelial cells upon the interaction of growth factors such as VEGFs, FGFs, and TGFβ [88]. Angiogenesis also needs the participation of fibroblasts and macrophages. The angiogenesis does not cease until new granulation tissue fills the wound [93]. ECs mainly secrete VEGFs, granulocyte-macrophage colony-stimulating factor (GM-CSF), etc.

Fibroblasts: will be reviewed in detail at 1.2.3.

Hair follicles stem cells (HFSCs): HFSCs are localized at the bulge of hair follicle (HF) constituted of epidermal and dermal compartments. HSFCs regulate hair regeneration (cycling) with a strict interaction with niches that remains to be clearly elucidated [94]. Interestingly, it is documented that the anagen phase of HF accelerated wound healing *in vivo* with alternations in endothelial, epithelial and inflammatory cell populations [95]. Furthermore, HFSCs contributes to acute wound repair by rapidly providing short-lived "transit amplifying" cells [96].

These cells communicate each other through signalling transduction where membrane receptors are able to selectively recognize growth factors or cytokines. The following will provide more details about several members amongst them, with a global view presented in Table 2.

PDGF: The family of PDGF includes PDGF-AA, PDGF-AB, PDGF-BB, PDGF-CC, and PDGF-DD [97]. PDGF not only attracts neutrophils, monocytes and fibrobalsts migrating to wound site, but also amplifies the production of ECM. In addition, PDGF is

reported to stimulate fibroblasts to contract wound and so mediate myofibroblast phenotype switch [98]. PDGF has been clinically used to treat human ulcers [99].

IL-6: IL-6 is a pleiotropic cytokine involved in the growth and differentiation of numerous cell types, including those of dermal and epidermal origin. While epidermal keratinocytes are the primary producer of IL-6 within the skin, macrophages, Langerhans cells and fibroblasts in the dermis also produce it. In wound healing, IL-6 acts as both a pro- and anti-inflammatory cytokine, and induces angiogenesis as well [100]. IL-6 was reportedly associated with vascularization during wound healing, during tumor growth and in reproductive system. IL-6 has also been shown to induce the proliferation of fibroblasts [101]. Signalling initiated by this cytokine occurs in association with its respective specific α-subunits interacting with the ubiquitous signal transducer gp130. Typically, this complex phosphorylates janus kinases (JAK), a tyrosine kinase, leading to the recruitment of adapter molecules such as signal transducer and activator of transcription (STAT)-3 and SH2 domain-containing tyrosine phosphatase (SHP-2), which permits the activation of the Ras-Raf-ERK pathway [102].

KGF: KGF is a member of the fibroblast growth factor family, known as FGF7. It can modulate epithelial cell growth by paracrine effect. It is produced by stromal cells in different tissues including lung, stomach, mammary gland, and skin. KGF is considered important in tissue development, morphogenesis and cutaneous injury repair, and has been implicated in hair regeneration [103].

VEGF: This family includes five isoforms, i.e., VEGF-A, VEGF-B, VEGF-C, VEGF-D, VEGF-E and placenta growth factor (PLGF). Their principal function as a mitogen derived mainly from arteries, veins and lymphatics is to promote ECs growth [104]. Furthermore, VEGF is a vascular permeable factor due to that it induces vascular leakage. Recently, it was also demonstrated that VEGF has a positive effect in scar formation in different wound healing models [105].

Connective tissue growth factor (CTGF): Also known as CCN2, CTGF is a member of CCN family of matricellular proteins which play distinct roles in wound repair, breast cancer, inflammation and fibrosis. CCN2 is considered as a stimulator for the proliferation and chemotaxis of fibroblasts [106] and has been documented as a conductor of skeletogenesis in cartilage development [107]. Interestingly, it promotes ECM deposition (collagen type I, fibronectin) and thus has certain function in scar formation [108].

In summary, cytokines and growth factors crosstalk each other and play vital roles in all phases of wound healing. For instance, studies have suggested the synergy between CTGF/CCN2 and TGFβ in the genesis and maintance of fibrotic response *in vivo* [109]. In addition, CTGF/CCN2 was able to bind to VEGFR and thus repressed the angiogenic effect of VEGF [110]. Additionally, both IL-6 and TNFα exert their functions during the inflammation phase of wound healing and collaborate to recruit other cells.

Table 2 Cytokines/growth factors in skin wound healing

Growth factor/Cytokine	Cell Source	Functions in wound healing	Ref.
FGF1 and FGF2	platelet, macrophage, fibroblast, endothelial cell	mitogen for most types of cells; promote angiogenesis.	111
FGF7, FGF10 and FGF22	keratinocyte, fibroblast	mitogen for epithelial cells; re-epithelialization.	88,111
PDGF	platelet, keratinocyte	attracts fibroblasts, smooth muscle cells, monocytes, vascular endothelial cells and neutrophils into the wound; coagulation and angiogenesis.	112
VEGF	endothelial cell, macrophage, keratinocyte	mitogen for vascular endothelial cells; stimulates angiogenesis.	113
TGFα	platelet, macrophage, keratinocyte	stimulates proliferation of epithelial cells, fibroblasts and vascular endothelial cells; re-epithelialization.	112,114
TGFβs	macrophage, lymphocyte, fibroblast, keratinocyte, platelet	inhibits proliferation of many cell types in vitro, including keratinocytes, endothelial cells and macrophage; may stimulate fibroblast differentiation; promotes granulation tissue formation, wound contraction.	115,116
IGF-1	fibroblast, macrophage, platelet	may promote migration of endothelial cells into the wound; mitogenic for fibroblasts.	112,117
EGF	platelet	stimulates proliferation and migration of epithelial cells, fibroblasts and vascular endothelial cells.	112,118–120
HB-EGF	macrophage	mitogenic for keratinocyte; angiogenic.	88,121

Table 2
(continued)

Growth factor/Cytokine	Cell Source	Functions in wound healing	Ref.
CTGF	fibroblast	stimulates proliferation and chemotaxis of fibroblasts; a potent inducer of extracellular matrix proteins.	108, 115
IL-6 and IL-8	keratinocyte, macrophage, Langerhans cell, fibroblast	stimulates inflammation; inhibits wound contraction; angiogenic.	112
IL-10	keratinocyte	inhibits inflammation and scar formation	122
IL-1α and IL-1β TNFα	polymorphonuclear leukocyte, macrophage	stimulates keratinocyte and fibroblast proliferation, synthesis and breakdown of extracellular matrix, fibroblast chemotaxis, and regulation of the immune response.	123-125
NGF	myofibroblast	stimulates nerve ingrowth; stimulates proliferation and inhibits apoptosis of keratinocytes in vitro.	125, 126
GM-CSF	macrophage, leukocyte, endothelial cell, fibroblast	mitogenic for keratinocytes; stimulate migration and proliferation of endothelial cell; chemotaxis for monocyte.	125,127, 128
Etc			

1.2.3 Fibroblasts in wound healing

1.2.3.1 Fibroblasts, myofibroblasts in wound healing

Fibroblasts are ubiquitous cells with a spindle-shape morphology and expressing interstitial collagens, which are normally found in the stroma of many tissues. They are rich in rough endoplasmic reticulum (RER), Golgi apparatus and thus have a high ability to synthesize proteins [129]. It is now accepted that they may be stemmed from transforming epithelial cells, resident cell populations and circulating precursors [130]. During wound healing, all these cells participate in tissue repair just following the appearance of

platelets that release different cytokines or growth factors attracting cell migration, wound cleanup, granulation tissue formation, collagen deposition, contraction, remodeling, etc. Fibroblasts are involved in granulation tissue formation, angiogenesis, wound contraction, skin reepithelialization and maturation given that they can synthesize ECM and collagen, the structural framework of animal tissue. Fibroblasts secrete IGF-1, FGF1, FGF2, TGFβ, PDGF and KGF [112, 131]. In the process of granulation tissue formation, fibroblasts provide ECM and growth factors triggering intercellular processes that move the fibroblasts into the reproductive phase of cell cycle. In contraction process, dermal fibroblasts are converted into "wound fibroblasts" (also called *myofibroblasts*) by TGFβ, which exhibit decreased proliferative behavior but increased synthesis of connective tissue proteins such as collagen type I contributing to the higher contractile strength in comparison to collagen type III [130, 131]. In the remodeling phase, fibroblasts synthesize a majority of the collagen, elastin, and proteoglycans that compose the dermal scar matrix. Fibroblasts are also a major source of MMPs that degrade the scar matrix, as well as their inhibitors, the tissue inhibitor of metalloproteinases (TIMPs) [125, 132]. Finally, these cells will gradually disappear with programmed cell death (PCD) along tissue mature as time goes.

Myofibroblasts are mesenchymal cells that have phenotypic characteristics of both fibroblasts and smooth muscle cells, including the formation of stress fibres in parallel with the long axis of the cell. The origin of myofibroblast was postulated from locally residing mesenchymal cells including fibroblasts, hepatic stellate cells (HSCs) (in liver), smooth muscle cells (SMCs) (in atheroma plaque formation) and endothelial cells (in lung) as well as bone-marrow circulating fibrocytes [133, 134]. In healing tissues, myofibroblasts are thought to play a major role in tissue contraction due to that they embrace more contractile force. It is documented that when cultured under mechanical strain and/or on a stiff substrate, fibroblasts develope actin stress fibres [135]. These cells starting to express smooth muscle actin are named proto-myofibroblasts, and they retract the wound with more force in contrast to fibroblasts and upregulate collagen synthesis. Also, under the action of TGFβ, proto-myofibroblasts differentiate into myofibroblasts, which are distinguished by the presence of α-smooth muscle actin (α-SMA), the specific marker of myofibroblasts [136]. Myofibroblasts can synthesize a large quantity of collagens type I and also produce ample cytokines and growth factors. During wound remodeling, the secreted collagen I predominates in ECM.

1.2.3.2 Fibroblasts interplay with other cells

In the process of wound healing, the interplay between keratinocytes and fibroblasts gradually shifts the microenvironment from inflammation milieu to granulation tissue, and also contributes to the basement membrane reestablishment [137]. As known, keratinocytes stimulate fibroblasts to secrete growth factors such as KGF/FGF7, which turn out to be stimulators for keratinocyte proliferation in a double paracrine manner [137]. This pattern of epithelial-mesenchymal interactions is part of the mechanisms regulating skin homeostasis. In addition, an *in vitro* model showed that the cooperation between fibroblasts and endothelial cells is essential for revasularization [138]. Moreover, the fibroblast/macrophage coculture was found to improve the chemokine production [139] and demonstrated that IL-22 could activate ECM gene expression as well as myofibroblast transdifferentiation, proving that IL-22 held unidentified functions in skin repair through immune cell/fibroblast interactions [140].

1.2.3.3 Growth factors and cytokines produced by fibroblast

During wound healing, fibroblasts produce different kinds of cytokines and growth factors that play key roles in promoting proteins synthesis, attracting cells migration, regulating inflammatory response, etc. As important players, FGF1 and FGF2 stimulate angiogenesis and the proliferation of fibroblasts that generate granulation tissue to fill up wound space/cavity. TGFβ not only participates in angiogenesis but also mediates the phenotype switch from fibroblast to myofibroblast.

1.2.3.3.1 FGFs

FGF family comprises 22 ligands that exert their functions through 4 highly conserved transmembrane tyrosine kinase receptors, i.e., FGF receptors (FGFR1, FGFR2, FGFR3, FGFR4) [141]. The basic structure of the FGF-FGFR complex consists of two receptor molecules, two FGFs and one heparan sulphate proteoglycan (HSPG) chain. FGFs signallings participate in fundamental developments and in addition, exert many physiological roles in adult organism, including in wound healing and angiogenesis [142]. FGFRs are expressed by many different cell types and regulate key cellular behaviours such as proliferation, differentiation, cell migration, survival and apoptosis. FGF binding leads to FGFR dimerization activating intracellular kinase domain and resulting in

intermolecular transphospharylation of the tyrosine kinase domains of intracellular tail. Phosphorylated tyrosine residues function as docking sites for adaptor proteins, leading to multiple signal transductions. FGFR substrate 2 (FRS2) is a crucial adaptor protein recruiting the Son of sevenless (SOS) and growth factor bound-2 (GRB2) to activate RAS and RAF-MAPK pathways. GRB2 also exerts the anti-apoptotic effect through PI3K/AKT pathway [143]. Elsewhere on the FGFRs, the Src homology 2 (SH2) domain of phospholipase Cγ (PLCγ) binds to phosphorylated tyrosine residues and is activated, which then activates diacylglycerol (DAG) and protein kinase C (PKC) triggering MAPK pathway by the phosphorylation of RAF. Several other pathways are also activated by FGFRs, depending on the cellular context, including the p38 MAPK and Jun N-terminal kinase (JNK) pathways, signal transducer and activator of transcription (STAT) signalling [144].

FGF1, also called acid FGF (aFGF), gene is made up by 105,893 base pairs (bp) and 10 exons. After translation, the FGF protein is encoded with one nuclear localization sequence (NLS) at N terminal, several receptor binding domains for FGFRs and a heparin binding domain at C terminal [143]. FGF1, with a low molecular weight of 16.5 kDa, is able to migrate to the nucleus by free diffusion in addition to NLS orientation [145, 146]. Recent study found out that integrin αvβ3 directly and specifically binds to FGF1 at the heparin binding site indicating the integrin-FGFR crosstalk mechanism [147]. Studies have revealed that FGF1 is widely expressed in different tissues and organs including colorectal and gastric tissues, tumor tissue, skin, breast, to just list a few, which correlate with its vast functions including angiogenesis, proliferation, development, wound repair, etc [111, 112]. In skin wound healing, FGF1 accelerated the full-thickness healing in rodents as reflected by the enhanced granulation tissue deposition, vascularization, epidermal growth, and closure [148].

FGF2, also called basic FGF (bFGF), gene has a length of 70990 bp and consists a 5' untranslated region (5'UTR), 3 exons, 2 introns and a long 3'UTR [149]. The regulatory elements located at 5'UTR and 3'UTR subtly control gene transcription according to cellular signals, e.g., growth factors, hormones, cell density, neurotransmitter, second messenger pathways, etc [149]. The transcribed mRNA stability varies due to the length of 3'UTR elements. FGF2 gene encodes 5 isoforms with different translation initiation sites [150]. The isoforms have biparite NLS as shown in Figure 3. The high molecular weight (HMW) isoforms initiate from CUG codons and embrace another glycine/arginine (GR)-repeat NLS while the 34 KDa isoform has an additional HIV-Rev-like NLS [151]. Amongst

them, the HMW isoforms are found in skin fibroblasts, aortic endothelial cells and retinal pigment epithelial cells. While LMW isoform mainly occurs in the cytoplasm, HMW isoforms are predominantly found in nucleus, which can be shuttled back into cytoplasm and also secreted into extracellular milieu. Functionally, FGF2 influences cell growth, migration, differentiation and survival, participating in various biological processes such as wound healing, tumorgenesis, angiogenesis and development.

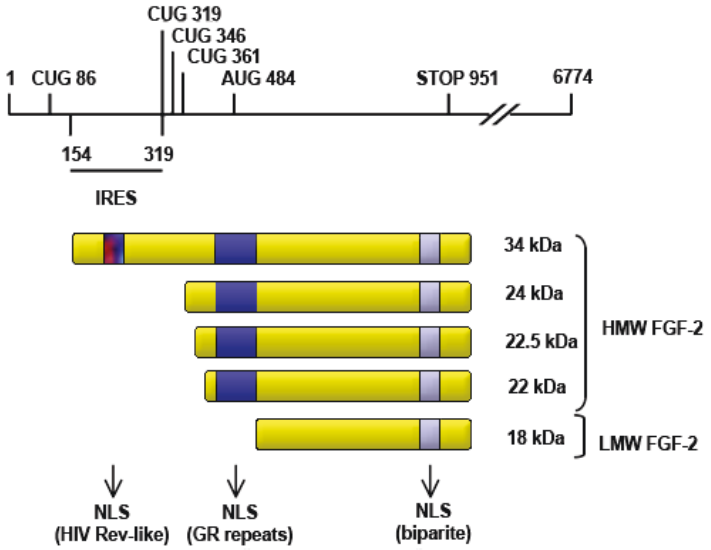

Fig. 3 Schematic representing human FGF2 isoform expression by alternative translation initiation. CUG, alternative leucine translation initiation codon; AUG, classical methionine translation initiation codon; IRES, internal ribosome entry sire; kDa, kilo Dalton; LMW, low molecular weight; HMW, high molecular weight; NLS, nuclear localization sequence; GR, Glutamic acid; HIV, human immunodeficiency virus [149].

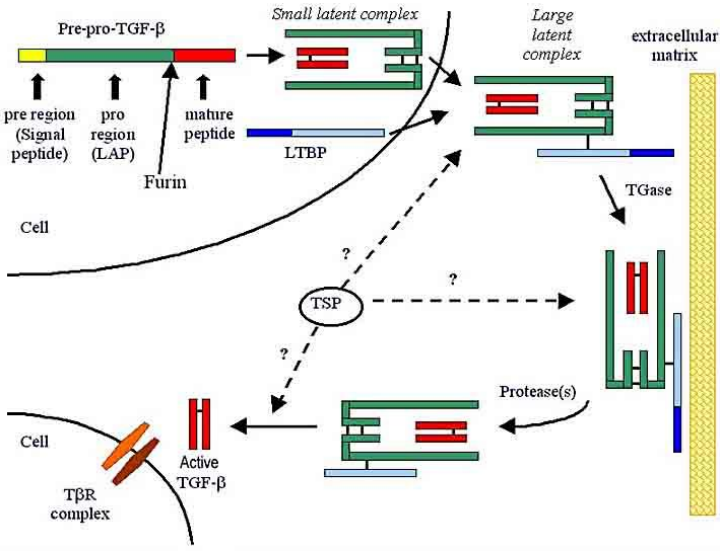

Fig. 4 Schematic picture of TGFβ activation [152]**.** TGFβs are produced as dimeric precursors (or pre-pro-TGFβ), in which the C-terminal forms active ligand following proteolytic processing. LAP and mature TGFβ remain non-covalently associated and form the SLC, which is biologically inactive. The released SLC is linked by disulfide bonds to one LTBP, forming LLC. (LAP, latency-associated peptide; LTBP, latent TGF-beta binding protein; SLC, small latent complex; LLC, large latent complex.)

1.2.3.3.2 TGFβ

The human transforming growth factor β (TGFβ) family consists of 33 members, most of them were encoded as dimeric, secreted polypeptides that control development, wound repair, morphogenesis, immune defence, and tumorgenesis. This family is characterized by a specific three-dimensional fold and a conserved number and spacing of cysteine residues in the C-terminus of the mature polypeptide.

Latent and active forms: TGFβs are synthesized and stay latent in ECM. In form of pre-pro-peptide precursor, they are cleaved twice to become active TGFβ. The first cleavage is to eliminate a hydrophobic signal peptide in the N-terminal region, yielding pro-TGFβ. The second cleavage removes latency-associated peptide (LAP), leading to mature TGFβ (Fig. 4). To keep latency in ECM, two isoforms exist, i.e., "small latent complex (SLC)" and "large latent complex (LLC)", where SLC is mature TGFβ-LAP complex and LLC is mature TGFβ-LAP and latent TGFβ–binding protein (LTBP) complex. The mature TGFβ dimer is noncovalently linked with LAP dimer that is associated by disulfide bonds in SLC. SLC is further linked to LTBP with one disulfide bond to become LLC [152].

Activation of latent TGFβs: Based on the noncovalent linkage between LAP and mature TGFβ, latent TGFβ was activated by acidification or heat treatment *in vitro* [153]. Besides, *in vivo* it is believed to be activated with proteolytic cleavage and conformational modification [154]. Studies discovered that plasmin and transglutaminase enhanced the activation of TGFβs by the specific cleavage [155, 156], whereas thrombospondin (TSP) achieved it via engaging the conformation change of LAP [154, 157]. Structural study also supported that tensile force across latent TGFβ was essential for its activation because the TGFβ become functioned with the aid of integrin attachment to cytoskeleton, LTBP to ECM and cellular contraction [154, 158].

Functions in brief: TGFβ family plays important roles in many essential cellular processes, including proliferation, differentiation, migration and apoptosis, according to cellular microenvironment. In the process of wound healing, fibroblasts can undergo a contractile phenotype transition that leads to their differentiation into myofibroblasts with the help of TGFβ [136]. Additionally, it has been reported that Smad signalling in response to TGFβ induced the expression of α-SMA gene [159].

1.2.4 Signallings related to cell growth and differentiation

1.2.4.1 A global view of cell signal transduction

Cells respond to their microenvironmental stimuli through different tools, in which signalling transduction is critical. In general, signalling transduction is initiated from ligand-receptor interaction, and then the receptor propagates message from extracellular milieu to cytosol and further pass into nucleus, as shown in Figure 5. How cells communicate in an efficient and coordinated way relies on the complicated signal transduction. This part will briefly present the global scenario of signalling transductions.

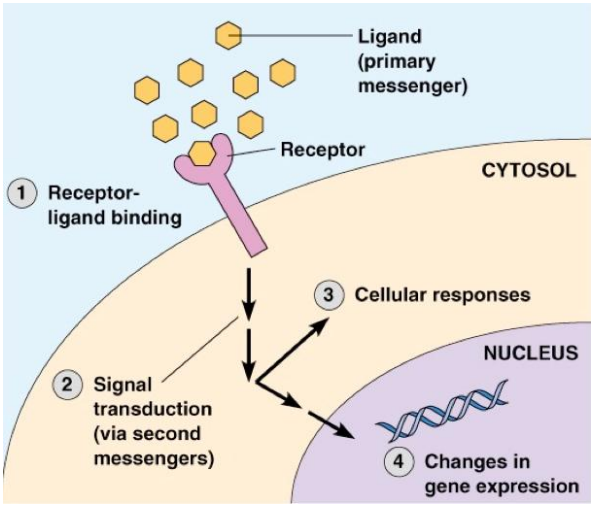

Fig. 5 Diagram of cell signalling transduction. From http://apbiomaedahs.weebly.com/3d-cell-communication-and-signal-transduction.html

1.2.4.1.1 The category of signal initiators

Cells in higher animals establish signalling route by a variety of molecules including gas (e.g. NO), proteins (e.g. growth factor), ions (e.g. Ca^{2+}), peptides (e.g. vasopressin), amino acid derivatives (e.g. epinepherine), steroids (e.g. testosterone), nucleotides (e.g. cAMP), fatty acids (e.g. polyunsaturated fatty acids), retinoids (e.g. tazarotene), etc.

1.2.4.1.2 Mechanisms of ligand-receptor binding

Ligand-receptor affinity model or lock-key model is the most widely accepted model to describe the specific recognition between the signalling molecules (ligands) and cell membrane molecules (receptors), even the detailed mechanisms for specific recognition is to be further elucidated. As known, the van der Waals, hydrophobic and electric-static forces are the principal forces involved in the protein-protein interactions [160]. The electrostatics holds a great role to drive them at a large distance after mutual 'sensing' [161] and thermal motion is thought as a model for ligand and receptor moving towards each other. Reportedly, electrostatic interaction mainly determines the stability, binding characteristics and function of proteins [162]. Additionally, the recognition between small molecules and proteins such as drug-receptor interactions, must consider cation-π interaction that is comparable to or stronger than a typical hydrogen bond. Cation-π interaction exists mainly in the recognition for the domain where the aromatic side-chain of phenylalanine, tyrosine or tryptophan plays the vital role [163].

With the advances in structural biology and computational biology, recent studies based on structure-recognition and energy-protonation provide fresh ideas for the fundamental mechanism of recognition. It is pointed out that almost any receptor-ligand binding is pH-dependent and protonation states of them must be appropriately set prior to and after the binding due to their direct relation with electrostatics [162]. Later on, the orientation or conformational changes will follow due to the flexibility of protein structure [164]. Pocket formation theory and transition state model are the other often mentioned mechanisms [165, 166]. Ligand-binding pocket is in a range of several hundred $Å^2$, with a shape that can firmly grasp or partially envelop their ligands. "Transition state" is defined by configurations in which the two proteins are shifted apart by 8 Å and the two binding surfaces are rotated away by 0 to 3 , and thus create proper orientation to form a complex.

1.2.4.1.3 The category of receptors

1.2.4.1.3.1 Enzyme-linked receptors

As transmember proteins, the ligand-binding domain locates outside of the plasma membrane and the intracellular domain possesses intrinsic enzyme activity or is associate directly with an enzyme. This group of receptors has six subgroups: receptor tyrosine kinases, tyrosine-kinase-associated receptors, receptor-like tyrosine phosphatases, receptor serine/threonine kinases, receptor guanylyl cyclases, and histidine-kinase-associated receptors. As we know, FGFR and TGFβRII belong to tyrosine kinase receptor and serine/theorine kinase receptor, respectively.

1.2.4.1.3.2 G-protein-linked receptors

These receptors usually have 7 transmembrane (TM) domains with an extracellular N-terminus and a cytosolic C-terminus. According to sequence analogy of the 7 TM domains, these receptors can be divided into 5 subfamilies: the frizzled/taste subfamily (24 members), the rhodopsin subfamily (701 members), the secretin subfamily (15 members), the adhesion subfamily (24 members), and the glutamate subfamily (15 members) [167]. Functionally, they modulate the activity of plasma-bound enzyme and ion channel via G proteins with three subunits-α, β, γ subunit. For example, some of them can affect the activity of adenylyl cyclase, and thus alter the intracellular cyclic AMP

concentration; and some of them influence Ca^{2+} signalling by protein kinase C (PKC), protein kinase A (PKA) and Ca^{2+}/calmodulin-dependent protein kinases (CaMK) [168].

1.2.4.1.3.3 Ion-channel-linked receptors

Ion-channel-linked receptors, also called transmitter-gated ion channels and ligand-gated ion channels, are transmembrane proteins involving in ion flux regulation. The ion channels work in a transient manner which allows them to concisely control the ion flow and thus affect cell functions. For example, transient receptor potential cation channel subfamily M member 7 (TRPM7) is one member in this group, which has six TM helixes and TRPM7 currents are detected in all cells [169]. Besides, nicotinic acetylcholine receptor (nAChR) consisting of α/β subunits from α2-α7and β2-β4 controls potassium (K^+) and sodium (Na^+) ions to enter the cells, in certain case, including Ca^{2+} influx [170].

1.2.4.1.4 Cell-signal interplay

There are four important aspects concerning the cell and signal interplay. 1) One vs. many: A great number of signal molecules provide enormous combinations for a specific cell behavior. On the other hand, one signal molecule is able to produce different outcomes if the target cells differ. For example, acetylcholine may promote secretion of salivary gland cell, induce contraction of skeletal muscle cell, or decreased the rate and force of contraction of heart muscle cell. 2) Memory and adaptation: for some treatments or exposures, cells can remember the intervention and sustain the effect for long time, say, by daughter cells, which are clearly revealed in immune response. Also, cells can adapt or desense to a stimulus, allowing cells to respond to signal molecules only in a concentration range. 3) Response or not: the signal induced consequence is embodied only if other signals are also indicated, such as in crosstalk and feedback regulation.

1.2.4.2 Signallings relevant to cell growth and differentiation

The “Pathway Interaction Database” in PubMed archives a variety of cell signalling pathways affecting cell proliferation and differentiation and the number of related research keeps increasing. To date, the signalling pathways related to cell proliferation include ERK1/2, PKC, p38, MAPKKK cascade, STAT1/3, EGR1, ErbB4/ErbB2/neurigulin 1β, IL5/IL5RA/syntenin, FOXO1, FOS, GATA2, Oct1, p70S6K,

MYC, CDK11 p58, PDGF/PDGFRs, uPA/uPAR, NF2, BRAF, JUN, JNK, CXCL4/CXCLR, αβ integrin, TGFβ/TGFβR, MAK, AR/RAK/Src, BRM/BAF57, glucosylceramide, etc.

As to the signalling pathways related to cell differentiation, similar literature search on PubMed using the key words "cell differentiation AND signalling". The signalling pathways are found mediated by the following molecules such as IL4, IL12, IL27, JAK, STATs, IFN, NFAT, JUN, FOS, Smads, PI3K, MAPKKK cascade, JNK cascade, TGF, to list the most discussed.

It is not difficult to note that TGFβ and MAPKKK cascade occupy an important position in both proliferation and differentiation pathways. The following will review their relevant details including TGFβ1, Smad pathway, ERK pathway (non-Smad pathway), and NF-κB signaling.

1.2.4.3 TGFβ1

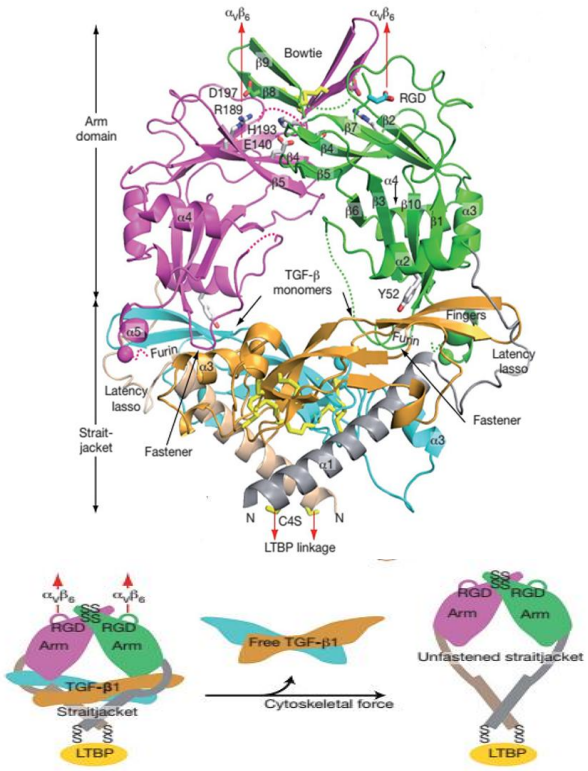

Fig. 6 Architecture of proTGFβ1. a) Overall structure; b) Schematic presentation of the structure and activation mechanism [170]**.**

As illustrated in Figure 6, TGFβ1 origins from a >100 kDa pre-proTGFβ1 with 390 amino acids. The pre-proTGFβ1 includes a signal peptide (1-29 amino acids) cleaved before secretion, LAP (75kDa, 30-278 amino acids) and mature peptide/mature TGFβ1 (25kDa, 279-390 amino acids) [152]. The signal peptide directs the secretory pathway, and the proTGFβ1 homodimer consists of mature TGFβ1 dimer with disulfide bonds at Cys356 itself and two LAP chains with disulfide bonds at Cys 223 and 225 [171]. The 3D structure in Figure 6 describes how the TGFβ1 dimer is located in proTFGβ1, held by straitjacket and encircled completely by the latency lasso loop, while LTBP is conjugated to straitjacket residue Cys4 [170]. In addition, the RGD motifs at each shoulder provide the recognition site for integrin α_v [170].

1.2.4.4 TGFβ signal transduction pathways

TGFβ, as a ligand, firstly binds to TGFβ receptor II (TGFβRII), a serine/theorine kinase receptor, which then recruits TGFβ receptor I (TGFβRI) forming a heterotetramer. TGFβRII then trans-phosphorylates TGFβRI, enabling the TGFβRI kinase domain to act on cytoplasmic proteins and thereby propel downstream signalling actions via Smad pathway and non-Smad signalling proteins. In Smad pathway, the activated TGFβRI kinase propagates the signal inside the cell through the phosphorylation of receptor-regulated Smads (R-Smads: Smad1, Smad2, Smad3, Smad5 and Smad8). The activated R-Smads form heteromeric complexes with Smad4 (common mediator Smad, or Co-Smad) translocating into nucleus to control gene expression in a cell-type-specific and ligand dose-dependent manner through interactions with transcription factors, coactivators and corepressors. Whereas in non-Smad signalling, due to TGFβR having the weak serine/tyrosine kinase attribute, TGFβRII also recruits GRB2 and SH2 and activates p38 MAPK signal pathway in addition to Ras-Raf-MEK-ERK signalling cascade [172, 173].

1.2.4.5 Smad pathways

The Smad pathway is activated by TGFβ superfamily members and also by other signalling molecules. Bone morphogenic protein (BMP) uses Smad1, 5, 8 as R-Smads, and Smad6, 7 as inhibitor Smads (I-Smads), whereas TGFβs mainly use Smad2, 3 as R-Smads and only Smad7 as I-Smads [174]. Smads have the conserved domains that indicate their important functions in molecular interaction, i.e., the Mad-homology 1 (MH1)

domain at N terminus and C-terminal, the MH2 domain at R-Smads and Co-Smad as well as the PY motif at R-Smads and I-Smads (Fig. 7) [174].

The L3 loop in the MH2 domain of Smad2 acts with the L45 loop of TGFβRI, resulting in the phosphorylation of the Ser residues (S465 and S467) and then the dissociation of Smad2 from the receptor complex (Fig. 8) [175]. The conserved loop-strand region in the MH2 domain of Smad4 mediates the heterodimer formation with the released Smad2. This signal transduction is blocked by Smad6, 7 via competing binding to receptor, where three amino residues, i.e., Phe411, Lys401 and Cys406 at the L3 loop in Smad7, hold a critical role [176]. Besides, Smad7 also initiate degradation by recruiting E3 ubiquitin ligases Smurf1, Smurf2 and Nedd4L, appealed to degrade TGFβRI through ubiquitin-dependent pathway [177]. In BMP mediated signalling, Smad6 also competes with Smad1 in the formation of Smad4/R-Smad dimer [176, 178].

As the key regulator of TGFβ signalling, Smad7 and its regulators YAP (Yes kinase-associated protein), Smurf1, Smurf2 and Nedd4L interact each other through the PY motif in Smad7 (Fig. 9) [179]. Both Smurf 1, 2 interact with Smad7 through a unique domain. YAP interacts with Smad7 only through the WW1 domain and Nedd4L uses WW2 domain to bind to the PY site of Smad7. However, R-Smads (Smad1, Smad3) require a WW pair to interact with the four regulator proteins. It is also reported that Smad4 recognizes its negative regulator Ski by the interaction between the L3 loof of Smad4 and the I loop from Ski [180]. While translocated into nucleus, the Smads can bind to specific DNA sequence. For example, the MH1 domain of Smad3 recognizes a palindromic Smad binding element (SBE, GTCTAGAC) [181, 182]. In addition, after binding to DNA and to their transcriptional partners, Smads require histone acetyltransferases and co-activators, such as C/EBP-binding protein (CBP), p300 and p300/CBP-associated factor (P/CAF), for the initiation of transcription [183].

Smad signalling is involved in a variety of functions such as in fibrosis, cell transdifferentiation, inflammation, bone growth, development and regeneration, acute and chronic liver injuries, etc. [184, 185].

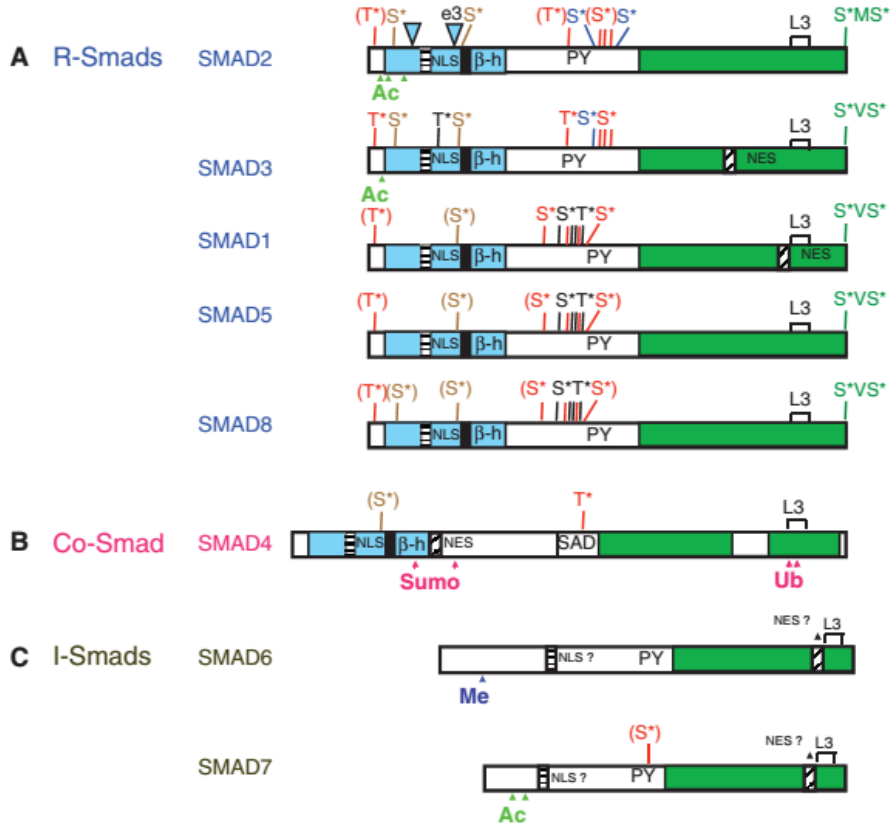

Figure 7. The Smad family [174]. Simplified structures of the eight human Smad proteins divided into (A) Receptor-activated (R) Smads; (B) common- mediator (Co) Smad; and (C) inhibitory (I) Smads.

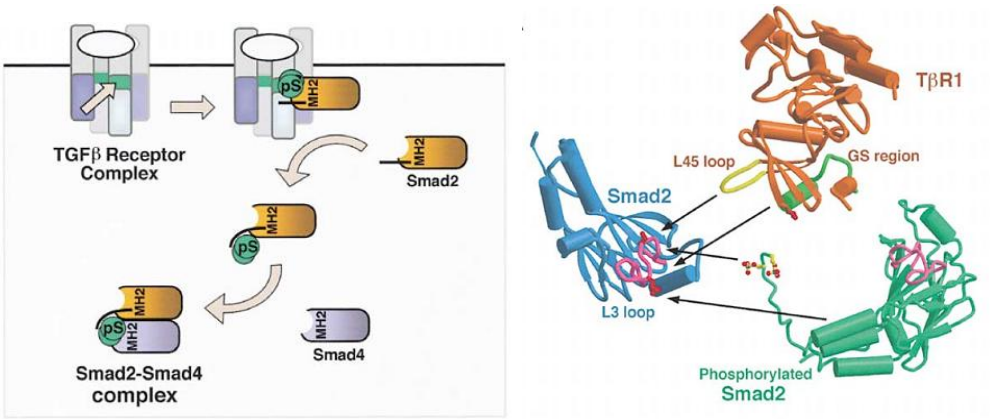

Figure 8. TGFβRI initiates Smad pathways through Smad2 [186].

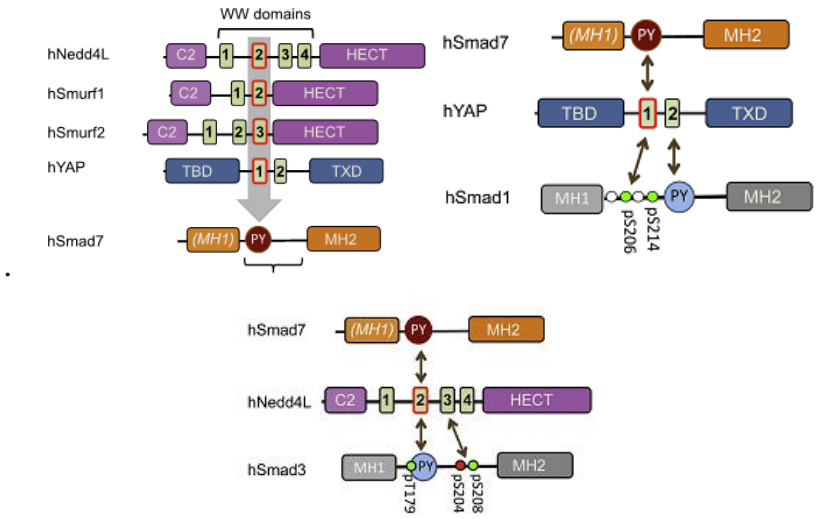

Figure 9. Schematic presentation of the different binding modes for Smurf1 and Smurf2 WW domains with respect to R- and I-Smad linkers [181].

1.2.4.6 Non-Smad pathways: ERK

TGFβ induced signal transduction can also propagate through non-canonical, non-Smad pathways including ERK [187]. As showed Figure10, MAP kinase cascades are divided into three groups: JNK, p38 MAPK, and extracellular-signal-regulated kinase (ERK) pathways. In ERK pathway, the signal binds to its receptor on plasma membrane, and the receptor recruits Ras with adaptor proteins (Shc, Grb2, Sos) and continues the cascade Ras/Raf/MEK/ERK [187, 188]. The activated ERK can be dephosphorylated by MAP kinase phosphatases (MKPs) as feedback regulation [189]. In addition, Raf is not the only MAP3K but the following molecules including TPL2 protoongogene, interleukin-1 receptor-associated kinase (IRAK), MLK-like mitogen activated protein triple kinase (MLTK) [190-192], all can activate ERK1/2. Many substrates of ERK have been reported, including Elk1, Ets family, c-Fos, c-Jun, ribosomal S6 kinase (RSK) family, etc. RSK family exerts their efforts through such molecules as nuclear factor-κB (NF-κB), CREB, nuclear factor of activated T cells 3 (NFAT3), serum response factor (SRF), estrogen receptor-α, and the transcription initiation factor TIF1A [193].

Structurally, as shown in Figure 11, ERK has N-, C- lobes, with a catalytic loop in the middle. At N-lobe, a glycine-rich loop helps the position of ATP phosphates; and the activation segment determines the substrate binding and catalytic efficiency. In active form, the lobes are closed together where DFG motif faces to the ATP-binding pocket

and adjusts Mg^{2+}. In inactive state, the two lobes are tilted away [194]. A recent study proposed the interaction of MAPK:KIM motif (kinase interaction motif, or D motif) structures for their mutual selectivity [195].

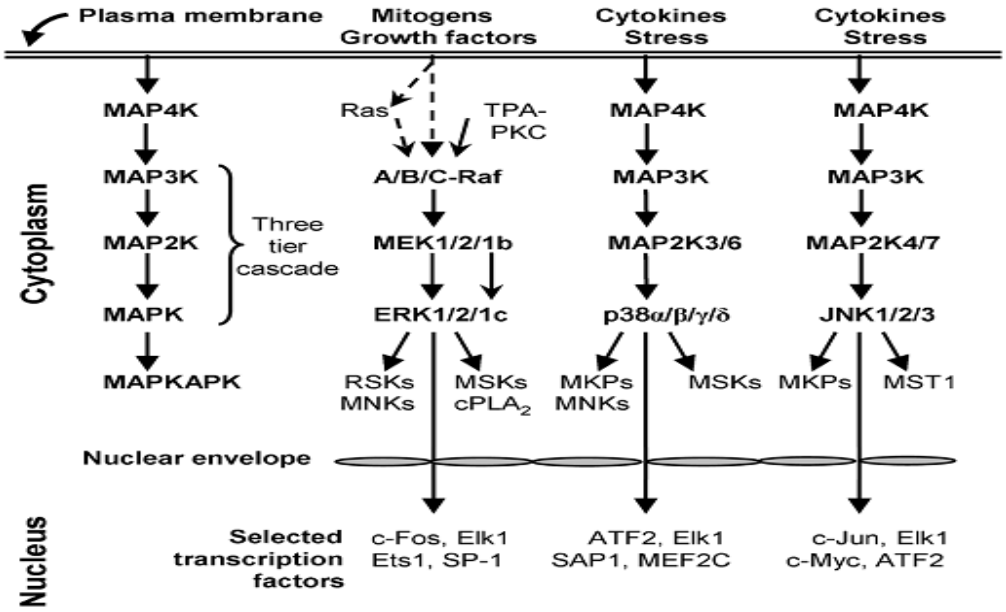

Figure 10. MAP kinases cascade [194].

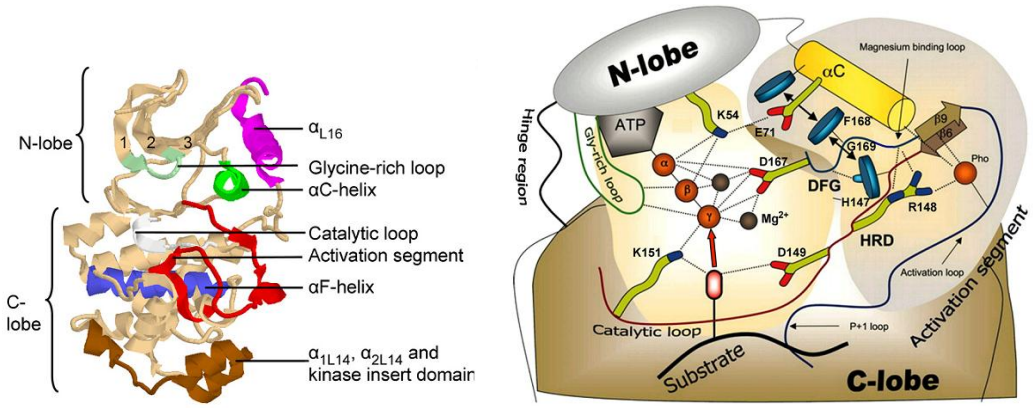

Figure 11. The structure of ERK and diagram of the inferred interactions between the human ERK2 kinase catalytic core residues [194].

ERK pathways regulate numerous functions such as cell survival, growth, apoptosis, motility, differentiation and adhesion, being an important player in tissue regeneration, development, tumorgenesis, and wound healing [188, 196-198].

1.2.4.7 NF-κB signalling

NF-κB is a transcription factor complex consisted of homo- and heterodimers of five members of the Rel family including p50/p105 (NF-κB1), p52/p100 (NF-κB2), RelA (p65), RelB, and c-Rel [199]. In general, NF-κB can be activated through canonical, alternative and atypical pathways. In canonical pathway, NF-κB signalling pathway starts from membrane receptors such as Toll-like receptors (TLRs), interleukin-1 receptor (IL-1R), tumor necrosis factor receptor (TNFR) and antigen receptors. These receptors often recruit adaptors which continue to recruit and activate IκB kinase (IKK) complex. IKK complex then phosphorylates IκB at two serine residues leading to the release of NF-κB translocating into nucleus and binding to target genes. In alternative or non-canonical pathway, the differences are the membrane receptors and partial degradation of p100 to p52. The receptors include B-cell activation factor receptor (BAFFR), lymphotoxin β-receptor (LTβR), CD40 receptor, receptor activator for nuclear factor κB (RANK), TNFR2 and Fn14 receptor [200-202]. The atypical pathway is triggered by genotoxic stress, with NF-κB essential modulator (NEMO or IKKγ) migrating into nucleus and then ubiquitinated (Fig. 12) [201].

Functionally, NF-κB signalling pathway controls B and T cell development where it involves TCRβ-NF-κB dependent survival step not only in the CD4-CD8-double negative 3 (DN3) to DN4 stage and but also in the αβ T cell selection and maturation [203]. In addition, inflammation and cancer are also regulated by this pathway [201]. It also responds to cell apoptotic signal, i.e., causing cytoplasmic relocalization of nucleophosmin [204], and tuning cell cycle and differentiation [205, 206].

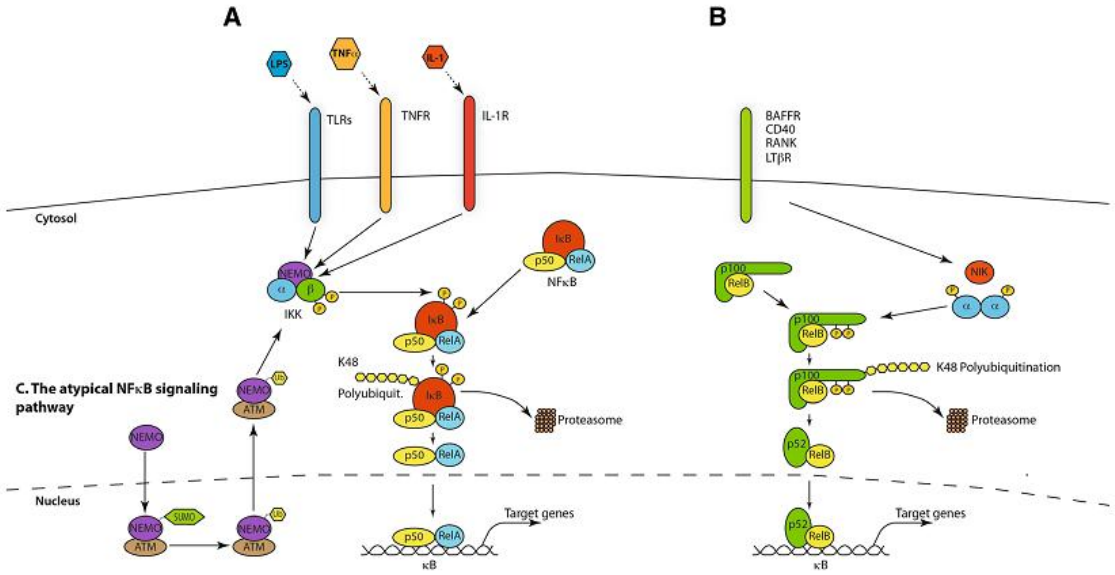

Figure 12. The canonical (A), non-canonical (B) and the atypical (C) NF-κB signalling pathways [201].

1.2.5 EF/ES in wound healing

1.2.5.1 The principle of transepithelial potential

The most widely documented EF related to wound healing is called transepithelial potential or TEP. In health state, the epidermis is well stratified and keratinocytes link with tight junctions giving high electrical resistance, i.e., restriction to free ion transportation across skin. Directional transport of cations like Na^+ inwards across epithelium leads to internal positive potential (TEP) [207]. As shown in Figure 13, when wound occurs, the tight junction is broken and outwards current of cations occurs, resulting in 0 mV TEP at the wound site. This causes potential difference between the wound site and the neighbour region that maintains high cation concentration because of the intact epithelium. This potential difference generates electric current (in form of ion flow) to the wound from surrounding tissues. As a consequence, an electrical field (EF) at wound is built up and persists until epithelium reseals the wound. It is reported that wound EF acts as an early cue to attract epithelial cell migration, which was demonstrated as galvanotaxis *in vitro* under a physiological electrical strength [18, 35]. The healing of cornea was found faster in higher TEP or EF by modulating ion channel activity [208, 209]. *In vitro*, EF reported to influence cell cycle of epithelial cells [210]. In addition, some reports pointed out that *in vitro* ES can trigger fibroblasts to change their behaviours including Ca^{2+} influx, proliferation, and collagen secretion [62, 63]. In particular, recent studies have

shown that direct current (DC), one type of ES, not only enhanced fibroblast viability but also increased the expression of IL-6 and IL-8 [211]. Researches in the field of EF and wound healing are encouraged to find out the mechanisms in this type of regulation and hope to apply this principle to make better and faster wound healing.

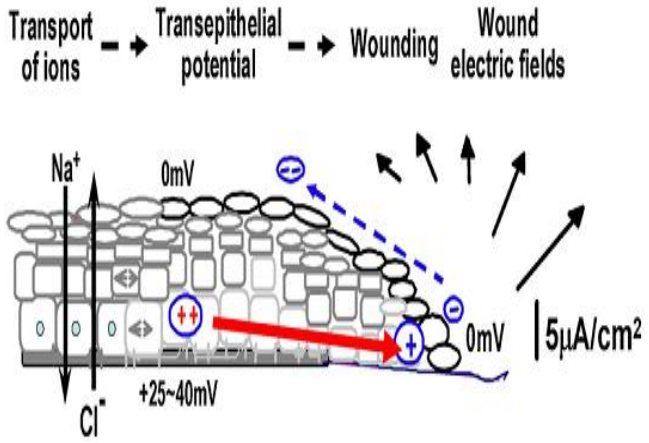

Figure 13. The mechanism of generation of wound electric fields [212].

For the measurement of endogenous EF in wound, it is difficult to give the precise values due to the limitation in tools and the dynamic nature of wound EF. In bovine cornea, the EF was measured as 42 mV/mm at 0.25mm from the wound edge [213], while in Guinea pig skin it measured 140 mV/mm at wound edge and declined towards the wound center [207]. In addition, the EF at skin changes temporally such that at cornea wound this value measured 4 μA/cm^2 at start, 10 μA/cm^2 within 60 mins and 4-8 μA/cm^2 later on [18].

1.2.5.2 Evidence of ES helped wound healing

Considering the potential effect of endogenous EF on wound healing, studies regarding the application of ES to facilitate wound healing have been conducted both in animals and in patients. Positive outcomes were reported but the criteria of selecting ES methods vary.

1.2.5.2.1 ES in animal wound healing

Various animal models have been used in electrical stimulated wound healing. Guinea pigs with 3 cm linear incision were treated with a uniderectional pulsed current of 300-

600 mA, 80 pulse per second (pps). The ES regimen was reported beneficial for wound healing regardless of the polarity of ES [214]. Experiment using diabetic mice indicated that ES induced collagen deposition in excisional wounds [215]. Also, Rowley et al. reported that ES in form of 1.0 mA DC treatment contributed to wound healing in rabbits by showing bacteriostatic effect [216]. In dogs, it was reported that an ES of 300 mV, 67 Hz, with a current of 0.04 μA, improved the healing of large surface full-thickness wounds [217].

1.2.5.2.2 ES in human wound healing

ES has been used in human mainly to treat non-union of bone and skin ulcers. While the effect of ES on wound healing is mostly reported with positive outcomes, it is still inconclusive in terms of the optimal ES program for a specific condition due to the variety of ES designs (duration, intensity, forms, frequency, etc.) [218]. According to recent database, high voltage ES at 100 V, although it only generates very small inductive field in tissue, accelerates the healing rate of ulcers in patients [219]. Pulsed ES with a frequency of 128 pps and a current of 29.2 mA was reported providing beneficial effect on the healing of chronic dermal ulcers of stages II, III and IV [220]. Diabetic ulcers were also improved effectively with the ES treatment with asymmetric biphasic square wave pulse or electrical nerve stimulation [221, 222]. Another form of ES is called frequency rhythmic electrical modulation system (FREMS), which was reported to improve diabetic ulcer healing [221]. Also showing clinic efficacy is the low voltage pulse current (LVPC) with the charge dosage of 250–500 μC/s [224], and the low-intensity direct current (LIDC) in the range of 200–800 μA [225].

1.2.6 Abnormal healing

There should be no pathologic sufer if normal wound healing proceeds. However, tissue repair is so complex that only a small error would lead to dysfunction of the injured tissue or organ. Abnormal healing should be thought as an abnormal process of the dynamic and delicate balance.

1.2.6.1 Inadequate regeneration

The first example is central nervous system (CNS) regeneration.Because of the complexity of brain and spinal cord and the very limited ability of adult neurons to

regenerate, CNS injury or degeneration often appears irreversible. Bone nonunion is another example. Corneal ulcers represent a challenge in epithelial regeneration.

1.2.6.2 Inadequate scar formation

Diabetic foot ulcers could not proceed through normal inflammation and proliferative phases; as a result, the ulcers stay in prolonged inflammation phase with delayed granulation tissue formation [226]. Inadequate blood supply induced pressure sores and venous stasis ulcers also reflect inadequate scar formation.

1.2.6.3 Excessive regeneration

The over-regeneration in peripheral nerve tissue leads to neuroma [227]. Hyperkeratosis is a process of thickening growth in stratum corneum in concert with the over-expression of keratin, which could be found in cutaneous psoriasis or adenomatous polyp formation in the colon [228, 229].

1.2.6.4 Excessive scar formation

The pathogenesis of fibrosis is attributed to the aberrant or exuberant wound healing in response to injury. In pulmonary fibrosis, fibroblasts and myofibroblasts synthesize a large quantity of ECM, a process that could be jointed by epithelial cells to produce pro-fibrotic mediators such as TGFβ, CTGF and sonic hedgehog (Shh) [230]. Liver cirrhosis also undergoes an excessive production of fibrous connective tissue. In hypertrophic scarring or keloid formation, studies recorded high activity of fibroblasts in the deposition of collagen *in vitro* [231].

1.3 Methods and electrically conducting polymers

1.3.1 Methods in ES research

To deliver ES to target cells or tissues in the context of wound healing, a variety of methods have been developed. Amongst them, some deliver ES through conductive substrate or scaffold to which cells are attached, some apply ES by electrodes that are in

contact with medium but do not in touch with cells, and others impose ES “noninvasively” via external electromagnetic field.

1.3.1.1 ES based on conducting substrate

In this approach, a conductive substract is chosen to culture cells and to mediate ES. A variety of conductive matrices are manufactured including PPy/PLA and PEDOT/PLA composites, graphene based materials, PEDOT/PPy-coated fabrics, electronspun conductive sheets, to list a few [29, 232-243]. These materials exist in different forms such as electrodes, gels, sheets, nanoparticles, fabrics, membranes [239, 240, 244-247], or in different scales ranging from nanometers to micrometers [232, 232, 236], or in 2-dimensional, 3-dimensional, porous, smooth, rigid and flexible states [234, 235, 247-254]. Some scaffolds are modified to acquire conductivity or electroactivity, such as electroconductive hydrogel, conductive nanocellulose and collagen gel [239, 254-258]. Recently, bioinspired conductive materials such as those surface modified with peptides, nucleotides and amino acids represent the new "blood" [259-263]. As documented, incorporating laminin peptide to PEDOT enhanced neurite growth [264]. Conductive collagen gel by mixing polyaniline (PANI) or PEDOT nanofibres with type I collagen demonstrated cytocompatible and induced PC12 cell differentiation [256]. Also, skin dermal fibroblasts cultured on PPy-PLA composite proliferated well and responded in favor of wound healing upon direct current ES [241, 254].

1.3.1.2 ES based on electrodes

There are metallic electrodes and salt bridges employed in research and in clinics. *In vitro*, electrodes deliver EF to the cultured cells through culture medium without contacting cells. In tissue, EF is often formed inside the tissue between two or multiple electrodes that are in direct contact with tissue or skin. Metallic electrodes in direct contact with culture medium or body fluid may induce the electrolysis of water causing pH alternation, gas production and electrode dissolution. It may damage tissues or cells if the exposure is not appropriate [265, 266]. In vitro, salt bridge (or agar/agarose salt bridges) technique uses two agar bridges to connect metal electrodes with culture medium, preventing the diffusion of the toxic substances from metal electrodes as well as joule heating [267, 268]. Clinically used instruments include transcutaneous electrical nerve stimulator (TENS) and frequency-modulated electromagnetic neural stimulation (FREMS).

1.3.1.3 Electromagnetic field induced ES

This type of ES is based on the principle that when electrical current passes a coil an electromagnetic field (EMF) is generated perpendicular to the current flow. When such an external EMF is generated near the wound, the EMF will penetrates and induce EF in the tissue [269].

1.3.1.4 ES parameters

In literatures related to ES, a large quantity of articles is found where researchers have utilized different ES modes. ES can take place as constant or pulsed electrical potential or current, or as alternative current. The intensity was found as high as hundred volts or as low as mV. The frequency was reported in the range of Hz to kHz. The exposure duration differs from microseconds to days. Because of the differences in ES methods and parameters, it is difficult to compare the outcomes of different studies in terms of current or potential intensity inside tissues.

1.3.2 Conducting polymers

1.3.2.1 Intrinsically conductive polymers (ICPs)

ICPs are the synthetic macromolecules conducting electricity without conducting fillers such as metals or carbon blacks. These polymers are characterized by the conjugated chemical chains. Through a process of 'doping', the insulating polymer chain can be either positively or negatively charged due to oxidization or reduction and consequently becoming electrically conductive [270]. Uniquely characterized by their physical and chemical properties of organic polymers and the electrical attributes of metals, ICPs have attracted much interest in the past 30 years [232]. Among ICPs, poyaniline (PANI), PPy, polythiophene (PT) and polyphenylene are among the most investigated. In biomedicine, PPy and poly(3,4-ethylenedioxythiophene) (PEDOT) are the most intensively studied.

ICPs have already made progress in several fields and built a number of promising and attractive research and/or application profiles such as biosensors, fuel cells, electromagnetic interference shielding, biomedical materials, and tissue engineering scaffolds [271-273]. ICPs represent a number of important advantages including

biocompatibility, the ability to entrap and controllably release biological molecules, and the feasibility to change their physical, chemical and electrical properties to adapt specific applications [274, 275]. Furthermore, ES through ICPs was reported promoting cell growth, including neurons, fibroblasts and osteoblasts, leading to the development of ICPs for medical applications [276].

1.3.2.2 Charge carrier and transport in conductive polymer

Unlike metals that are rich in free moving electrons as charge carriers, the neighboring single and double chemical bonds in conductive polymers become conjugated upon doping and form delocalized charge carriers called polaron or bipolaron depending on the oxidation state. In analog to solid state physics, the change from localized conjugation to delocalized mobile polaron or bipolaron is the change from valence band (VB) to conduction band.(CB). The width between VB and CB is called bandgap which determines the intrinsic electrical properties of the material. In an undoped conjugated polymer, this bandgap is too large to allow the free movement of charge carriers. Upon oxidation, i.e., the removal of an electron from the chain, the ionization energy becomes lower. Thus the "delocalized electrons" are generated and can move in an EF. For chemists, polaron is a radical ion associated with a re-equilibriumed lattice, and the presence of localized electronic state is referred to as polaron state [277, 278]. The conductive entity includes a oligomeric cation/anoin and a counterion that comes from the oxidative/reductive agent or from specifically added dopants. If the second electron is removed from the entity, then a bipolaron forms with a strong local lattice distoration and high mobility. The charge carriers travel along the conjugated polymer chain and also are capable to jump from chain to another, called hopping [279]. Therefore the length of the polymer chain and extent of defects have significant effect on the conductivity of conductive polymers.

1.3.2.3 Polypyrroles (PPy)

PPy is polymerized from pyrrole monomer whose chemical formula is C4H5N, a five-membered aromatic ring (Fig. 14A). PPy is synthesized either by oxidant or oxidative electrical potential as show in Figure 14B. Pyrrole is easily oxidized by oxidants including oxidative transition-metal ions, acid, and peroxide. The common oxidants in lab for PPy production are ferric salts, e.g., $FeCl_3$, $Fe(ClO)_3$ and $FeBr_3$. Oxidized PPy is electrostatically interacted with counterions, which can be anions from oxidant such as

Cl^- or from other molecules added during or after polymerization. When counterions get lost, e.g., dissolved in an aqueous solution, the polymer will be reduced and conductivity also goes away.

A B

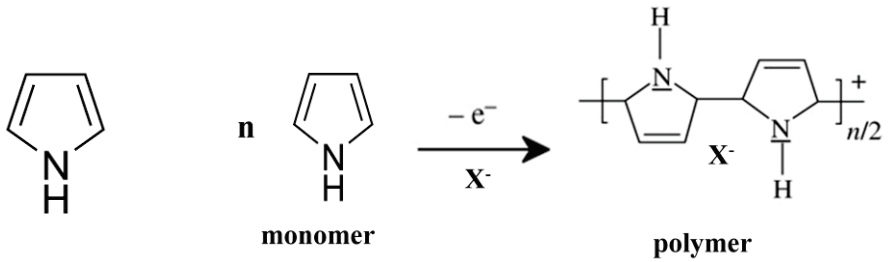

Figure 14. A: The structure of a pyrrole monomer. B: The polymerization of PPy .

PPy has generated profound research interests owing to its easy synthesis, reasonable environmental stability, and the unveiled biocompatibility both *in vitro* [280-282] and *in vivo* [282, 283]. Because of the sensitivity of the conductivity of PPy to environmental factors, PPy has been widely investigated in sensoring technology. It was used as carbon dioxide gas sensor because CO_2 molecules generate weak bonds with the π-electrons of PPy [284]. Composite of PPy and multi-walled carbon nanotube was employed in environmental pollution detection to trace mercury, lead and iron ions [285]. PPy was also studied as a candidate to replace the platinum counter electrode in dye-sensitized solar cells [286]. In biomedical applications, PPy-based immunosensor showed various capacities in response to amperometric, conductometric and potentiometric changes [287]. As documented, PPy has been applied to flexible substrates such as papers and textiles [288, 289]. PPy was reported capable of supportting the proliferation of many cells such as mesenchymal stem cells (MSCs), endothelial cells, PC12, fibroblasts and glial cells from dorsal root ganglia (DRG) [290-292]. In addition, PPy can also be bioactivated by using biomolecules as dopant. For instance, arginine–glycine–aspartic acid (RGD) peptide was dopped to the chlorine-doped PPy surface and thus ameliorated PC12 cell adhesion [293], so did other candidate peptides

such as Arg–Gly–Asp–Ser (RGDS) peptide and 12-amino acid peptide (THRTSTLDYFVI, T59) [294, 295].

1.4 Aims of the study

1.4.1 Background

Endogenous EF is one of the many factors participating normal biological processes and wound healing. Literatures have shown that externally applied ES can interfere with a wide range of cellular activities, including proliferation, migration and production of growth factors. From tissue regeneration point of view, EF becomes a valid and valuable parameter in the equation controlling the complex tissue repair and regeneration process. Therefore, interactions between exogenous EF and biological process have been studied with the purpose to understand and modulate these natural processes. However, the mechanisms related to EF and cell interactions important to wound healing remain poorly understood. The biomaterials suitable to introduce EF to biological systems are also very limited.

In the processe of wound healing, fibroblasts play very important roles from proliferative phase to reepithelialization phase. One of such roles is their trandifferentiation into myofibroblasts contributing to wound closure. The studies from our laboratories and other researchers indicated that ES was able to change the behaviours of fibroblasts and to help wound healing. Based on the *in vivo* and *in vitro* results reported in literatures, it is reasonable to study the relationship between ES and the activities of fibroblasts at cellular and molecular levels, and the underlining mechanisms in particular.

1.4.2 Hypothesis

Fibroblasts proliferate and transdifferentiate into myofibroblasts by sensing and adjusting to pulsed electrical signal.

1.4.3 Objectives

The general objective of this work is to investigate the communications between ES and dermal fibroblast in the context of wound healing.

The four specific aims are:

1. To design PPy-coated conductive fabrics suitable for skin fibroblast culture and PES exposure;

2. To investigate the behaviours of skin fibroblast due to PES;

3. To study the signalling pathways related to fibroblast transdifferentiation due to PES;

4. To preliminarily study the phenotypic stability of electrically activated fibroblast *in vivo*.

1.4.4 Research design

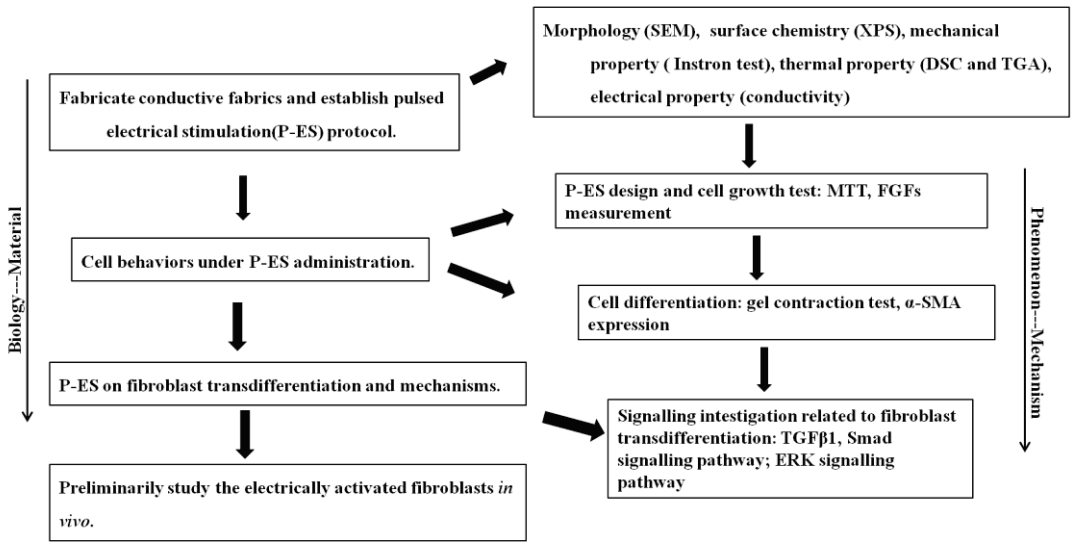

Figure 15. The schematic of research design.

CHAPTER II

CONDUCTIVE MATERIAL PREPARATION AND CHARACTERIZATIONS

PPy-coated PET fabrics and electric pulse-stimulated fibroblasts

Yongliang Wang[1,2,3], Mahmoud Rouabhia[1] and Ze Zhang[2,3]

[1]Groupe de recherche en écologie buccale, Faculté de médecine dentaire, Université Laval, Québec (QC), Canada; [2]Département de chirurgie, Université Laval; [3]Centre de recherche Hôpital Saint-François d'Assise, CHU, Québec (QC), Canada

Keywords: PPy, PET fabrics, electrical stimulation, pulse, fibroblasts

J. Mater. Chem. B, 2013,**1**, 3789-3796 **DOI:** 10.1039/C3TB20257G

2.1 Abstract

Inherent in biological systems, the electrical field is involved in regulation of many physiological processes. Exogenous electrical stimulation has been used to modulate cellular activity and enhance wound healing. In this study, electrically conductive polypyrrole (PPy) was synthesised through a two-step method and subsequently used to cover the surface of polyethylene terephthalate (PET) fabric microfibres which were used to investigate the effect of electrical pulse on human skin fibroblasts. Scanning electron microscopy (SEM) revealed a very thin, uniform PPy coating on the PET microfibres, which was supported by a surface chemical analysis by X-ray photoelectron spectrometry (XPS). An Instron machine, a thermogravimetric analyser (TGA), and a differential scanning calorimeter (DSC) were used to analyse the mechanical and thermal properties of the fabrics, which showed no significant change following treatment with PPy. The average surface and bulk electrical resistivity of these fabrics were measured to be 63 kU per square and 138 ohm m, respectively. The bulk resistivity increased to 213 ohm m after 24 h pre-incubation in cell culture medium, and then increased by another 22% following a pulsed electrical stimulation protocol in cell culture medium for additional 24 h. Human skin fibroblasts were seeded on the PPy-coated PET fabrics and cultivated thereafter with or without pulsed electrical stimulation (PES). PES was found to enhance fibroblast proliferation, as confirmed by MTT and Hoechst staining. These findings demonstrate that PES is effective in promoting fibroblast growth. It also shows that PPy-coated PET fabrics are electrically stable enough to mediate sufficient PES. This study therefore lays the groundwork for the use of PPy-coated fabrics to mediate ES in biomedical research.

2.2 Introduction

Electrical phenomena are intrinsic in biological systems. For example, cells generate a potential gradient across a plasma membrane due to ion transportation with the help of ion channels and pumps. Protein receptors at the cell membrane sense environmental changes, including electrical potential, and then propagate signals to the downstream executors. Ions such as K^+, Na^+, Ca^{2+} and Cl^- are ubiquitous, as they participate in each life function [1-4], and their movement and distribution are also sensitive to the electrical field (EF). Consequently, the EF is widely involved in various physiological regulations, such as molecular transportation, signal transduction, embryo development, heart rhythm, and wound healing, to name a few [5,6]. In vitro and in vivo studies have demonstrated the

effect of EF on important cellular activities including the destruction of microorganisms [7], increased migration and proliferation of epithelial cells [8, 9], increased attraction of macrophages to the wound site [8,10], and improved wound healing associated with endogenous electrical currents at the wound [11, 12]. Based on this knowledge, doctors have used electrical stimulation (ES) to cure bone non-union [13, 14] and for cardiac resuscitation [15, 16]. This has also motivated researchers to investigate ES in regenerative medicine and tissue engineering.

Polypyrrole (PPy) is a synthetic conductive polymer that displays reasonable biocompatibility both in vitro and in vivo [17-20]. Due to its highly conjugated molecular structure, PPy is unprocessable unless it is combined with other processable polymers. In our previous research, Shi et al[21] and Meng et al [22] developed a processable PPy – polylactide (PLA) composite demonstrating sufficient electrical conductivity and stability. It was also shown that ES in the form of a constant direct current voltage applied through this composite was indeed able to enhance the growth of human cutaneous fibroblasts and to promote the secretion of cytokines and growth factors [23, 24].

Medical textiles are an important category of materials that are widely used in medicine in applications such as wound dressings, hernia patches, and vascular grafts. These textiles have many attractive properties, including flexibility, porosity, and suturability, making them excellent candidates to form composites with conductive polymers. Milliken Research Corporation reported PPy-coated textiles called Contex prepared through wet chemistry [25]. Tessier et al. deposited PPy on the surface of polyethylene terephthalate (PET) fabrics through plasma and chemically activated surface grafting polymerisation [26]. These fabrics were shown to be non-cytotoxic *in vitro* [20] and tissue compatible *in vivo* [27]. In contrast to the PPy–PLA composite membrane, however, the PPy-coated fabric was shown to easily lose its electrical conductivity in an aqueous environment, particularly under continuous ES [28], due to the unavoidable conductivity deterioration of intrinsically conductive polymers under aqueous conditions, particularly when the PPy layer was thin. Electrical stability thus becomes a critical issue when the goal is to use conductive textiles to provide electrical interaction with a biological system.

In this study, PPy-coated PET fabrics were prepared and characterised, and their electrical stability was subsequently investigated using pulsed electrical potential. The efficacy of the PES on fibroblast proliferation was tested and demonstrated for the first

time. This work revealed the feasibility of using conductive polymer-coated textiles to mediate ES in a biological system.

2.3 Materials and Method

2.3.1 Two-step synthesis of PPy-coated PET fabrics

Pyrrole (98%, Laboratoire MAT, Beauport, QC, Canada) were distilled and stored in a refrigerator at 4ºC prior to use. PET fabrics (Testfabrics, West Pittston, PA, USA) were thoroughly washed three times in methanol (Laboratoire Mat) followed by isopropanol (Laboratoire Mat). After a final wash in deionised water for 10 min, the PET fabrics were placed in a pyrrole solution (12% v/v) of methanol and water (50:50) for 60 min, then transferred to an aqueous solution of $FeCl_3$ (12% w/ v)(Laboratoire Mat) water solution for 15 min to complete polymerisation. The PPy-coated fabrics were then washed three times with deionised water and were dried in a desiccator overnight.

2.3.2 Electrical conductivity

The surface resistivity (R) of the dry PPy-coated fabrics was measured with a four-point method using a Jandel Multiheight Probe (Jandel Engineering, Linslade, Bedfordshire, UK). The four probes had a separation of 1 mm and a diameter of 500 μm. To measure coating uniformity, three specimens 2.5 × 4.5 cm^2 in size were tested on both sides, with 9 measurements (3 x 3) taken on each side. Average resistivity was calculated and compared. The surface conductivity (σ, s. □) of a fabric is the inverse of its surface resistivity or sheet resistivity (ρ , ohm/□), where the symbol of square is dimensionless.

2.3.3 Electrical stability

To ensure the usefulness of conductive fabrics in an aqueous environment, the decline of its conductivity must be in a narrow range. To test this aspect, PPy-coated PET fabrics were cut into specimens 2.5 × 4.5 cm^2 in size, and these specimens were assembled on the bottom of a homemade multi-well electrical cell culture plate designed by Meng [29]. The assembly was then sterilised with ethylene dioxide (EO) gas so as to simulate cell culture conditions. The two longitudinal edges of each specimen, extending to the outside of the culture well, were firmly pressed against two copper (99.99%) electrodes connected to a

waveform generator (Tabor Electronics, Tel Hanan, Israel). Dulbecco's modified Eagle's medium (DMEM) (M-0268, Sigma Chemical Co., St. Louis, MO, USA) was then added into the plate. There was no contact between the electrodes and the medium. Incubation was carried out in a standard cell culture incubator at 37 ºC for 24 h with no changing of the medium. Square wave pulses of DC voltage were then applied through the electrodes to the conductive fabrics for another 24 h. The pulse amplitude, width, and period were 5 volts, 10 seconds, and 1200 seconds, respectively. The current-time function was recorded with the Keithley 2700 Digital Multimeter/Data Acquisition System (Keithley Instruments, Cleveland, OH, USA). This experiment was repeated eight times.

The bulk electrical resistivity (ρ) of the fabrics was calculated based on the following formula: $\rho = (R \times A)/L$, where R (ohm) is the resistance of the fabric specimen, A is the cross-sectional area (m^2) of the fabric specimen, and L is the length (m) of the fabric specimen or the distance between the two copper plates. Because the width of the fabric was 2.5 cm and the thickness was 1 mm, the area A was 2.5×10^{-5} m^2. L was 4 cm. R was calculated from the voltage (5 V) and measured current (A) passing through the fabric specimen.

2.3.4 Tensile testing

The stretch–strain behaviour of the fabrics was tested by means of an Instron 5848 MicroTester (Instron, Norwood, MA, USA). Each fabric was cut into 5×50 mm^2 long specimens in the weft direction of the fabric. The specimens were then placed firmly between two clamps, leaving an effective sample length of 20 mm. During testing, the fabric samples were stretched at a rate of 1 mm min^{-1} until broken. The recorded stretch–strain curves thus generated the Young's modulus, maximum force, and strain at failure.

2.3.5 Thermal analysis

The mechanical property and biostability of PET depends highly on its molecular morphology which can be readily monitored by measuring the thermal properties [30]. A DSC 823e system (Mettler-Toledo, Columbus, OH, USA) was used to analyse the crystallinity, glass transition, and melting temperatures of virgin and PPy-coated PET fabrics at a scanning rate of 20 ºC min^{-1} between 25 and 350 ºC. The weight of the specimens ranged between 6 and 10 mg. The thermal degradation of the fabrics, an

indicator of material stability, was measured with a TGA/SDTA 851e thermogravimetric analyser (Mettler-Toledo) at a scanning rate of 20 ºC min^{-1} between 25 and 800 ºC. Each measurement was performed in triplicate.

2.3.6 Electric pulse-stimulated culture of fibroblasts

The electrical cell culture plates were the same as those used in the electrical stability test, as previously described. PPy-coated PET fabrics of 2.5 × 4.5 cm^2 in size were fixed on the bottom of the electrical cell culture plate and connected to the wave generator through external electrodes. The surface area exposed for cell culture was 1.7 × 1.7 cm^2. Both the plate and the fabrics were then sterilized with EO gas at 37 ºC according to standard industrial procedures. Prior to seeding the cells, the fabrics were pre-conditioned by immersion in DMEM for 24 h under cell culture conditions to remove any residual chemicals remaining in the fabrics following PPy synthesis. After the culture medium was refreshed, human skin fibroblasts (Clonetics, San Diego, CA, USA) were seeded (1×10^5 cells per well) on the test fabrics and cultured for 24 h with or without PES (amplitude 5 V, width 10 sec, and period 1200 sec). Following stimulation, the fibroblasts were cultured for another 24 and 48 h prior to being stained with Hoechst dye for adhesion observation or evaluation by MTT assay.

2.3.7 Hoechst staining

The cells on the fabrics were washed three times with PBS and fixed thereafter with a mixture of methanol in acetone (3:1) for 10 min. The cells were then incubated with a solution of 2 mg ml^{-1} Hoechst 33342 (Riedel de Haen, Seele, Germany) in PBS for 15 min at room temperature. Finally, the fabrics were subsequently washed, observed under an epifluorescence microscope (Axiophot, Zeiss, Oberkochen, Germany), and photographed.

2.3.8 Cell viability test (MTT assay)

MTT [(3-(4,5-dimethylthiazol-2-yl)-2,5-di-phenyl-tetrazolium-bromid)] is reduced to purple formazan in live cells, which is a widely used method to measure cell viability and proliferation, as fluorescence intensity is proportional to the number of live cells. The

prepared MTT solution (5 mg ml^{-1}) was stored at 4ºC prior to use. The fibroblasts selected for analysis were refreshed with new medium containing 10% (v/v) MTT (Sigma-Aldrich Canada) and were cultivated in a standard incubator for another 4 h without light. Thereafter, the supernatant was carefully removed and lysis solution (2 ml HCl in isopropanol (0.04N)) was added. Fifteen minutes later, 200 µl of solution (in triplicate) was transferred from each well to a 96-well flat-bottom plate, and the absorbance of the MTT (formazan) was determined at 550 nm by means of an ELISA reader (Model 680, BioRad Laboratories, Mississauga, ON, Canada).

2.3.9 Statistical analysis

All of the data were presented as mean ± SD when appropriate. A *t*-test was applied to compare the difference between the PPy-coated and virgin PET fabrics. The variance of conductivity uniformity test was determined by one-way ANOVA. A significant difference was indicated when $p < 0.05$.

2.4 Results

2.4.1 Electrical conductivity of the PPy-coated PET fabrics

The average surface electrical resistivity of the dry PPy-coated PET fabrics was measured to be 63.4 ± 0.9 kΩ per square and showed no significant difference among samples on either side. The relatively small SD generated from nine measurements performed on each sample surface revealed a uniform coating of PPy on the fabrics. The average resistance of the fabric specimens (4 cm long × 2.5 width × 0.1 cm thick) in air of about 60% humidity was 2.2×10^5 ohm, which increased to 3.4×10^5 ohm in the culture medium at the end of the first 24 h incubation. The bulk electrical resistivity of the dry and wet fabrics was calculated to be 138 and 213 ohm.m, respectively. Electrical stability was defined as the remaining percentage of electrical conductivity of the conductive fabrics following the electrical stability test relative to the conductivity at the beginning of the second 24 h incubation. As can be seen in Fig. 16, the conductivity of the PPycoated fabrics slowly decreased over the stimulation time (n= 8). However, after 24 h of pulsed stimulation, the conductivity of the PPy-coated PET fabrics continued to retain 78% of the conductive ability relative to that at the end of the first 24 h incubation. Fig.

16 also presents the change of bulk electrical resistivity over time, showing the absolute values of the fabric resistivity.

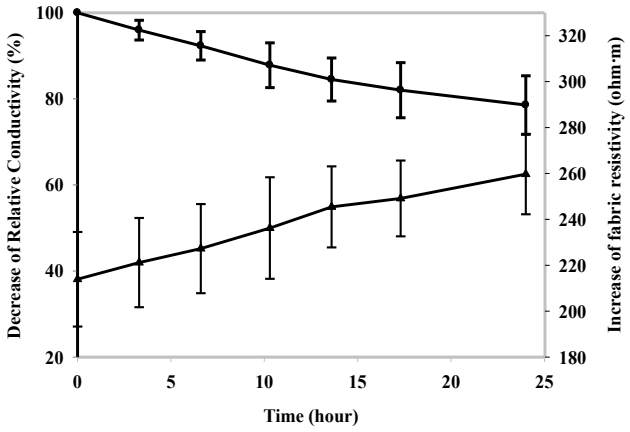

Fig. 16 Electrical stability tests, showing the slow decline of conductivity over time.

2.4.2 Surface morphology

At low magnification (Fig. 17A1 and B1), the PPy-coated fabric showed the same textile structure as the virgin fabric, with no blocking of the fibre interstices. At a higher magnification (Fig. 17A2 and B2), individual fibres displayed a similar diameter of approximately 25 μm, with patches of extra materials appearing on the PPy-coated fibres. At even higher magnification (Fig. 17A3 and B3), the characteristic granular morphology of PPy growth revealed a very thin, uniform layer of PPy coating on the PET fibre. The size of most of the PPy grains was less than 100 nm (arrow, Fig. 17B3). This layer of PPy was not visible at the cross section and its thickness could not be determined under SEM (Fig. 17A4 and B4).

2.4.3 Surface chemistry

Table 3 presents the surface elemental composition of the PPy-coated, virgin PET, and pure PPy specimens. Clearly, nitrogen (N) in the PPy-coated PET fabric was significantly elevated, compared to that observed in the PET. Because nitrogen only exists in PPy (0.5% in PET is considered to be normal contamination), the high nitrogen content thus indicated the presence of PPy. However, both the nitrogen concentration and the doping

ratio (Cl/N) in the PPy on PET were lower than those recorded by the pure PPy, which were 9.5% vs. 16.5% and 0.13 vs. 0.19, respectively.

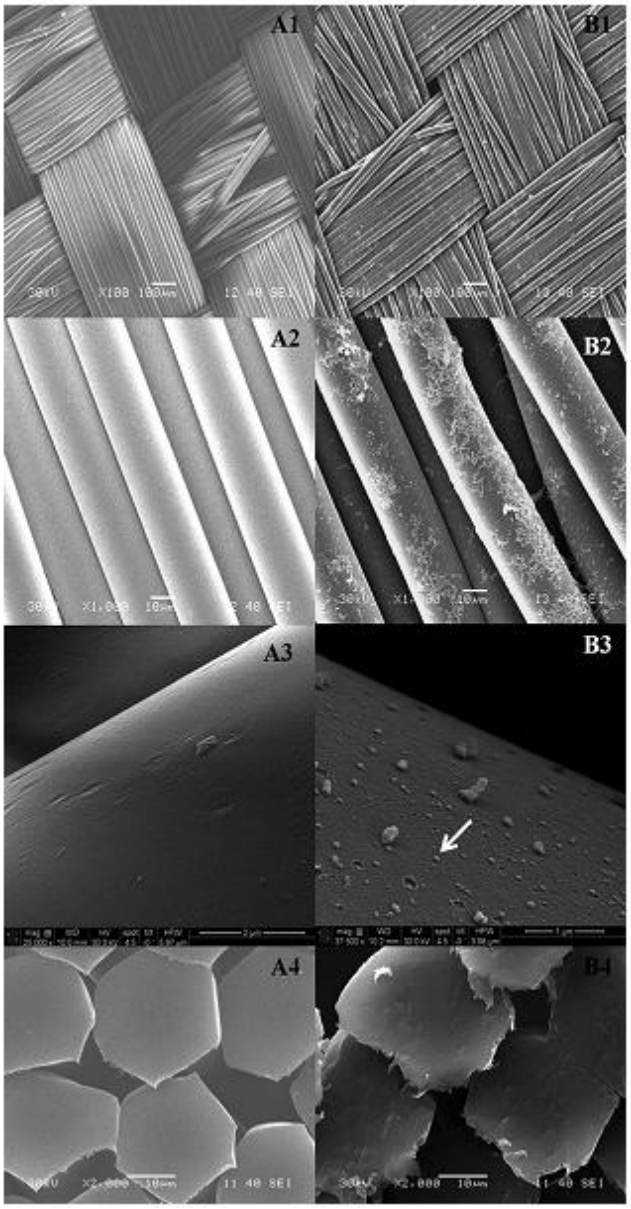

Fig. 17 SEM photomicrographs of the PET (A) and PPy-coated PET fabrics (B), showing thin and uniform PPy on the surface of the microfibres without blocking inter-fibre space. The arrow indicates a PPy granule less than 100 nm in size.

The high-resolution XPS spectra of nitrogen were used to identify the neutral and positively charged nitrogen atoms in the PPy. The N1s spectra of both the PPy-coated PET fabric and the pure PPy showed one major peak, with a distinct shoulder at the higher binding energy side and a tail at the lower binding energy side (Fig. 18). This significant peak was assigned to neutral pyrrolylium nitrogen (-NH-) at 399.1 eV and the

shoulder to the two charged nitrogen species at 400.2 and 402.4 eV, namely, polaron (-$N^{+}H$-) and bipolaron (-$N^{2+}H$-), while the tail observed at 396.9 eV was assigned to the deprotonated imine group (=N-) [23].

Table 3. Surface elemental composition of the fabrics measured by XPS (%)

Specimens	C_{1s}	N_{1s}	O_{1s}	Cl_{2p}	Cl/N
PET	74.4	0.5	25.1	-	-
PPy	74.6	16.5	5.7	3.2	0.19
PPy-PET	65.9	9.5	23.4	1.2	0.13

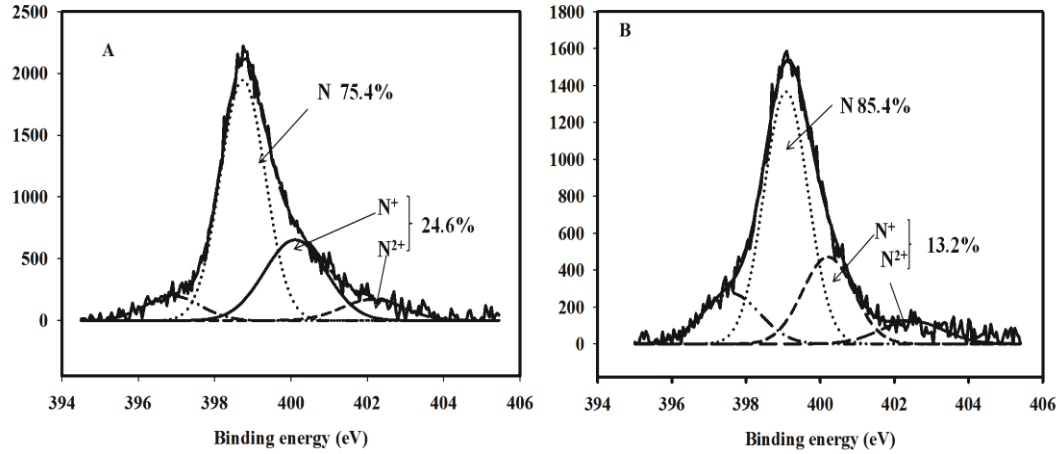

Fig. 18 XPS N1s spectra of pure PPy (A) and PPy-coated PET fabrics (B), showing oxidized nitrogen (N^{+}, N^{2+}), neutral nitrogen (–NH–) and deprotonized nitrogen (–N=).

2.4.4 Thermal analysis

Fig. 19A shows the melting behaviour of the fabrics measured with DSC. Both the PET and the PPy-coated PET fabrics recorded a sharp melting behaviour close to 284 ºC, with a crystallinity of 37.5% for the PET and 38.8% for the PPy-coated PET, thereby showing no significant difference (Table 4). Fig. 19B presents similar thermal degradation curves measured with TGA. Before 200 ºC and after 700ºC, the weight loss of both of these fabric specimens was less than 1%, whereas the PPy-coated fabric lost more weight before 200 ºC and less weight after 700 ºC.

Table 4. Thermal property of the fabrics

	Melting (DSC)			Weight loss % (TGA)		
	Peak(°C)	Heat of fusion ($W \bullet g^{-1}$)	Crystallinity (%)	0~200°C	200~700°C	700~800°C
PPy-PET	283.3± 0.5	54.5±3.6	38.8±2.4	0.8± 0.18[a]	83.7±0.8	0.9±0.02[a]
PET	284.0± 1.2	52.5± 5.0	37.5± 3.5	0.1± 0.09[a]	84.6± 1.3	0.6± 0.09[a]

[a] A significant difference was found.

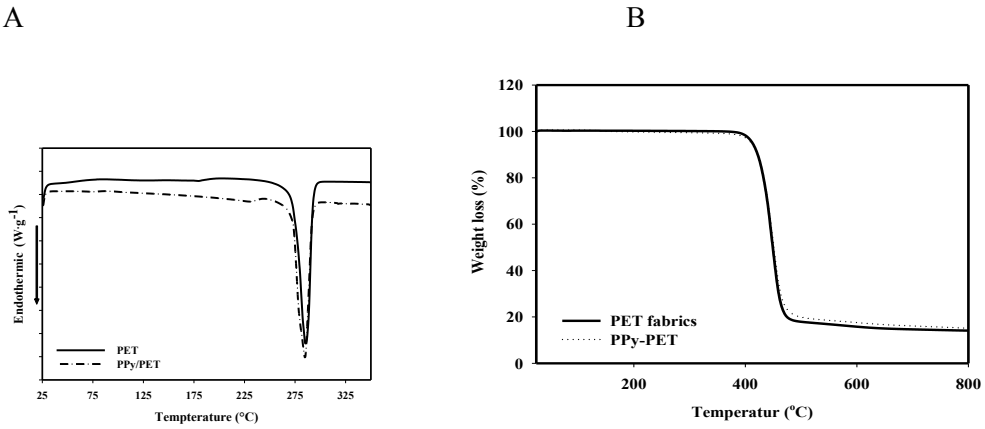

Fig. 19 Thermal analyses of the fabrics. (A) Endothermic behaviour measured with DSC and (B) thermal degradation measured with TGA.

2.4.5 Tensile properties

Table 5 and Fig. 20 present the tensile property test results. Both fabrics exhibited a highly similar behaviour by showing almost linear stretch-strain curves prior to failure. While the Young's modulus and failure strain were not different ($p > 0.05$, $n = 3$), the maximum load of the PPy-coated fabric was significantly lower than that of the virgin fabric, which revealed a decreased strength of the PET specimen following PPy treatment. Nevertheless, the stress-strain curves were almost overlaid prior to the 20% stain. The small upper flexure at ca. 3% was probably caused by the engagement of the initially unstretched fibres.

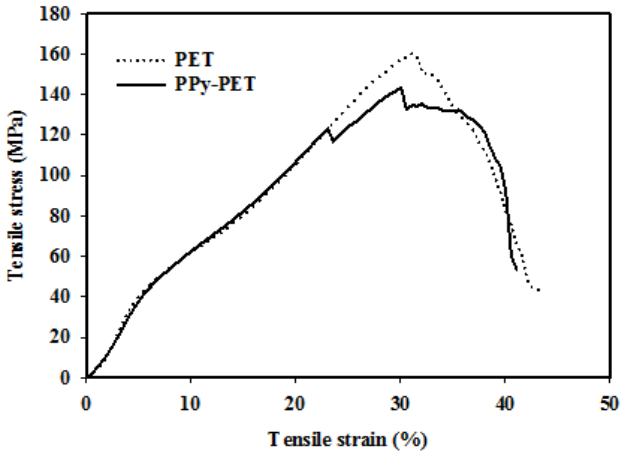

Fig. 20 Typical stress–strain behaviour of the PET and PPy-coated PET fabrics.

Table 5. **Tensile property of the fabrics**

	Young's modulus(10^3MPa)	Maximum load (N)	Failure strain (%)
PET	9.5 ± 0.6	155 ± 4.1[a]	32 ± 1.0
PPy-PET	8.3 ± 0.3	134 ± 2.6[a]	32 ± 1.4

[a] A significant difference was found, $p \leq 0.05$.

2.4.6 Cell viability

Fig. 21A shows cells adhered to the surface of the fabrics after 24 and 48 h of PES. The cellsunder PES (c, d) appeared to be similar to those without ES (a, b). However, the MTT optical density was significantly higher for the electrically stimulated cells than for the non-stimulated group (0.110 vs. 0.083), indicating that the electrically stimulated fibroblasts displayed greater viability and possibly a higher number of cells as well. This post-ES upregulation effect remained for at least 48 h (0.153 vs. 0.138). Similar upregulated cell viability was reported previously where PPy/PLLA composite membranes were used as substrates [18,24].

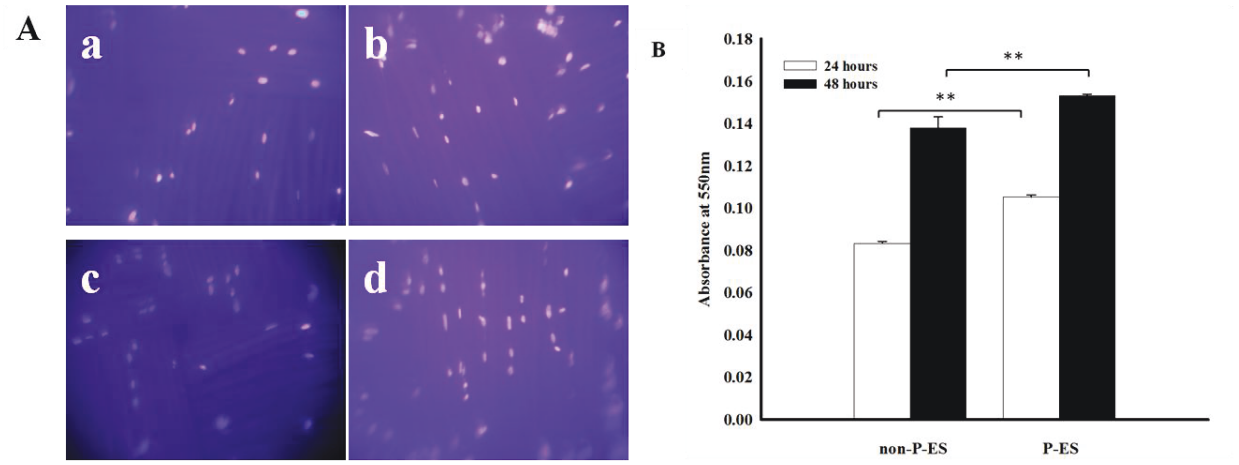

Fig. 21 Adhesion and viability of human skin fibroblasts on PPy-coated fabrics, showing comparable cell adhesion ((A), Hoechst staining) for both electrically stimulated (c and d) and non-stimulated (a and b) cells, and increased viability following PES (B), MTT assay. **: $p < 0.01$.

2.5 Discussions

PPy, a biocompatible conductive polymer, can be easily synthesised and modified chemically by means of various pyrrole derivatives [31]. PET fabric, on the other hand, is widely used in medical implants, such as vascular prostheses, because of its mechanical strength, porous structure, easy manipulation, and superior biostability.

The first objective of this study was to render PET fabric electrically conductive while retaining its morphological and mechanical strength. Its porous structure allows for cell infiltration and tissue ingrowth, both essential in wound healing. The conductive fabrics developed for this study had a very thin layer of PPy on only the surface of the microfibres without sealing any spaces between the microfibres. This was achieved by limiting the polymerisation of PPy to the grains in micro- and mostly nano-scale. As demonstrated, this surface modification did not affect the textile structure, as revealed by SEM, nor the PET molecular morphology, as indicated by DSC and TGA analyses. Consequently, the mechanical property (stretch-strain behaviour) of the conductive fabrics matched that of the virgin fabrics up to 20% of strain. This strain is beyond the normal conditions in medical use, for example, as patches or vascular grafts. The decrease in maximum load appearing at 32% of strain of the conductive fabrics was probably due to the plasticiser effect on fibre surface which was likely caused by various chemicals, such as the isopropanol, alcohol, and methanol used to wash the fabrics. Compared to previous research, PPy-coated fabrics, such as those developed by Milliken

[25] for industrial use, were coated with a thick layer of heavily doped PPy that was not adequate for medical use because of the excessive PPy and potentially cytotoxic dopants. The PPy-coated PET fabrics previously reported by our group require surface activation using phosphorylation [26]. In comparison, the technique developed in this study is just as effective yet far simpler.

The second objective of this study was to prove that a thin layer of PPy had enough electrical conductivity to introduce ES to cells in an aqueous environment. Although the conductivity of a thin layer of conductive PPy was shown to decrease rapidly in aqueous environment, particularly under electrical potential [32], the present study confirms that by adopting an appropriate ES protocol, such as the PES used here, PPy-coated PET fabrics can effectively provide ES to cells under standard cell culture conditions. The stability test showed that with this PES protocol, the conductivity of the fabrics decreased as anticipated but rather slowly. Compared to the conductivity at the end of the first 24 h preincubation, the fabrics retained close to 80% of their original conductivity after 24 h of ES stimulation. Therefore during ES, the fibroblasts were exposed to a relatively stable electric field (Fig. 16). This slowly deteriorating conductivity in DMEM likely occurred because of the short accumulated ES time and the redoping during the 1190-second "off" period. More importantly, this work proves that the same PES protocol has the proliferative potential for fibroblast. We previously reported that continuous ES upregulated fibroblast proliferation [23] and cytokine secretion [24] in a solid PLLA/PPy composite membrane. Our research continues here to non-continuous ES protocols that warrant the use of a thin layer of PPy and consequently PPy-coated PET fabrics.

The thickness of the PPy coating was difficult to directly measure and was therefore estimated through XPS. The XPS data of the PPy-coated fabrics revealed not only PPy but also strong PET signals (see the high oxygen value shown in Table 3). This indicates that either the PET was not completely covered by PPy or/and the PPy layer was less than 100 Å (XPS sampling depth). Should most of the microfibres be covered by PPy, as evidenced by SEM (Fig. 17, B3), the thickness of the PPy layer would be less than 100 Å.

Electrical phenomena widely occur in such physiological regulations as nerve signal transmission and cardiomyocyte contraction. ES has therefore been explored as a tool to manipulate cellular function. While the mechanisms are not well understood, ES has been shown to influence cell proliferation and migration and to have a strong relationship with growth factor production [33, 34] and calcium transportation [35,36]. ES has also developed

research interests in more diverse areas, including the stimulation of retinal ganglion cells with multi-electrode arrays [37], of human embryonic stem cells [38], and of muscle cells [39]. In light of these studies, conductive substrates, particularly those that can be used as scaffolding materials, show great potential for applications in regenerative medicine. Among other things, there are two essential requirements for such conductive substrates: sufficient electrical conductivity in an aqueous environment and basic scaffold characteristics, meaning non-cytotoxic, porous, and processable. The conductive fabric presented in our study meets these requirements.

To perform electrically stimulated cell culture, special attention should be paid to the setup of ES device and the possible disturbance to the culture medium. Culture medium contains a variety of inorganic ions such as Na^+, Ca^{2+}, K^+ and organic ions such as charged peptides and proteins. Those charged species move in electrical field, a well-known phenomenon called electrophoresis. A continued ES using electrodes may therefore cause the depletion or enrichment of those charged species near the electrodes, a secondary effect of EF that may affect the normal growth, distribution and migration of the cells. Using pulsed ES may reduce or eventually eliminate such electrophoresis, providing that the pulse duration be short enough to avoid ion migration. Another important issue is to avoid electrochemical reactions at the electrodes if there is a direct contact of the electrodes with the culture medium, because such reactions generate cytotoxic products. An effective approach is to avoid the direct contact of the electrodes with the medium, such as using salt-bridges [5]. Under the experiment configuration of this work, the conductive fabric was integrated in a closed electrical circuit instead of as an electrode, thus avoided electrophoresis and electrochemical reaction. Readers are referred to recent reviewing articles to understand the features of different ES devices [40, 41].

Interest in the interactions between electrical fields and biological systems continues to grow and has generated a promising research field. In the future, developing ES-activated cell responses, targeting transduction receptors and signalling pathways, and integrating ES into biomaterials will be imperative for both basic science research and clinical applications.

2.6 Conclusion

A two-step polymerisation process was developed to synthesise PPy on PET fabrics. This simple wet chemistry technique efficiently rendered PET fabric electrically conductive

without affecting its mechanical and thermal properties. A PES protocol was established to work with the conductive fabrics. This research reveals for the first time that medical textiles covered with a very thin layer of conductive polymer can have sufficient electrical conductivity and stability to mediate effective ES to mammalian cells.

2.7 Acknowledgements

This work was supported by The Canadian Institutes of Health Research. We are grateful to Stéphane Turgeon for his technical assistance and constructive discussions on XPS. Our thanks go to Sebastien Meghezi for his technical assistance with the mechanical test.

2.8 Conflict of interest

The authors declare no conflicts of interest.

References

1. MacKnight ADC, Leaf A. Regulation of cellular volume. *Physiol Rev*. 1977; 57: 510–573.
2. Fabiato A, Fabiato F. Calcium and Cardiac Excitation-Contraction Coupling. *Ann Rev Physiol.* 1979; 41: 473–484.
3. Faraci FM, Heistad DD. Regulation of the cerebral circulation: role of endothlium and potassium channels. *Physiol Rev*. 1998; 78: 53–97.
4. Toled-Aral JJ, Brehm P, Halegoua S et al. A single pulse of nerve growth factor triggers long-term neuronal excitability through sodium channel gen induction. *Neuron*. 1995; 14: 607–611.
5. McCaig CD, Rajnicek AM, Song B et al. Controlling cell behaviour electrically: current views and future potential. *Physiol Rev*. 2005; 85: 943–978.
6. Funk RH, Monsees T, Ozkucur N. Electromagnetic effects - From cell biology to medicine. Prog Histochem Cytochem. 2009; 43: 177–264.
7. Kincaid CB, Lavoie KH. Inhibition of bacterial growth in vitro following stimulation with high voltage, monophasic, pulsed current. *Phys Ther*. 1989; 69: 651–655.
8. Kloth LC, McCulloch JM. Promotion of wound healing with electrical stimulation. *Adv Wound Care*. 1996; 9: 42–45.

9. Alvarez OM, Mertz PM, Smerbeck RV et al. The healing of superficial skin wounds is stimulated by external electrical current. *J Invest Dermatol*. 1983; 81: 144–148.
10. Orida N, Feldman JD. Directional protrusive pseudopodial activity and motility in macrophages induced by extracellular electric fields. Cell Motil. 1982; 2: 243–255.
11. Karba R, Semrov D, Vodovnik L et al. Electrical stimulation for chronic wound healing enhancement. Part 1. Clinical study and determination of electrical field distribution in the numerical wound model. *Bioelectrochem Bioenerg*. 1997; 43: 256–270.
12. Mehmandoust FG, Torkaman G, Firoozabadi M et al. Anodal and cathodal pulsed electrical stimulation on skin wound healing in guinea pigs. *J Rehabil Res Dev.* 2007; 44: 611–618.
13. Scott G, King JB. A prospective, double-blind trial of electrical capacitive coupling in the treatment of non-union of long bones. *J Bone Joint Surg Am*. 1994; 76, 820–826.
14. Hughes MS, Anglen JO. The use of implantable bone stimulators in nonunion treatment. *Orthopedics.* 2010; 151-157.
15. Wellens HJ, Schuilenburg RM, Durrer D. Electrical stimulation of the heart in patients with ventricular tachycardia. *Circulation*. 1972; 46: 216–226.
16. Spurrell RA, Sowton E, Deuchar DC. Ventricular tachycardia in 4 patients evaluated by programmed electrical stimulation of heart and treated in 2 patients by surgical division of anterior radiation of left bundle-branch. *Br Heart J*. 1973; 35: 1014–1025.
17. Wang X, Gu X, Yuan C et al. Evaluation of biocompatibility of polypyr-role in vitro and in vivo. *J Biomed Mater Res A*. 2004; 68: 411–422.
18. Wang Z, Roberge C, Dao LH et al. In vivo evaluation of a novel electrically conductive polypyrrole/poly(D, L-lactide) composite and polypyrrole-coated poly(D, L-lactide-co-glycolide) membranes. *J Biomed Mater Res A*. 2004; 70: 28–38.
19. Kotwal A, Schmidt CE. Electrical stimulation alters proteinadsorption and nerve cell interactions with electrically con-ducting biomaterials. *Biomaterials*. 2001; 2: 1055–1064.
20. Zhang Z, Roy R, Dugre FJ et al. In vitro biocompatibility study of electrically conductive polypyr-role-coated polyester fabrics. *J Biomed Mater Res*. 2001; 57: 63–71.

21. Shi G, Rouabhia M, Wang Z et al. A novel electrical conductive and biodegradable composite made of nanoparticles and polylactice. *Biomaterials.* 2004; 25: 2477–2488.
22. Meng S, Rouabhia M, Shi G et al. Heparin dopant increases the eletrical stability, cell adhesion, and growth of conducting polypyrrole/poly(L, L-lactide) composites. *J Biomed Mater Res A*. 2008; 87: 332–344.
23. Shi G, Rouabhia M, Meng S et al. Electrical stimulation enhances viability of human cutaneous fibroblasts on conductive biodegradable substrates. *J Biomed Mater Res A*. 2008; 84: 1026–1037.
24. Shi G, Zhang Z, Rouabhia M. The regulation of cell functions electrically using biodegradable polypyrrole-polylactide conductors. *Biomaterials*. 2008; 29: 3792–3798.
25. Milliken and Co., Milliken. http://www.milliken.com
26. Tessier D, Dao LH, Zhang Z et al. Polymerization and surface analysis of electrically conductive polypyrrole on surface activated polyester fabrics for biomedical applications. *J Biomater Sci: Polym Ed*. 2000; 11: 87–99.
27. Jiang X, Marois Y, Traoré A et al. Tissue reaction to polypyrrole-coated polyester fabrics: an in vivo study in rats. *Tissue Eng*. 2002; 8: 635–647.
28. Wang Z, Roberge C, Wan Y et al. A biogdegradable electrical bioconductor made of polypyrrole nanoparticle/poly(D,L-lactide) composite: A prelininary in vitro biostability study. *J Biomed Mater Res A*. 2003; 66: 738–746.
29. Meng S, Zhang Z, Rouabhia M. Accelerated osteoblast mineralization on a conductive substrate by multiple electrical stimulation. *J Bone Miner Metab.* 2011; 29: 535–544.
30. Woo L, Ling MTK, Cheung W. Advanced testing for biomaterials. In: Szycher M, ed. High Performance Biomaterials. Lancaster, PA: Technomic. 1991; 91–123.
31. Khan W, Marew T, Kumar N. Immobilization of drugs and biomolecules onin situ copolymerized active ester polypyr-role coatings for biomedical applications. *Biomed Mater*. 2006; 1: 235–241.
32. Jiang X, Tessier D, Dao LH et al. Biostability of electrically conductive polyester fabrics: an in vitro study. *J Biomed Mater Res.* 2002; 62: 507–513.
33. Chao PH, Lu HH, Hung CT et al. Effects of Applied DC Electric Field on Ligament Fibroblast Migration and Wound Healing. *Connective Tissue Res*. 2007; 48:188–197.
34. Bai H, Forrester JV, Zhao M. DC electric stimulation upregulates angiogenic factors in endothelial cells through activation of VEGF receptors. *Cytokine*. 2011; 55: 110-115.

35. Cho MR, Marler JP, Thatte HS et al. Control of calcium entry in human fibroblasts by frequency-dependent electrical stimulation. *Front Biosci.* 2002; 7: a1–8.
36. Bourguignon GJ, Jy W, Bourguignon LY. Electric stimulation of human fibroblasts causes an increase in Ca^{2+} influx and the exposure of additional insulin receptors. *J Cell Physiol.* 1989; 140: 379–385.
37. Sekirnjak C, Hottowy P, Sher A et al. Chichilnisky. Electrical stimulation of mammalian retinal ganglion cells with multielectrode arrays. *J Neurophysiol.* 2006; 95: 3311–3327.
38. Serena E, Figallo E, Tandon N, C et al. Electrical stimulation of human embryonic stem cells: cardiac differentiation and the generation of reactive oxygen species. *Exp Cell Res*. 2009; 315: 3611–3619.
39. Burch N, Arnold AS, Item F et al. Electrica pulse stimulation of cultured murine muscle cells reproduces gene expression changes of trained mouse muscle. *PLoS One*. 2010; 5: e10970.
40. Meng S, Rouabhia M, Zhang Z. Applied Biomedical Engineering, Intech Open Access Publisher, Croatia. 2011; 37-62.
41. Balint R, Cassidy NJ, Cartmell SH. Electrical stimulation: A novel tool for tissue engineering. *Tissue Eng Part B*. 2013; 19:48-57.

CHAPTER III

STUDY THE CELL RESPONSE TO PULSED ELECTRICAL STIMULATION: PART 1

Pulsed electrical stimulation modulates fibroblasts' behaviour through the Smad signalling pathway

Yongliang Wang[1, 2], Mahmoud Rouabhia[1], Denis Lavertu[3] and Ze Zhang[2]

[1]Groupe de Recherche en Écologie Buccale, Faculté de Médecine Dentaire, Université Laval, Québec, QC, Canada

[2]Axe Médecine régénératrice, Centre de Recherche du CHU de Québec, Département de Chirurgie, Faculté de Médecine, Université Laval,
QC, Canada

[3]Département de Chirurgie Plastique, Hôpital Saint-François d'Assise, Québec, Canada

Keywords: wound healing; fibroblasts; electrical stimulation; signalling; Smad

JOURNAL OF TISSUE ENGINEERING AND REGENERATIVE MEDICINE
J Tissue Eng Regen Med (2015)
Published online in Wiley Online Library (wileyonlinelibrary.com) DOI:
10.1002/term.2014

3.1 Abstract

The aim of this study was to investigate the healing characteristics and the underlying signalling pathway of human dermal fibroblasts under the influence of pulsed electrical stimulation (PES). Primary human dermal fibroblasts were seeded on polypyrrole-coated polyester fabrics and subjected to four different PES protocols. The parameters of the rectangular pulse included potential intensity (50 and 100 mV/mm) and stimulation time (pulse width 300s within a period of 600 s, and pulse width 10 s within a period of 1200s). Our study revealed that PES moderately improved the ability of the cells to migrate in association with a statistically significant ($p < 0.05$) increase of FGF2 secretion by the PESexposed fibroblasts. These exposed fibroblasts were able to contract collagen gel matrix up to 48h and this collagen gel contraction paralleled an increase in α-SMA mRNA expression and protein production from the PES-exposed fibroblasts. Interestingly, the effect of PES on the human fibroblasts involved the Smad signalling pathway, as we observed higher levels of phosphorylated Smad2 and Smad3 in the stimulated groups compared to the control groups. Overall, this study demonstrated that PES modulates fibroblast activities through the Smad signalling pathway, thus providing new mechanistic insights related to the use of PES to promote wound healing in humans.

3.2 Introduction

Electrical signal is involved in a variety of life processes in both physiological and pathological situations [1, 2]. Endogenous electrical field (EF) is known to play an important role in development and is thus an attractive cue to induce stem cell differentiation [2, 3]. Electrical stimulation (ES) was shown to increase DNA synthesis [4], activate p53 [5], increase TGFβ receptor expression [6] and upregulate fibroblast growth factor secretion [7]. Cells also responded to exogenous ES via intracellular signalling pathways, such as phosphatidylinositol-3-OH kinase (PI3K)–Akt, MAPK–ERKs, integrin and Rho [8, 9]. Cells migrate toward an electrode and their orientation is modulated according to the direction of the EF [10]. ES was also shown to influence cell growth and differentiation [11, 12].

Because of its various effects on cell behaviour, ES has aroused keen interest in medicine in such applications as the pacemaker, brain stimulation and the healing of ulcers [13]. Our group thus proposed and demonstrated the hypothesis that direct current modulates wound healing by promoting fibroblast-to-myofibroblast transdifferentiation [7].

Wound healing evolution includes four overlapping phases: haemostasis and coagulation, with the formation of a provisional wound matrix; inflammation, with neutrophil and monocyte recruitment; proliferation and repair, with the formation of granulation tissue and the restoration of the vascular network as well as reepithelialization; and a remodelling phase [14, 15]. During wound healing, fibroblasts proliferate and migrate into a wound fibrin clot and produce new extracellular matrix (ECM; collagens, proteoglycans and elastin) contributing to the formation of granulation tissue [16, 17]. Following migration into the wound site, fibroblasts gradually change to profibrotic phenotypes and switch their major function to protein synthesis and wound contraction [18].

It is well known that fibroblasts secrete many useful growth factors and cytokines, including platelet-derived growth factor (PDGF), acidic fibroblast growth factor (aFGF or FGF-1) and basic fibroblast growth factor (bFGF or FGF-2) [19]. During the remodelling phase, certain fibroblasts transdifferentiate to a contractile phenotype, viz. myofibroblasts, expressing a high level of contractile fibre α-smooth muscle actin (α-SMA) proteins. Myofibroblast differentiation was reported to involve TGFβ through the Smad signalling pathway [20]. This may be modulated by ES delivered through conductive polymers. As pertains to the present study, inherently conductive polymers (ICPs) that embrace conductivity were chosen to deliver the ES because of their progress in several fields in a number of promising and attractive studies [21, 22].

Substrate conductivity can be achieved through polypyrrole (PPy), which is a conductive polymer, not only easy to synthesize but also easy to incorporate anionic biomolecules (dopants) to enhance biocompatibility and target cellular function [23]. Several recent studies have demonstrated that PPy doped with bioactive molecules can influence cell survival and differentiation [23, 24]. Our group also demonstrated that PPy-coated polyester fabrics retained sufficient long-term electrical stability/conductivity when ES was used, thus providing an opportunity to directly apply a conductive textile matrix as a scaffold for ES delivery [25]. In this study, we sought to investigate the effects of pulsed electrical stimulation (PES) on dermal fibroblast migration following monolayer scratch, FGF2 secretion, collagen matrix contraction, α-SMA expression and the Smad signalling pathway. We provided evidence that PES mediated fibroblast migration and increased FGF2 secretion. The PES-exposed fibroblasts contracted collagen matrix and expressed a high level of α-SMA. The effect of PES on dermal fibroblasts involved the Smad2/3 signalling pathway. This study thus provides greater insight into the mechanism of ES in

modulating wound healing, and the electrically activated cells may prove a clinically relevant cell therapeutic strategy.

3.3 Materials and methods

3.3.1 Materials

A two-step method was used to coat PPy onto the surface of polyethylene terephthalate (PET) fabrics, as we previously reported [26]. The anti-smooth muscle α-actin, HRP-anti-rabbit and HRP-anti-mouse were from Sigma-Aldrich (St. Louis, MO, USA). A Smad2/3 sampler kit was bought from Cell Signalling Technology (Danvers, MA, USA; cat. no. 12747). An FGF2 ELISA kit was purchased from R&D Systems (Minneapolis, MN, USA) and rat tail collagen I was obtained from Gibco (Life Technologies, Burlington, ON, Canada), while the primers were obtained from Invitrogen (Burlington, ON, Canada).

3.3.2 PES programme design

Endogenous EF in human wounds has been reported in the range 40–200 mV/mm [27]. Accordingly, four PES protocols were designed, using a combination of two pulse intensities (50 and 100 mV/mm) and two trains of rectangular pulses (pulse width 300 s within a period of 600 s; and pulse width 10 s within a period of 1200 s).

3.3.3 Primary human dermal fibroblast extraction and culture

Human skin biopsies were collected from patients following their informed consent and with the approval of the Université Laval–CHUQ Ethics Committee. The biopsies were treated with thermolysin (500 μg/ml) to separate the epidermis from the dermis. To isolate the fibroblasts, the dermal tissue was placed in a collagenase P solution (0.125 U/ml) for 18 h at 4°C. The isolated cells (2×10^6) were then seeded in 75 cm3 flasks (Falcon, BectonDickinson, Cockeysville, MD, USA) and grown in Dulbecco's modified Eagle's medium (DMEM; Invitrogen) supplemented with 10% fetal bovine serum (FBS) in a humidified incubator at 37°C with 5% CO_2. The medium was changed three times a week. The fibroblasts were used when the cultures reached 90% confluence.

3.3.4 Delivery of PES to the human dermal fibroblasts

ES was delivered by directly connecting the conductive fabric outside of the culture medium to an external power source [28]. The PPy–PET fabrics were assembled into a homemade multiwell electrical culture plate (Fig. 22) under sterile conditions, and then used for cell culture and exposure to PES. Briefly, primary dermal human fibroblasts (6×10^5) were plated in each chamber in 10% FBS-supplemented culture medium, and then incubated overnight in a 5% CO_2 humid atmosphere at 37°C to promote cell adhesion. The following day, PES was introduced by means of a waveform generator, according to predetermined protocols, for 24 h. It is important to mention that, during the 24 h of exposure to ES, there was no contact between the metal connector and the medium at the circuit–fabric interface, as the current only went through the PPy layer, with no medium bubbles or colour changes, as occurs in a redox reaction (Fig. 22). Following each PES regime, the culture medium was refreshed and the cells were maintained in culture for an additional 24 h prior to their detachment and use for various analyses.

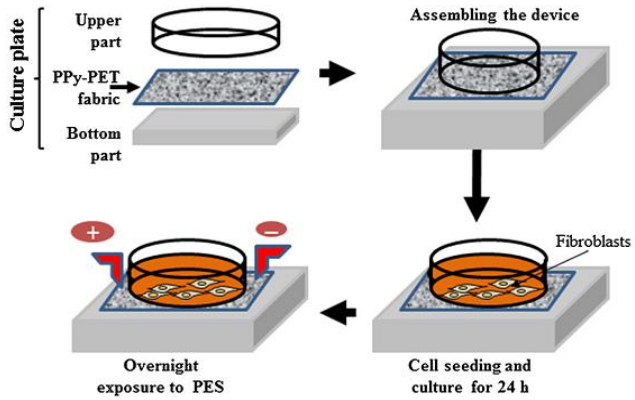

Fig. 22 Schematic protocol for the electrical stimulation experiment. The PPy–PET membranes were cut into rectangular pieces and assembled tightly into a home-made electrical cell culture plate to prevent the culture medium from leaking. Fibroblasts were seeded into the culture, adhering well to the PPy–PET conductive membrane. The edges of the PPy–PET membrane were linked to a DC power source through two metal plates. It is important to note that the metal plates were not in contact with the culture medium, preventing any redox reaction and ionic current formation

3.3.5 Scratch wound assay

Migration was measured with a wound-healing migration assay. Briefly, the PES-exposed fibroblasts were plated in six-well plates and grown to confluence. A mechanical scratch was made with a 200 µl sterile pipette tip, crossing the centre of the confluent cell monolayer and resulting in a denuded area. The scratched monolayer was extensively rinsed with PBS to remove non-adherent cells and debris, after which fresh medium was added and the culture was maintained at 37°C in a 5% CO_2 humid atmosphere. The denuded area was followed and imaged with a phasecontrast microscope at 0, 6, 12 and 24 h post-wounding. The images were used to measure the denuded area, using the NIH ImageJ public domain image-processing program. The experiment was repeated six times independently for statistical analyses. Data were presented as percentages of the healed wound area at 6, 12 and 24 h over the area at time 0 (initial wound).

3.3.6 ELISA assay of the FGFs

We sought to demonstrate that ES promoted fibroblast growth and wound healing through wound-healing mediators, notably FGFs and MMPs. We therefore measured FGF1 and FGF2 levels in the cell culture supernatant. To do so, supernatants were freshly collected, filtered through 0.22 µm filters and used to measure growth factor level. ELISA plates (R&D Systems) were read at 450 nm and analysed by means of a Microplate Reader Model 680 (Bio-Rad, Philadelphia, PA, USA). According to the manufacturer, the minimum detectable concentrations are < 14 pg/ml for FGF1 and 0.07 pg/ml for FGF2. Each experiment was repeated four times (n = 4) to calculate mean ± SD.

3.3.7 Quantitative PCR and α-SMA gene expression assay

PES-exposed and control dermal fibroblasts were used to extract total RNA by means of the Illustra RNAspin Mini kit (GE Healthcare UK Ltd, Buckingham, UK). The quality, concentration and purity of the extracted RNA were then determined, using an Experian system with an RNA StdSens analysis kit, according to the manufacturer's instructions (Bio-Rad, Hercules, CA, USA). RNA was reversely transcribed to complementary DNA (cDNA), using a cDNA synthesis kit (Bio-Rad). The cDNA was then used to investigate the mRNA transcripts by means of quantitative PCR (qPCR), using the CFX96 Bio-Rad

real-time PCR detection system. The reaction was performed using a PCR supermix from Bio-Rad (iQ SYBR Green supermix). Specific primers were then added to the reaction mix at a final concentration of 250 nM; 5 µl cDNA were added to a 20 µl PCR mixture containing 12.5 µl iQ SYBR Green supermix (Bio-Rad), 0.5 µl specific primers (α-SMA, GAPDH; Invitrogen Life Technologies) and 7 µl nuclease-free water (MP Biomedicals, Solon, OH, USA). The reaction was performed in a Bio-Rad CFX96, with the cycling conditions as follows: after an initial hold for 2 min at 50°C and 10 min at 95°C, the samples were cycled 40 times at 95°C for 15 s, then at 60°C for 60 s. The primer sequences used were as follows: for α-SMA, forward 5'-AAAGACAGCTACGTGGGTGACGAA-3',reverse 5'-TTCCATGTCGTCCCAGTTGGTGAT-3'; for GAPDH, forward 5'-ATGCAACGGATTTGGTCGTAT-3', reverse 5'-CTGAGGGCTGAGATGCCG-3'. GAPDH produced uniform expression levels, varying by < 0.5 cycle of threshold (CTs) between the sample conditions, and was therefore used as a reference gene for this study. The results were analysed using the $2^{-\Delta\Delta CT}$ relative expression method.

3.3.8 Collagen contraction assay

PES-exposed and control dermal fibroblasts (3×10^4 cells) were mixed with a 3 mg/ml rat tail type I collagen solution (cat. no. A 10483-01; Gibco-Invitrogen) and then poured into 35 mm diameter tissue-culture plates. Following collagen gel polymerization, the edges of the gel sheets were detached from the wall of each well; then 2 ml fresh culture medium was added to each well, followed by incubation in a 5% CO_2 humid atmosphere at 37°C. Follow-up was performed at 6, 12, 24 and 48 h to scan the size of the collagen gel. These scans were then used to measure the area of the collagen gels at each time point, using an NIH public domain image-processing program. Each experiment was performed in triplicate, with the data presented as the percentage of the gel area at each time point relative to that at time 0.

3.3.9 Immunohistochemical staining for α-SMA

For the PES-exposed and control fibroblast monolayer cultures, the cells were detached from the conductive fabrics and subsequently subcultured onto tissue-culture glass slides for 48 h, prior to being fixed with 4% paraformaldehyde for 60 min for immunohistochemical staining. For the fibroblasts in collagen gel, after 48h of culture the

gels were fixed in 4% paraformaldehyde for 60min, dehydrated with ascending grades of alcohol and then embedded in paraffin; 5 μm-thick sections were cut at cross-section and used for immunohistochemical staining. To stain, the cell monolayers on the glass slides and the tissue in the paraffin slides were first permeabilized with 100% methanol at 20°C for 10min, incubated in 2:3 acetone:alcohol at 20°C for 10min, then treated with peroxidase blocking solution for 15min and finally incubated for an additional 30min in 10% bovine serum albumin (BSA). After two washes with PBS, anti-α-SMA primary antibody (Sigma-Aldrich) at 1:150 dilution was overlaid on the specimens for 60min at 37°C. The specimens were then washed twice with PBS and subsequently incubated with HRP-conjugated secondary antibody (Cell Signalling Technology) for 45 min at room temperature. Following two washes with PBS, 3,3-diaminobenzidine-(DAB)–HRP substrate solution was added for 5 min to the specimens, which were then washed with distilled water. Mayer's haematoxylin (Dako Canada Inc., Burlington, ON, CA) was then applied for 1 min to label the nuclei. Mounting was performed using mounting solution (Fisher Scientific, Ottawa, ON, CA). The stained samples were observed under a microscope and photographed to identify the α-SMA-positive cells.

3.3.10 Western blotting for the Smad signalling pathway

To detect the Smad signalling pathway, cells were cultured for an additional 30 min following the stimulation regimes. The cells were first detached from the conductive fabrics. Cell lysates were then prepared, using lysis buffer [25 mM Tris–HCl, pH 8.0, 150 mM NaCl, 1 mM EDTA, 10% glycerol, 0.1% SDS, 0.05% sodium deoxycholate, 1% Triton X-100 and anti-protease (Sigma-Aldrich, cat. no. P2714) supplemented with anti-phosphatase cocktail III (Sigma-Aldrich, cat. no. P0044)]. Extracted protein concentrations were quantified by means of the Bradford assay. Equal amounts of total protein (20–40 μg) in reducing sample buffer (61.5 mM Tris, 100 mM DTT, 2% SDS, 10% glycerol) were boiled for 5 min and migrated using 4% stacking gel, followed by 10% acrylamide SDS–PAGE. The proteins were then transferred to PVDF membranes, using a refrigerated Tris–glycine transfer buffer (25 mM Tris, 192 mM glycine, 100 μM Na3VO4, 20% methanol) for 1 h at 100 V. The blots were then incubated overnight with primary antibody (P-Smad2 at 1:1000; Smad2 at 1:1000; P-Smad3 at 1:1000; Smad3 at 1:200; and β-actin at 1:5000). The membranes were then washed and incubated for 1 h with appropriate peroxydase-conjugated secondary antibodies. Detection was performed using the VersaDoc 5000MP Imaging System (Bio-Rad) and photographs were taken with Quantity One VersaDoc (Bio-Rad).

3.3.11 Visualization by immunofluorescence of the Smad2/Smad3 dimer translocation in the cytosol and the nucleus

Fibroblasts were collected from the conductive PPy–PET fabrics, washed twice, then seeded on glass slides and allowed to reach half-confluence. The cells were then fixed and stained with anti-Smad2/Smad3 primary antibody (1/200; Cell Signalling Technology) for 60 min, after which they were washed twice, followed by incubation with the FITClabelled secondary antibody for 60 min in the dark. Cell nuclei were then counterstained with Hoechst (1mg/ml, 1:2000 dilution; Invitrogen, Carlsbad, CA, USA) for 10 min. The slides were subsequently mounted with PBS–glycerol–gelatin and visualized under a Zeiss Apotome® microscope with a ×63/1.4 NA lens and AxioVision 4.8.2 scanning software (Carl Zeiss, Gottingen, Germany).

3.3.12 Statistical analysis

Data were presented as mean ± standard deviation (SD) of at least three separate experiments. Statistical comparison among the groups was performed using one-way ANOVA and the statistical difference between two groups was determined using Student's t-test. Differences were considered significant at $p < 0.05$.

3.4 Results

3.4.1 PES-enhanced cell migration/wound healing

Fig. 23 shows PES-modulated fibroblast migration, as ascertained by the reduced wound area in the PES exposed compared to the non-exposed scratched monolayer cultures. While a statistically significant difference was obtained for the short-time PES regime (10 s), a greater effect was observed with the long-time PES regime (300s). Fibroblasts exposed to 300 s of stimulation demonstrated greater cell migration in both potential intensities (50 and 100mV/mm). These effects were statistically significant ($p < 0.05$), particularly at later culture periods (12 and 24 h). Because fibroblast migration suggests cell activation with possible fibroblast-to-myofibroblast phenotype shifting, non-exposed and PES-exposed fibroblasts were seeded onto culture glass slides, then stained with anti-α-SMA antibody. The data in Fig. 24 indicate the presence of a high number of α-SMA-

positive cells in the PES-exposed cells compared to the non-exposed cells. Interestingly, at 300 s exposure to PES, the level of α-SMA-positive cells was significantly ($p < 0.05$) higher than in the 10 s exposure. This supports the cell migration results shown in Fig. 23, suggesting that PES modulated fibroblast growth/migration and stimulated the fibroblasts to express α-SMA.

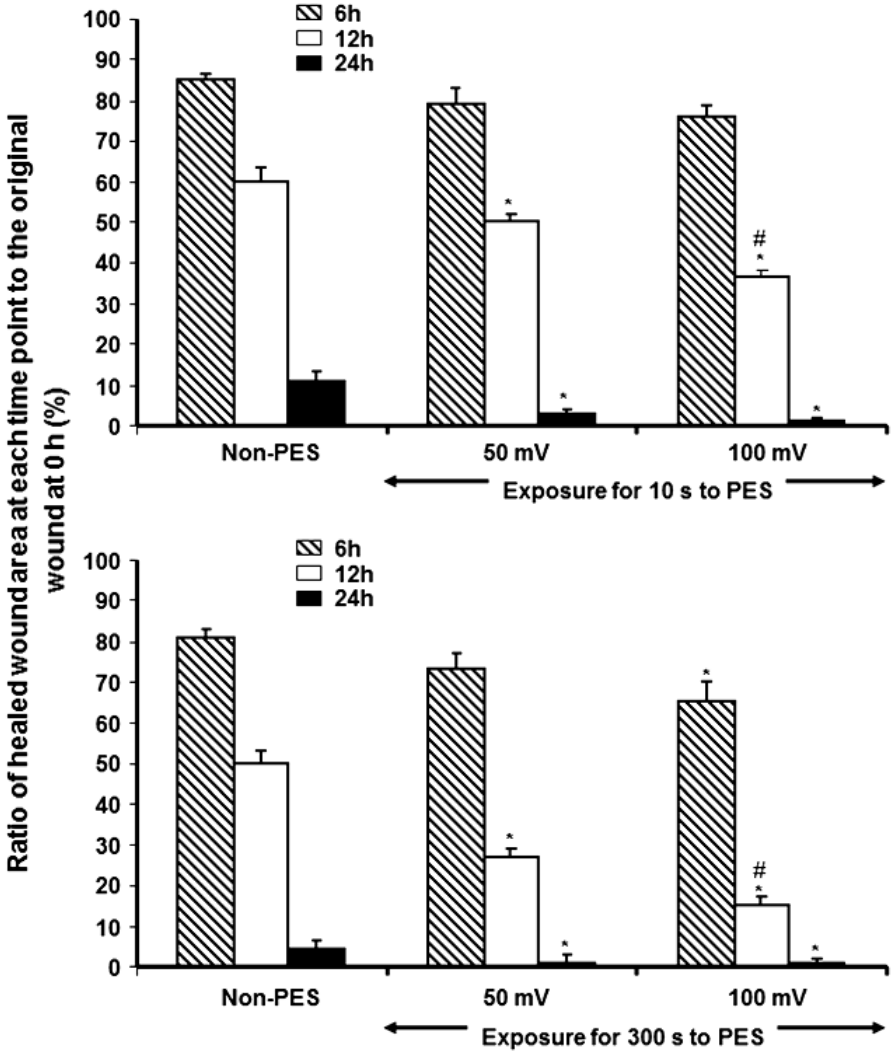

Fig. 23 PES increased the wound healing rate in primary human dermal fibroblast monolayer. Cells were cultured on PPy–PET conductive fabric for 24 h and then exposed to PES for 24 h, followed by an additional 24 h of culture without ES. The cells were detached from each membrane, seeded in Petri dishes and cultured until confluence. Scratches were then made on each monolayer and the medium was refreshed, with the cultures maintained for various time periods prior to observation and determination of wound recovery. Percentage changes in wound area over time are presented as a ratio to the initial wound size (time zero after wound); values are presented as mean ± SD (n = 6). The PES-exposed and non-exposed cultures were compared, with the difference considered statistically significant at $p < 0.05$.

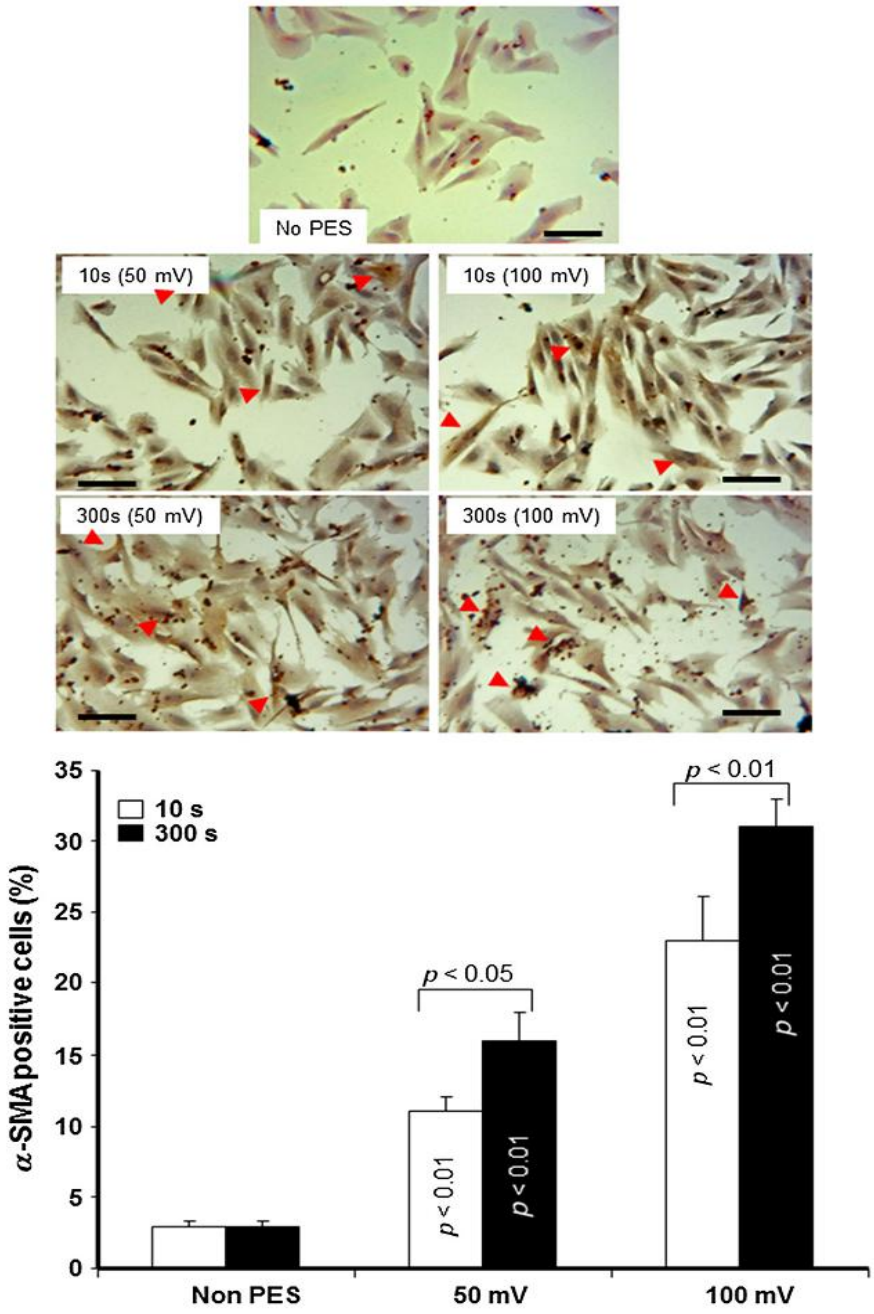

Fig. 24 Presence of α-SMA-positive fibroblasts in the PES-exposed monolayer. Following exposure to different PES regimes, fibroblasts were detached and cultured on glass slides for 48–72 h. They were then immunostained with α-SMA-specific antibody. Representative phase-contrast photomicrographs are shown; scale bars = 10 μm; n = 4. The α-SMA positive cells (arrows poinited) in each condition were counted and presented as a percentage of total cells counted in different photos. Statistical significances were obtained by comparing the non-PES and PES data, also by comparing the 10 s and 300 s exposures of PES; the differences were considered statistically significant at $p < 0.05$.

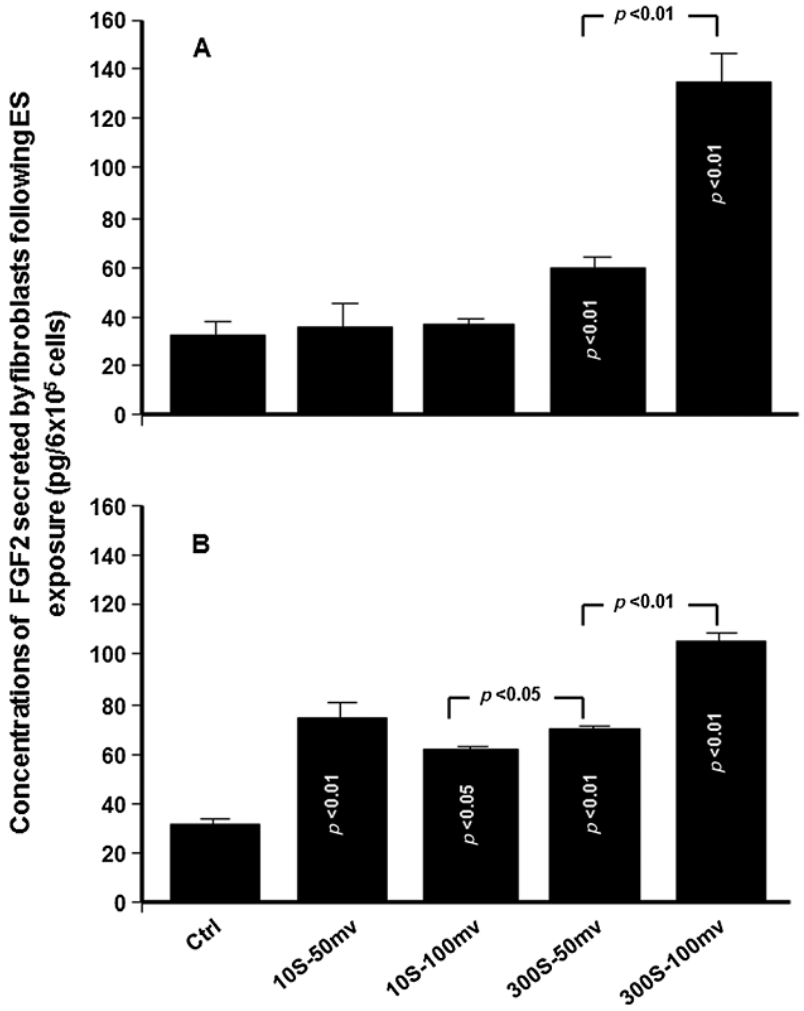

Fig. 25 PES promoted FGF2 secretion by normal human dermal fibroblasts. Following exposure to PES, culture medium was collected immediately (A) and 24 h post-ES (B). The collected media were used to measure the FGF-2 concentrations by sandwich enzyme-linked immunosorbent assays; values are given as mean ± SD (n = 4). The ES-exposed and non-exposed cultures were compared, with the difference considered statistically significant at $p < 0.05$.

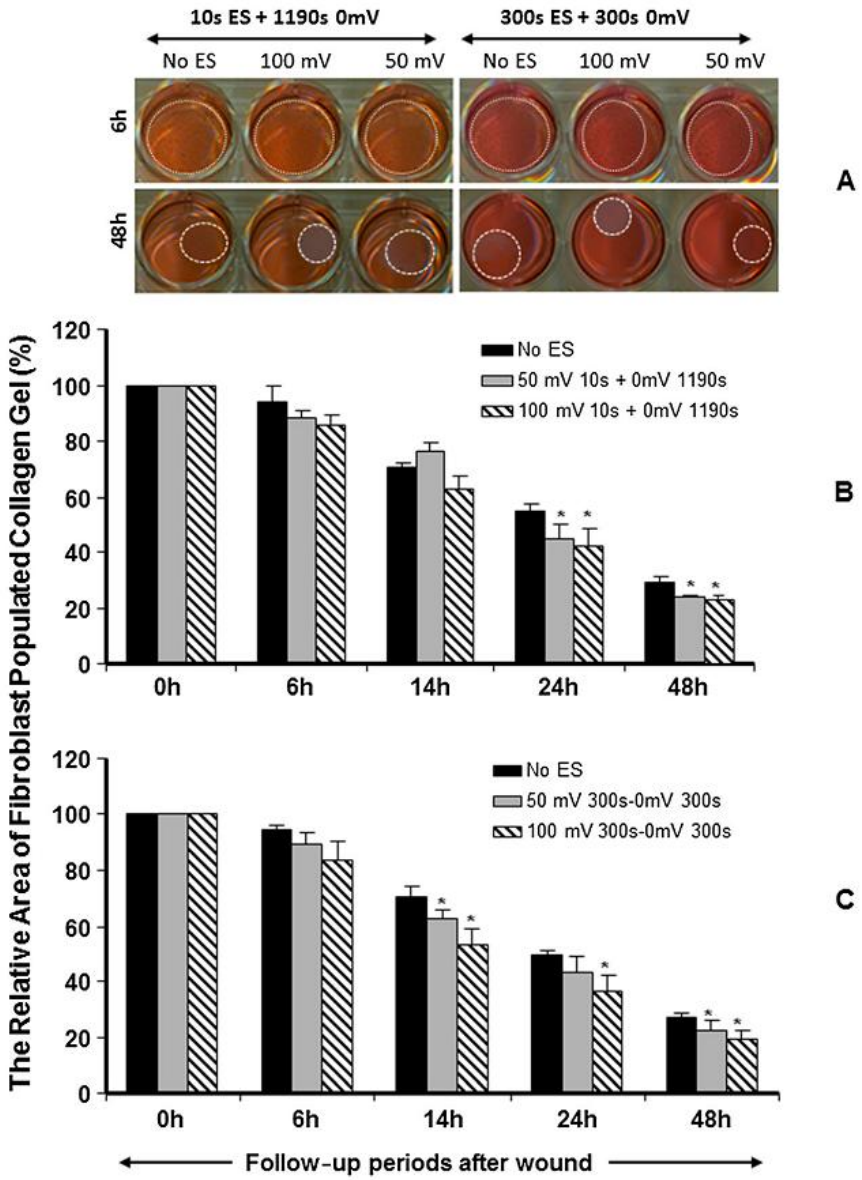

Fig. 26 PES promoted fibroblast activity to contract collagen gel. Following exposure to PES, the fibroblasts were detached, seeded in collagen gel and cultured. The diameter of each collagen gel was measured at different time points. Representative photographs show the capacity of the PES-exposed fibroblasts to contract the gel. Collagen gel size was measured and plotted. Values are given as mean ± SD (n = 5). The ES-exposed and non-exposed cultures were compared, with the difference considered statistically significant at $p < 0.05$.

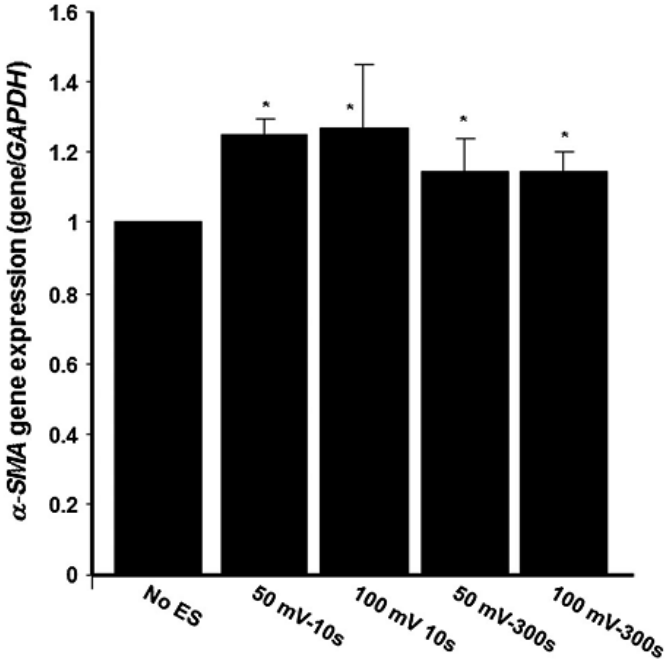

Fig. 27 Dermal fibroblasts expressed high levels of α-SMA mRNA following exposure to PES. Fibroblasts were exposed to PES for 24 h prior to RNA extraction. These were then used to analyse α-SMA mRNA expression by means of qRT–PCR (n = 4).

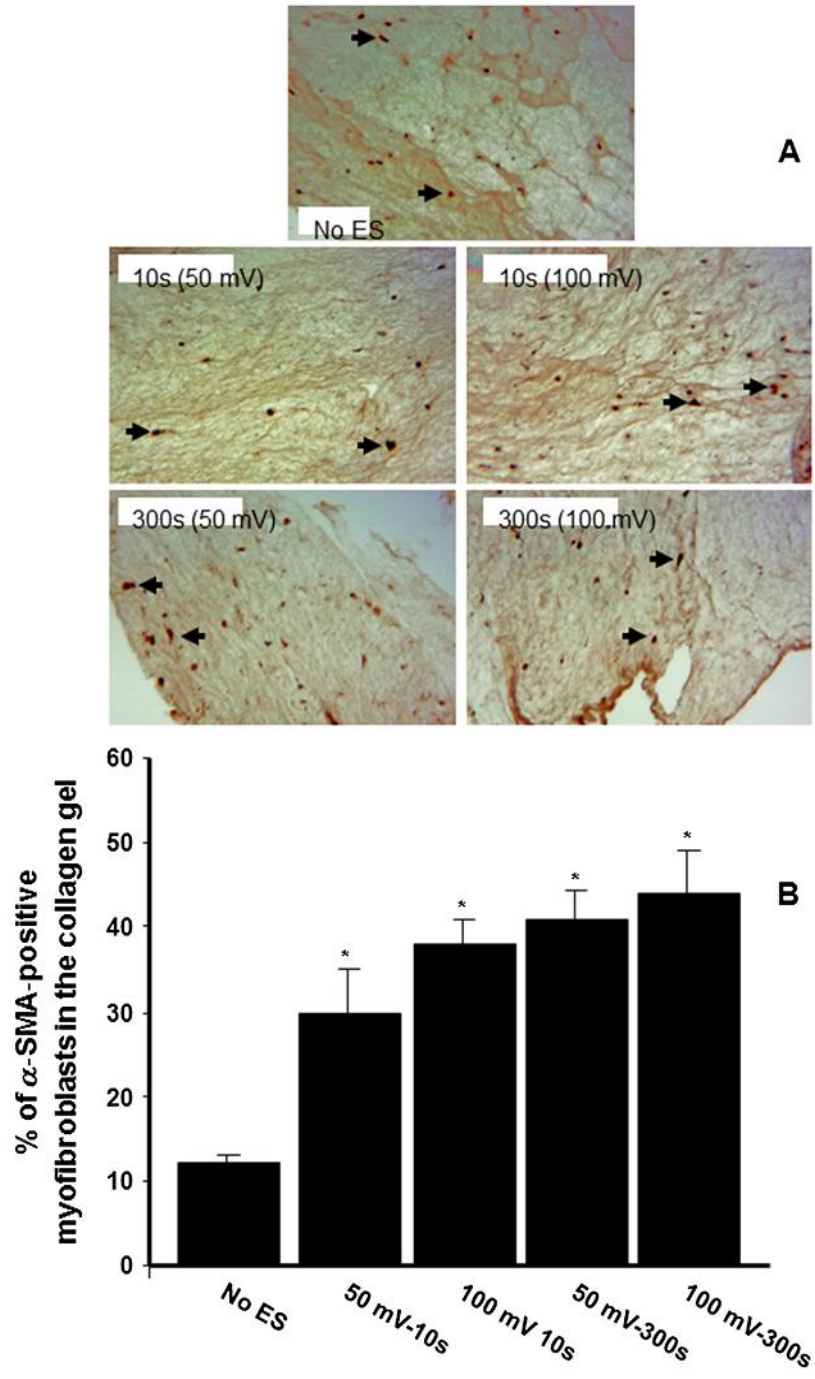

Fig. 28 Immunostaining of α-SMA-positive fibroblasts in the contracted collagen gels. Following exposures to PES, the fibroblasts were detached and used to engineer dermal equivalents, using collagen gel matrix. The gels were processed after 48 h of culture to identify α-SMA-positive cells. (A) α-SMA-positive cells (arrows); (B) percentage of α-SMA-positive cells in total number of cells; data are shown as mean ± SD (n = 5). The ES-exposed and non-exposed cultures were compared, with the difference considered statistically significant at $p < 0.05$

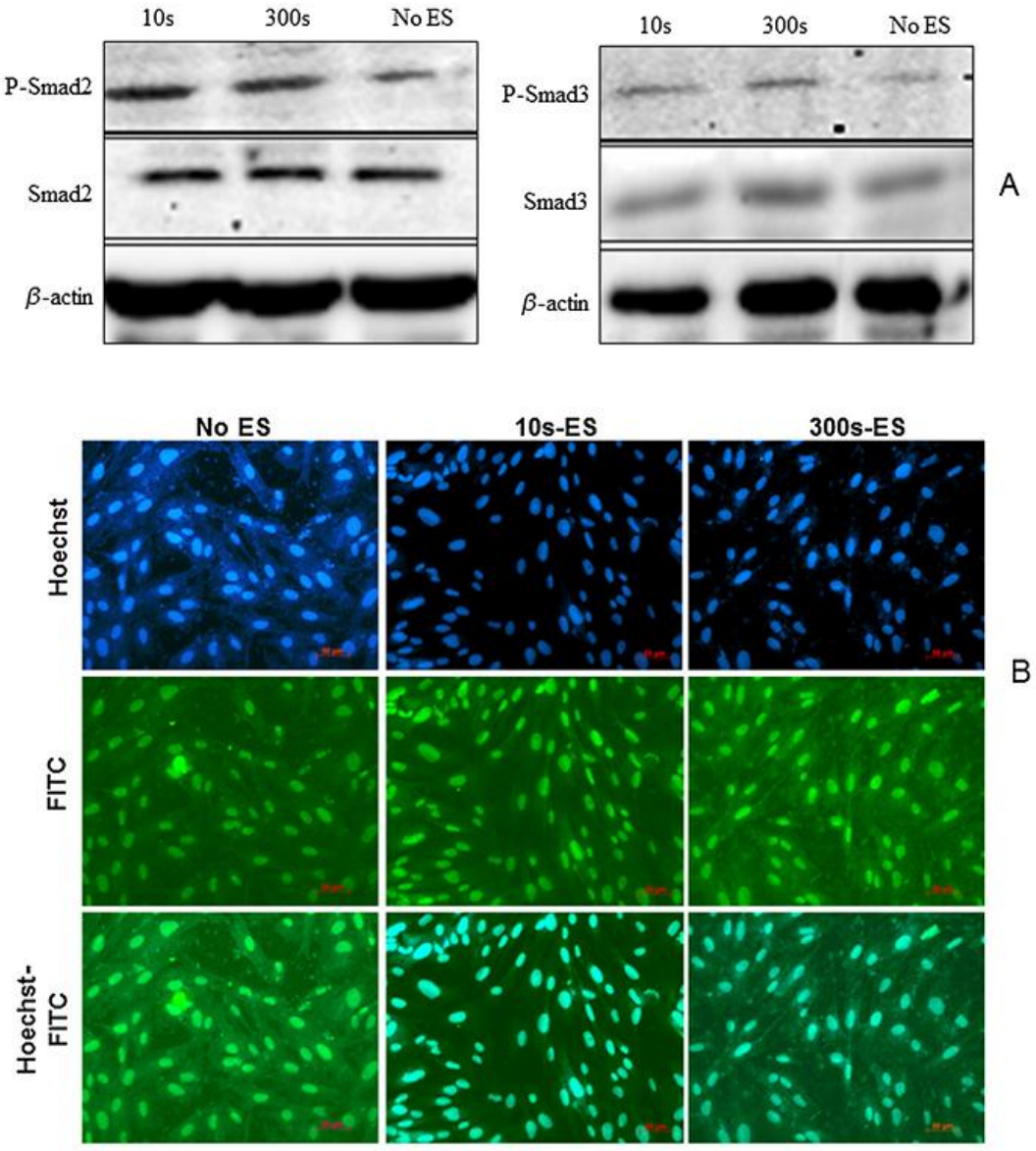

Fig. 29 PES promoted Smad2 and Smad3 phosphorylation and Smad2/3 translocation from the cytoplasm to the nucleus of dermal fibroblasts. Following exposure to PES, the cells were either used to extract total proteins for western blotting or seeded onto glass slides for immunofluorescence analyses. (A) Western blot results. (B) Cells stained with primary anti-Smad2/3 monoclonal antibody and FITC secondary antibody; the cell nucleus was revealed by Hoechst (n = 4). The stained slides were visualized under a Zeiss Apotome® microscope with a ×63/1.4 NA lens and AxioVision 4.8.2 scanning software

3.4.2 PES increased FGF2 secretion

Because FGF2 is known to play a role in fibroblast migration and wound healing, the increased cell migration following PES may take place through FGF2. Measuring FGF2

in the culture supernatant demonstrated a higher level of FGF2 in the PES groups than in the controls. Immediately following long-time (300 s) PES, the FGF2 concentration increased from approximately 40 pg in the control to approximately 60 pg and 140 pg in the PES-stimulated groups (Fig. 25A). Of great interest was the elevated amount of FGF2 still secreted by the fibroblasts 24 h after PES (Fig. 25B). All four PES regimes promoted FGF2 secretion by the dermal fibroblasts. The most important effect, however, was obtained with the strongest regime, i.e. 300 s and 100 mV/mm (Fig. 25B). Overall, these data show that, following PES, the secretion of FGF2 in human dermal fibroblasts was upregulated, and that the PES regime of 300 s + 100 mV/mm was more effective in promoting this secretion. FGF1 measurement showed no statistically significant difference (data not shown).

3.4.3 PES promoted collagen gel contraction by the stimulated fibroblasts

In order to measure the contribution of PES-exposed fibroblasts to wound closure, we imitated wound healing by designing a collagen gel 3D matrix containing PES-exposed fibroblasts, to evaluate gel contraction. Fig. 26 shows that the area of collagen gel was reduced in the PES groups compared to the non-exposed control specimens ($p < 0.05$). The short-time PES regime, viz. 10s at 100 mV/mm, revealed statistically significant gel contraction at later time points (Fig. 26B). However, the longtime PES regime was more effective in contracting the collagen matrix. This was specifically statistically significant ($p < 0.05$) at the 14, 24 and 48h follow-ups (Fig. 26C). In short, PES did indeed lead to better contraction ability of the fibroblasts, suggesting its possible involvement in assisting wound repair.

3.4.4 PES increased α-SMA gene expression and protein production

As a higher number of α-SMA-positive cells was identified in the PES groups, and because these cells were more contractile, we hypothesized that this contraction was due to the expression of α-SMA fibres by the PES-exposed fibroblasts. To confirm this, we examined α-SMA gene expression in these fibroblasts. As shown in Fig. 27, the exposure of primary human dermal fibroblasts to PES led to an increase in α-SMA mRNA expression. Both short- and long-time exposure at either 50 mV/mm or 100 mV/mm increased the gene expression of α-SMA in the fibroblasts ($p < 0.05$). This gene modulation supports the α-SMA staining and gel contraction results. Fig. 28A shows the

presence (arrows) of α-SMA-positive cells in the gels containing the PES-exposed fibroblasts compared to the non-exposed ones. We recorded a higher number of α-SMA-positive cells in the PES groups than in the controls (Fig. 28B). Overall, these data demonstrate that PES increased α-SMA gene expression and protein production.

3.4.5 PES promoted fibroblast-to-myofibroblast differentiation through the Smad signalling pathway

In order to analyse the signalling pathway involved in the differentiation of fibroblasts into myofibroblasts expressing α-SMA following exposure to PES, we performed a western blot analysis related to the Smad pathway. Fig. 29A shows that both PES regimes increased total Smad2 and Smad3, compared to the control. This was paralleled by an increase of phosphorylated Smad2 and Smad3 (P-Smad2, P-Smad3). Notably, long-time exposure (300s) induced more total and phosphorylated Smads than did the short-time exposure (10s). The signalling pathway was confirmed by the translocation of the Smad2/3 dimer in the nucleus. Fig. 29B shows the presence of the Smad2/3 dimer (green staining, FITC) in the cytoplasm of both the PES-exposed and nonexposed fibroblasts. However, an overlap of the greenstained Smad2/3 and the blue-stained nucleus (Hoechst) revealed a turquoise colour only in the PES-exposed fibroblasts. This confirms the implication of the Smad signalling pathway in the fibroblast-to-myofibroblast transdifferentiation caused by exposure to PES.

3.5 Discussions

To better understand how ES affects fibroblast behaviours and their implication in wound healing, this experiment was designed to study the signalling pathway and the efficacy of a new conductive substrate. Because all cellular activities studied, such as migration, transdifferentiation and wound closure, are closely linked to wound healing [18], this work not only reveals the molecular mechanisms in ES-activated fibroblasts but also demonstrates the potential of this approach as a clinically relevant cell therapy.

Studies on the signalling pathways related to EF or ES remain very limited and fundamental at best, with voltage-gated calcium channels and downstream activities being the most investigated [29-31], if not the only, mechanisms reported, and despite some studies reporting that ES may activate specific genes, with or without protein production

[32]. The mechanisms involved are, however, rarely mentioned. The present study demonstrates for the first time that PES at 50 and 100 mV/mm intensities likely induces fibroblast transdifferentiation through a Smad signalling pathway involving P-Smad2 and P-Smad3. The Smad signalling pathway is known as a general TGFβ-induced differentiation pathway [33]. Its activation leads to stress fibre expression by fibroblasts embracing a higher level of contractibility [34], and thus may help wound closure, as partly confirmed by the gel contraction experiment. Further studies on TGFβ will undoubtedly provide greater insight.

Textiles are widely used in medical applications such as vascular prostheses, healing patches and wound dressings and bone non-union fixations. Conductivity adds value to medical textiles and can potentially expand their applications where ES is required or can be applied [35]. While conductive polymer membranes are capable of mediating ES to cultured cells [36], a fibrous structure does provide additional advantages [34]. With respect to solid or porous polylactide–PPy membrane [37], PPy–PET fabric displays high flexibility, can be easily moulded into the required size and form, and can also be sutured. To tackle the electrical instability of a thin-layer PPy in an aqueous environment, as in the case of PPy–PET fabrics in culture medium under constant ES, PES was developed [26]. This work proves for the first time that, under appropriate conditions, a thin layer of PPy is able to sustain sufficiently strong ES to alter fibroblast behaviour. This research thus expands the conductive scaffold approach from composite membranes to surface-coated textiles. Considering the wide availability of medical textiles in terms of materials and textile structures, herein lies the proof of principle, opening the door to more extensive and novel uses for conductive biomaterials.

Cell migration is a key factor in wound healing. ES or EF was shown to accelerate cell migration and provide direction [36]. However, this effect is mostly, if not all, the result of electrotaxis, or is due to the indirect effect of protein deposition in the EF [38]. The higher cell migration speed in the present study is totally different, because the cells were replated and the migration occurred in the absence of ES. It is well known that cell migration involves cytoskeleton molecules such as actin and integrin. While the cell migration mechanism was not the focus of this study, it is likely that high amounts of α-SMA in the PES-exposed fibroblasts contributed to the migration speed. Evidently, this remains a hypothesis and requires further *in vitro* and *in vivo* investigation.

ES affects cell behaviour at different levels, with various outcomes. Both constant ES using direct current and PES offer some advantages [39, 40]. For example, direct current ES accelerated osteoblast proliferation and calcification [40], while PES promoted cell growth and differentiation [38]. Adding to these findings, this study shows that PES may indeed serve as a tool to stimulate fibroblasts into synthesizing more active proteins, such as FGF2, and to provide greater α-SMA expression, all of which are key in the wound healing process. As a cell growth modulator, FGF2 also plays a role in inducing angiogenesis in granulation tissue, to bring nutrients to the wound site for the repairing cells [41]. In addition, stress fibres, such as α-SMA, contribute to pulling the wound edges toward the middle, resulting in better re-epithelialization [42]. This needs to be supported by future in vivo studies.

3.6 Conclusion

This study reveals that PES-induced fibroblast-to-myofibroblast differentiation is associated with the Smad2/3 signalling pathway. It also demonstrates that, through determined PES regimes, PPy-coated textiles effectively mediated ES to modulate such skin fibroblast functions as the synthesis of growth factors and stress fibres, such as α-SMA, which are all-important to wound healing. This study thus provides greater insight into PES-wound healing mechanisms. However, further study on how cellular activities are electrically tuned, to reveal the molecular pathways and to design clinically implantable electrical devices enabling electrical stimulation in vivo, are mandatory. The purpose is to advance this approach to preclinical and clinical levels to benefit public health.

3.7 Conflict of interest

The authors declare no conflicts of interest.

3.8 Acknowledgements

This study was supported by the Canadian Institutes of Health Research and the Centre de Recherche du CHU de Québec. Thanks go to Eric Jacques and Hyunjin Park for their technical assistance.

References

1. Song B, Zhao M, Forrester JV et al. Nerves are guided and nerve sprouting is stimulated by a naturally occurring electrical field in vivo. *J Cell Sci*. 2004;17: 4681–4690.
2. Thrivikraman G, Madras G, Basu B. Intermittent electrical stimuli for guidance of human mesenchymal stem cell lineage commitment towards neural-like cells on elctroconductive substrates. *Biomaterials*. 2014;35(24): 6219–6235.
3. Mooney E, Mackle JN, Blond DJ et al. The elelctrical stimulation of carbon nanotubes to provide a cardiomimetric cue to MSCs. *Biomaterials*. 2012;33(26): 6132–6196.
4. Bourguignon G, Bourguignon L. Electric stimulation of protein and DNA synthesis in human fibroblasts. *FASEB J.* 1987;1(5): 398–402.
5. Fukuda R, Suico MA, Koyama K et al. 2013; Mild electrical stimulation at 0.1 ms pulse width induces p53 protein phosphorylation and G2 arrest in human epithelial cells. *J Biol Chem*.2013; 288(22): 16117–16126.
6. Falanga V, Bourguignon G, Bourguignon L. Electrical stimulation increases the expression of fibroblast receptors for transforming growth factor-β. *J Invest Dermatol.* 1987;88: 488–492.
7. Rouabhia M, Park H, Meng S et al. Electrical stimulation promotes wound healing by enhancing dermal fibroblast activity and promoting myofibroblast transdifferentiation. *PLoS One.* 2013;8(8): e71660.
8. Fukata M, Nakagawa M., Kaibuchi K. Roles of Rho-family GTPases in cell polarisation and directional migration. Curr Opin Cell Biol. 2003;15: 590–597.
9. Li F, Wang H, Li L et al. Superoxide plays critical roles in electrotaxis of fibrosarcoma cells via activation of ERK and reorganization of the cytoskeleton. *Free Radic Biol Med*. 2012;52: 1888–1896.
10. Nishimura KY, Isseroff RR, Nuccitelli R. Human keratinocytes migrate to the negative pole in direct current electric fields comparable to those measured in mammalian wounds. *J Cell Sci*. 1996;109: 199–207.
11. Meng S, Rouabhia M, Zhang Z. Electrical stimulation modulates osteoblast proliferation and bone protein production through heparin-bioactivated conductive scaffolds. *Bioelectromagnetics*. 2013;34(3): 189–199.
12. Prindeze NJ, Jo DY, Paul DW et al. Regional neurovascular inflammation and apoptosis are detected after electrical contact injury. *J Burn Care Res*. 2014;35(1): 11–20.

13. Feedar JA, Kloth LC, Gentzkow GD. Chronic dermal ulcer healing enhanced with monophasic pulsed electrical stimulation. *Phys Ther*. 1991;71(9): 639–649.
14. Reinke JM, Sorg H. Wound repair and regeneration. *Eur Surg Res.* 2012;49(1): 35–43.
15. Monaco JL, Lawrence WT. Acute wound healing an overview. *Clin Plast Surg.* 2003;30: 1–12.
16. Kurkinen M, Vaheri A, Roberts PJ, Stenman S. Sequential appearance of fibronectin and collagen in experimental granulation tissue. *Lab Invest.* 1980;43: 47–51.
17. Woodley DT, O'Keefe EJ, Prunieras M. Cutaneous wound healing: a model for cell–matrix interactions. *J Am Acad Dermatol.* 1985;12: 420–433.
18. Wiegand C, White R. Microdeformation in wound healing. *Wound Repair Regen.* 2013;21(6): 793–799.
19. Barrientos S, Stojadinovic O, Golinko MS et al. Growth factors and cytokines in wound healing. *Wound Repair Regen.* 2008;16(5): 585–601.
20. Midgley AC, Rogers M, Hallett MB et al. Transforming growth factor–β1 (TGFβ1)-stimulated fibroblast to myofibroblast differentiation is mediated by hyaluronan (HA)-facilitated epidermal growth factor receptor (EGFR) and CD44 co-localization in lipid rafts. *J Biol Chem.* 2013;288(21): 14824–14838.
21. Tessier D, Dao LH, Zhang Z et al. Polymerization and surface analysis of electrically conductive polypyrrole on surface-activated polyester fabrics for biomedical applications. *J Biomater Sci Polym Ed*. 2000;11(1): 87–99.
22. Otero TF, Martinez JG. Biomimetic intracellular matrix (ICM) materials, properties and functions. Full integration of actuators and sensors. *J Mater Chem B*. 2013;1: 26–38.
23. Ateh DD, Navsaria HA, Vadgama P. Polypyrrole-based conducting polymers and interactions with biological tissues. J R Soc Interface. 2006;3: 741–752.
24. Zhang L, Stauffer WR, Jane EP et al. Enhanced differentiation of embryonic and neural stem cells to neuronal fates on laminin peptides-doped polypyrrole. *Macromol Biosci.* 2010;10(12): 1456–1464.
25. Jiang X, Tessier D, Dao LH et al. Biostability of electrically conductive polyester fabrics: an in vitro study. *J Biomed Mater Res*. 2002;62(4): 507–513.
26. Wang Y, Rouabhia M, Zhang Z. PPycoated PET fabrics and electric pulsestimulated fibroblasts. *J Mater Chem B.* 2013;1: 3789–3796.
27. Nuccitelli R. A role for endogenous electric fields in wound healing. *Curr Top Dev Biol.* 2003;58: 1–26.

28. Meng S, Rouabhia M, Zhang Z. Accelerated osteoblast mineralization on a conductive substrate by multiple electrical stimulation. *J Bone Miner Metab*. 2011;29(5): 535–544.
29. Barat E, Boisseau S, Bouyssières C et al. Subthalamic nucleus electrical stimulation modulates calcium activity of nigral astrocytes. *PLoS One*. 2012;7(7): e41793.
30. Xu J, Wang W, Clark CC et al. Signal transduction in electrically stimulated articular chondrocytes involves translocation of extracellular calcium through voltage-gated channels. *Osteoarthr Cartilage*. 2009;17(3): 397–405.
31. Brighton CT, Wang W, Seldes R et al. Signal transduction in electrically stimulated bone cells. *J Bone Joint Surg Am*. 2001;83A(10): 1514–1523.
32. Rattfält L, Lindén M, Hult P et al. Electrical characteristics of conductive yarns and textile electrodes for medical applications. *Med Biol Eng Comput.* 2007;45(12): 1251–1257.
33. Shi Y, Massagué J. Mechanisms of TGFβ signalling from cell membrane to the nucleus. *Cell.* 2003;113(6): 685–700.
34. Shirol PD, Shirol DD. Myofibroblasts in health and disease. *Int J Oral Maxillofac Pathol.* 2012:3(1):23-27.
35. Ghasemi-Mobarakeh L, Prabhakaran MP, Morshed M et al. Application of conductive polymers, scaffolds and electrical stimulation for nerve tissue engineering. *J Tissue Eng Regen Med.* 2011;5(4): e17–35.
36. Pullar CE, Isseroff RR, Nuccitelli R. Cyclic AMP-dependent protein kinase A plays a role in the directed migration of human keratinocytes in a DC electric field. *Cell Motil Cytoskel*. 2001;50(4): 207–217.
37. Zhang Z, Rouabhia M, Wang Z et al. Electrically conductive biodegradable polymer composite for nerve regeneration: electricity-stimulated neurite outgrowth and axon regeneration. *Artif Organs*. 2007;31(1): 13–22.
38. Forciniti L, Ybarra J 3rd, Zaman MH et al. Schwann cell response on polypyrrole substrates upon electrical stimulation. *Acta Bioater*. 2014;10: 2423–2433.
39. Ercan B, Webster TJ. Greater osteoblast proliferation on anodized nanotubular titanium upon electrical stimulation. *Int J Nanomed.* 2008;3(4): 477–485.
40. Wang Q, Zhong S, Ouyang J et al. Osteogenesis of electrically stimulated bone cells mediated in part by calcium ions. *Clin Orthop Relat Res*. 1998;348: 259–268.
41. Kottakis F, Polytarchou C, Foltopoulou P et al. FGF–2 regulates cell proliferation, migration, and angiogenesis through an NDY1/KDM2B–miR-101–EZH2 pathway. *Mol Cell.* 2011;43(2): 285–298.

42. Tomasek JJ, Gabbiani G, Hinz B et al. Myofibroblasts and mechano-regulation of connective tissue remodelling. *Nat Rev Mol Cell Biol*. 2002;3(5): 349–363.

CHAPTER IV

STUDY THE CELL RESPONSE TO PULSED ELECTRICAL STIMULATION: PART 2

Conductive polymer-mediated pulsed electrical stimulation benefits wound healing by activating skin fibroblasts through the TGFβ1/ERK/NF-κB axis

(Submitted)

Yongliang Wang[1, 2], Mahmoud Rouabhia[1], Ze Zhang[2]

[1]Groupe de Recherche en Écologie Buccale, Faculté de Médecine Dentaire, Université Laval, Québec, QC, Canada

[2]Axe Médecine régénératrice, Centre de Recherche du CHU de Québec, Département de Chirurgie, Faculté de Médecine, Université Laval,
QC, Canada

Keywords: Wound healing, Fibroblasts, Electrical stimulation, Signalling, ERK1/2, Conductive Polymer

4.1 Abstract

Electrical field at wound site participates in wound repair process. Dermal fibroblasts activated by conductive polymer-mediated electrical stimulation (ES) have shown myofibroblast characteristics which favor wound healing. However, the signaling pathway related to this phenotype switch remains unclear and the *in vivo* survival of the electrically activated cells has never been studied. In this work, polypyrrole (PPy) coated polyethylene terephthalate(PET) fabrics were synthesized and installed in a homemade electrical device. Human skin fibroblasts were activated by pulsed-ES mediated by a conductive substrate to show an upregulation of TGFβ1 measured as 121.2 ± 17.3 % and 135.6 ± 22.9% compared to noES, as detected by ELISA assay. Downstream ERK signaling was demonstrated by Western blot and visualization of the NF-κB nucleus translocation and was confirmed by inhibition experiments. Using qRT-PCR and immunocytochemistry, ES-fibroblasts were found to highly express α-smooth muscle actin after prolonged subculture. Subcutaneous implantation for 15 days revealed more myofibroblasts in the experimental groups, with a percentage of 65 ± 8.2% and 70 ± 9.6% %, compared to 24 ± 5.8% in the controls. These findings demonstrate for the first time the involvement of the TGFβ1/ERK/NF-κB signaling pathway in ES-cells and its relevance to fibroblast/myofibroblast transdifferentiation. Also shown for the first time is that the electrically acquired characteristics can be transferred to daughter cells. This work thus reveals new molecular mechanisms in electrically activated fibroblasts and demonstrates the potential of applying electrically activated cells to help wound healing.

4.2 Introduction

During cutaneous wound healing, dermal fibroblasts exert their functions from the proliferative phase to the remodeling phase. Most importantly, these fibroblasts deposit a large quantity of extracellular matrix (ECM) including collage I, III, and fibronectin to form the much needed extracellular matrix for cell migration and granulation tissue generation [1]. The vital transition step from fibroblast to myofibroblast, a contractile fibroblast phenotype that expresses rich alpha smooth muscle actin (α-SMA) [2, 3] contributes primarily to wound closure. Consequently, understanding the regulation of fibroblast transdifferentiation is of great scientific interest. Meanwhile, electrical field at wound site was measured [4, 5] providing internal function in skin wound repair [6, 7]. One active research field uses electrical field (EF) in wound healing as a cue to control cellular behaviors. To date, electrical stimulation (ES)-induced cell response has been found to

depend on cell type, ES mode, and type of electrical device. ES modulates epithelial cell migration [8], stem cell proliferation and differentiation [9, 10], Schwann cell regeneration [11, 12], and osteoblast mineralization [13].

Mechanistic studies on how cells react to EF have mainly focused on ion channels such as voltage-gated calcium channels. Indeed, it was reported that ES-induced secretion of nerve growth factors (NGFs) and brain-derived neurotrophic factors (BDNFs) by Schwann cells depended on calcium influx through T-type voltage-gated calcium channels (VGCCs) [12]. In addition, high-frequency ES was found to promote capillary morphogenesis of endothelial cells *in vitro* through the ERK pathway [14]. Furthermore, signaling pathways were shown to play a potential role in the ES-induced increase in paralyzed muscle mass [15]. ES was also reported to function via the LKB1-AMPK pathway [16]. Notably, ES-triggered TGFβ signaling has been identified in osteoblasts, dermal fibroblasts, monocytic cells, and skeletal muscle cells [17-19].

TGFβ has been shown to modulate cell activity including cell proliferation [20] and differentiation [21]. TGFβ mediates this differentiation through two signaling pathways: the canonical Smad pathway and the noncanonical nonSmad or MAPK/ERK pathway [22]. Following signal transduction, phosphorylase kinase targets molecules (JNK, p38MAPK, ERK1/2, etc.) and propagates the message into gene transcription through transcription factors (TFs), such as c-Jun, NF-κB, Elk1, MSK1, c-Myc, to name a few [23, 24]. These signaling cascades were shown to be initiated by various stimuli [25-27], but have not been associated with any cells exposed to electrical field. In this study, primary human dermal fibroblasts were subjected to electrical stimulation through polypyrrole (PPy)-coated polyethylene terephthalate (PET) conductive fabrics then used to analyze the TGFβ1-ERK1/2-NF-κB axis involving in fibroblast to myofibroblast transdifferentiation. We also investigated the fate of the electrically activated cells *in vivo* and whether the ES effect could be transferred to daughter cells. The answers to these questions are directly related to how likely electrically activated cells can be used in clinical applications.

4.3 Materials and methods

4.3.1 Conductive PPy-PET fabrics preparation and ES device

A two-step method was used to synthesize PPy on the surface of PET fabric to produce a conductive scaffold, as presented in our previous published work [28]. The topographic information for PPy coating was observed through scanning electron microscope (SEM). We designed an appropriate ES device in which the conductive fabrics were installed in each culture chamber to serve as cell culture scaffolds while delivering the electrical stimulation [29]. No electrodes were in contact with the culture medium during stimulation. This electrode-free setup completely rules out the potentially controversial interference of either the redox activity at the electrode/medium interface or the ionic current in the culture medium. This experimental setup was presented at Figure 30.

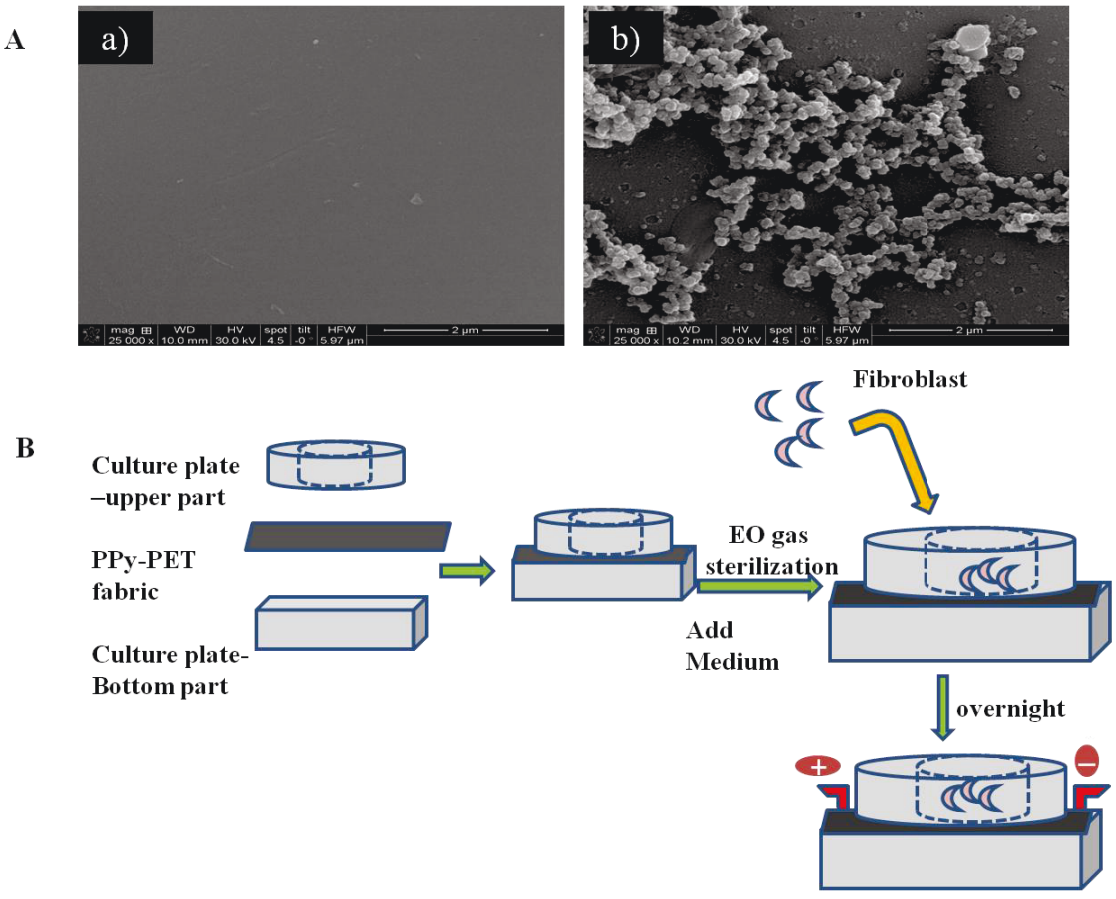

Figure 30 Experimental setup that combines substratum topography and electrical stimulation. (A) Scanning electron microscope (SEM) presents the non-coated PET (a) and PPy-coated PET fabrics (b). (B) Schematic graph shows the ES system and the electrodes directly linked to conductive membrane without touching medium. EO, ethylene oxide.

4.3.2 Cell culture and PES

Following approval by the Université Laval-CHU Ethics Committee, primary skin fibroblasts were extracted from human skin biopsies. Prior to the biopsies, the patients provided their informed consent regarding the proposed protocol. The biopsies were treated with thermolysin (500 μg ml^{-1}) to separate the epidermis from the dermis. The dermis was then incubated in the presence of collagenase to release fibroblasts from the extracellular matrix. The extracted fibroblasts were then seeded in 75-cm^2 flasks and grew in Dulbecco's modified Eagle's medium (DMEM) supplemented with 10% fetal bovine serum in a humidified incubator at 37°C with 5% CO_2. The medium was changed two to three times a week. The fibroblasts were used once the cultures reached 90% confluence. For the ES, the cells were used between passages 4 and 9. The ES device and conductive substrate were sterilized by ethylene oxide (EO) gas and pre-conditioned in DME medium overnight, followed by cell seeding (1.2×10^5 cells cm^{-2}). Twenty four hours following cell seeding, the medium was refreshed and a pulsed EF was applied at an intensity of 100 mV mm^{-1}, with a train of cycles of either a 10 s stimulation within a period of 1200 s, or a 300 s stimulation within a period of 600 s. Each pulsed ES lasted 24 h. Cells cultured in the same device without PES were used as controls.

4.3.3 Analysis of cell signalling

4.3.3.1 ELISA test for secreted TGFβ1

Immediately following PES, cell culture supernatant was collected for ELISA assay. The supernatant was first activated by 1 N of HCl and then incubated in the assay well. Following incubation with biotin-conjugate anti-human TGFβ1 antibody, streptavidin-HRP and downstream substrate were used to quantify TGFβ1 concentration. The TGFβ1 ELISA kit (OKAA0026_96W, Cedarlane, Burlington, ON, Canada) used in this experiment has a sensitivity of 15 pg ml^{-1}. The concentration of TGFβ1 in the experimental groups was normalized to the controls and presented as percentage change. The concentration of TGFβ1 in the experimental groups was normalized to the controls and presented as percentage change following the formula,

(TGFβ1 concentration at ES group - TGFβ1 concentration at noES)/ TGFβ1 concentration at noES × 100%.

Each experiment was repeated three times (n = 3).

4.3.3.2 Western blot for TGFβ1-ERK1/2 signalling detection

Thirty minutes after the PES regime, cells were harvested and lysed in 60 μl of radioimmunoprecipitation assay buffer (Sigma-Aldrich, Oakville, ON, Canada, cat. no. P2714) supplemented with anti-phosphatase cocktail III (Sigma-Aldrich, cat. no. P0044) to extract the protein. Protein concentration was quantified by means of the Bradford assay. For electrophoresis, 20 μg of protein were blotted to each lane. After transferring, the proteins on the blotting PVDF membrane were detected by antibodies including anti-TGFβ1 (1:1000, ab647, Abcam, Cambridge, MA, USA), anti-ERK1/2 (1:1000, MAB15761, R&D Systems, Minneapolis, MN, USA), anti-phosph-ERK1/2 (1:2000, AF1018, R&D Systems), and anti-β-actin (1:5000, A5441, Sigma-Aldrich). To confirm the signalling pathway, anti-TGFβ1 antibody (0.5 μg ml^{-1}, Ab647, Abcam) and phosph-ERK1/2 inhibitor PD98059 (50 μM, EMD Millipore, Billerica, MA, USA) were used to pre-treat the cells for 1 h prior to PES exposure. After PES and protein extraction, the phosph-ERK1/2, ERK1/2 and TGFβ1 were analyzed by Western blot.

4.3.3 3 Immunocytochemistry (ICC) for NF-κB translocation

The signal from the cytoplasm to the nucleus depends on nuclear factor NF-κB after electrical stimulation. Because the cellular culture scaffolds are not transparent and porous, it is not allowed to observe the NF-κB on the fabrics. Alternatively, immediately following their detachment from the conductive fabrics, the cells were reseeded on cover slides, incubated overnight in DME medium in a standard cell incubator, and fixed in 4% paraformaldehyde for 1 h the next day. Washed in PBS and permeabilized first in 100% methanol then in an acetone/alcohol (2:3) solution at -20°C, the samples were saturated in 10% BSA and incubated thereafter with anti-NF-κB (1:100, sc-109, Santa Cruz Biotechnology, Santa Cruz, CA, USA) for 1 h. Finally, the samples were incubated in an FITC-conjugated secondary antibody solution for 45 min at room temperature, after which time the cell nuclei were stained with Hoechst 33342, observed under a Zeiss Apotome microscope, and analyzed using AxioVision 4.8.2 software (Carl Zeiss, Gottingen, Germany).

4.3.3.4 Cell migration test with or without ERK inhibition

To verify whether ERK inhibition affected cell migration (further proof of TGFβ1/ERK/NF-κB pathway activation), the PES-exposed and non-exposed cells were harvested immediately after stimulation and were then reseeded in a standard six-well culture plate. When the cells reached confluence, a scratch was created in the form of a cross by means of a 200 μl pipette tip. After washing out the cell debris, fresh medium was added with or without ERK inhibitor PD98059 (50 μM). Cell migration was monitored thereafter with a phase contrast microscope and photographed at 0 and 10 h post-wound. The images were analyzed to calculate the denuded area using the NIH ImageJ public domain image processing program. The experiment was repeated four times (n = 4).

4.3.4 Quantitative PCR and gene expression assay for the descendent cells

To determine whether the cells could memorize the contractile property acquired through PES, PES-exposed and control fibroblasts were trypsinized following PES and reseeded in a six-well culture plate to proliferate. Because the cell cycle for dermal fibroblasts is normally less than two days, five days after PES, the cells were processed for total RNA extraction by means of the Illustra RNAspin Mini kit (Bio-Rad, Hercules, CA, USA). RNA was converted to complementary DNA (cDNA) with a cDNA synthesis kit (Bio-Rad), which underwent PCR using the CFX96 Bio-Rad real-time PCR detection system. A uniform expression level of GAPDH was used as reference for this study, i.e., varying by less than 0.5 cycle of threshold (CT) between samples. Results were analyzed using the $2^{-\Delta\Delta Ct}$ relative expression method. Detailed PCR protocol and primers were previously reported [29]. Concurrently, PES-exposed and control fibroblasts were also cultured on glass slides for α-SMA staining with HRP-conjugated secondary antibody and DAB detection protocol.

4.3.5 In vivo implantation and immunohistochemical(IHC) analysis

To investigate the fate and function of stimulated cells *in vivo*, stimulated and non-stimulated fibroblasts were collected immediately after PES and reseeded in a 3D porous collage matrix (Zimmer) for two days prior to subcutaneous implantation in the dorsal

region of nude mice at two areas per mouse. Each implant consisted of a round collagen sheet 5 mm in diameter and 1 mm in thickness produced by a biopsy punch. The animals were sacrificed at 15 days post-operation and the implants were harvested with the surrounding tissue. The implants were then detached from the encapsulating tissue, fixed in 4% paraformaldehyde, embedded in paraffin, and cut into 5-μm sections. Masson's trichrome stain was employed to examine graft shape and cellular distribution. To identify implanted human fibroblasts, the slides were labelled with either mouse monoclonal anti α-SMA (1:150; A2547, Sigma-Aldrich) or rabbit monoclonal anti-human HLA-ABC antibody (1:100; SAB5500118, Sigma-Aldrich). To determine the proportion of implanted human fibroblasts that also expressed α-SMA, double IHC staining was performed, namely, anti-rabbit rhodamine-conjugated secondary antibody (SAB4600398, Sigma) for the HLA-ABC and goat anti-mouse FITC-conjugated secondary antibody (A-11001, Life Technologies, Burlington, ON, Canada) for the α-SMA. The nuclei were marked by Hoechst stain. The slides were observed under an Olympus BX51 microscope and the photographs were processed with Image-Pro Express software (Opti-Ressources Inc., Québec, QC, Canada). The proportion of myofibroblasts in the implanted human cells was calculated using the following equation: (number of double stained cells/number of HLA-ABC$^+$ cells) × 100%.

4.3.6 Statistical analysis

Data were presented as mean ± standard deviation (SD) of at least three experiments. Variations between groups were analyzed by means of a *t-test*, with the difference deemed significant when *P* value was smaller than < 0.05.

4.4 Results

4.4.1 TGFβ1 expression increased in PES groups

Protein analysis by Western blot shows (Fig. 31A) dense protein bands in the ES groups compared to the control (non-ES) groups. An ELISA assay was performed to confirm this observation. Fig. 31B reveals that higher concentrations of secreted TGFβ1 were found in the ES groups. According to ELISA assay, the percent concentrations, 121.2 ± 17.3 % (10 s group) and 135.6 ± 22.9% (300 s group) were obtained relative to those of the non-ES controls which were considered 100 ± 0.0 %. Interestingly, the long stimulation

period (300 s) rendered the highest TGFβ1 concentrations, a significant difference with from those obtained with the shorter period of stimulation (10 s).

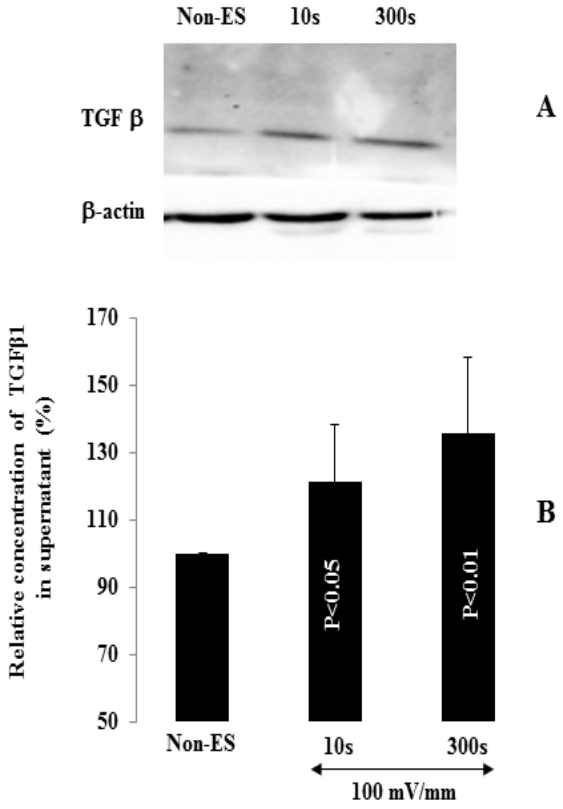

Fig. 31 **PES increased TGFβ1 expression in human dermal fibroblasts**. A: Western blot was performed, showing higher TGFβ1 expression in the PES groups. B: Following exposure to PES, the collected supernatant was used to measure TGFβ1 concentration by sandwich enzyme-linked immunosorbent assays; values are given as mean ± SD in percentage after normalized to non-ES value (n=4).

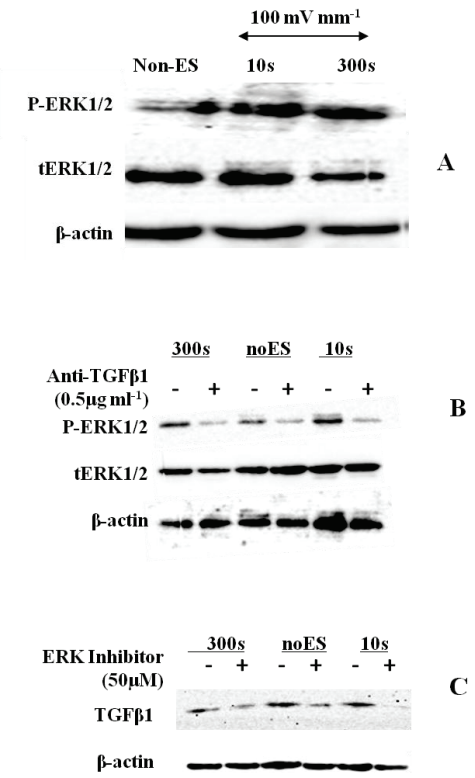

Fig. 32 **PES promoted ERK activation**. Proteins were extracted 30 min after ceasing PES exposure and used to blot TGFβ1, phospho-ERK1/2, total ERK, and β-actin. A: Western blot was performed, showing higher P-ERK1/2 expression in the PES groups. B: Signaling inhibition tests show that phosph-ERK1/2 was lower in each TGFβ1 neutralization than in the control. C: ERK signal blocking directly downregulates the TGFβ1 expression in (C).

4.4.2 ERK signalling pathway

Fig. 32A shows that PES increased the phosphorylation of ERK1/2. To further define the participation of the TGFβ1-ERK1/2-NF-κB signalling axis upon administration of PES, TGFβ1 inhibition and ERK1/2 phosphorylation were performed. Fig. 32B demonstrates a suppressed p-ERK1/2 expression in contrast to t-ERK due to the presence of anti-TGFβ1 antibody at 0.5 μg ml^{-1}, which confirms the participation of TGFβ1 in the PES-induced ERK activation. The ERK signaling does affect the expression of TGFβ1, supported by the fact that p-ERK1/2 inhibition led to a significant decrease in TGFβ1 expression (Fig. 32C).

4.4.3 NF-κB migration into nucleus

Although the stimuli has been off for overnight, the NF- κB still showed the nuclei targeting. Fig. 33 shows the green-stained NF-κB distributed within the cytosol and reaching the nucleus following PES (bright green as indicated by the arrows). By merging the NF-κB and Hoechst-stained images, the nuclei in both PES groups appeared turquoise in comparison with the light blue nuclei observed in the controls. The translocation of NF-κB to the nucleus appeared more evident in the 300 s group than in the 10 s group.

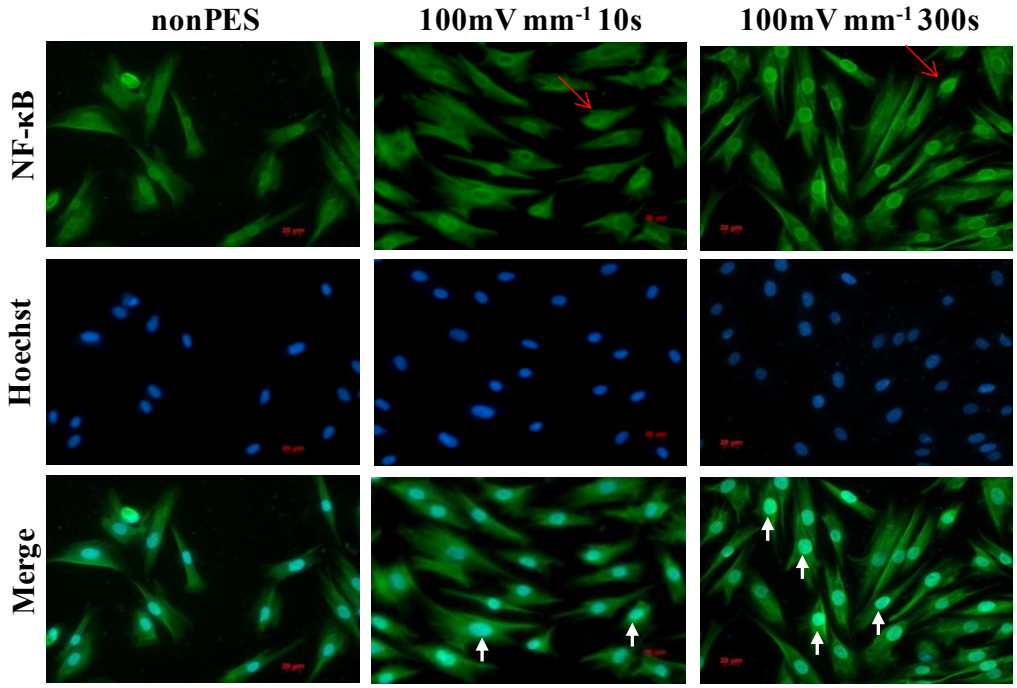

Fig. 33 **PES promoted NF-κB translocation from cell cytoplasm to nucleus**. Following exposure to PES, cells were seeded on glass slides for immunofluorescence analyses and then stained with primary anti-NF-κB monoclonal antibody and FITC secondary antibody, with the cell nucleus revealed by Hoechst (n = 4). Arrows show the NF-κB (sharp green) in the nucleus and turquoise color in the merge images. Scale bar = 20μm.

4.4.4 Cell migration and ERK pathway

Fig. 34 demonstrates the relationship between the PES-accelerated cell migration and the ERK pathway, as investigated using the *in vitro* cell monolayer wound model. Ten hours after initial wounding, the cells under PES recorded smaller wound areas, mainly because of the faster cell migration. Inhibiting the ERK pathway with PD98059 led to a significantly reduced migration of the fibroblasts in each paired groups (66.2 ± 0.5% vs. 72.8 ± 3.5% in noES pair, 61.2 ± 4.1% vs. 71.0 ± 6.2% in 10s ES pair, 60.4 ± 5.2% vs. 71.2 ± 4.3% in 300s ES pair), although the difference between PES and noES groups is not significant.

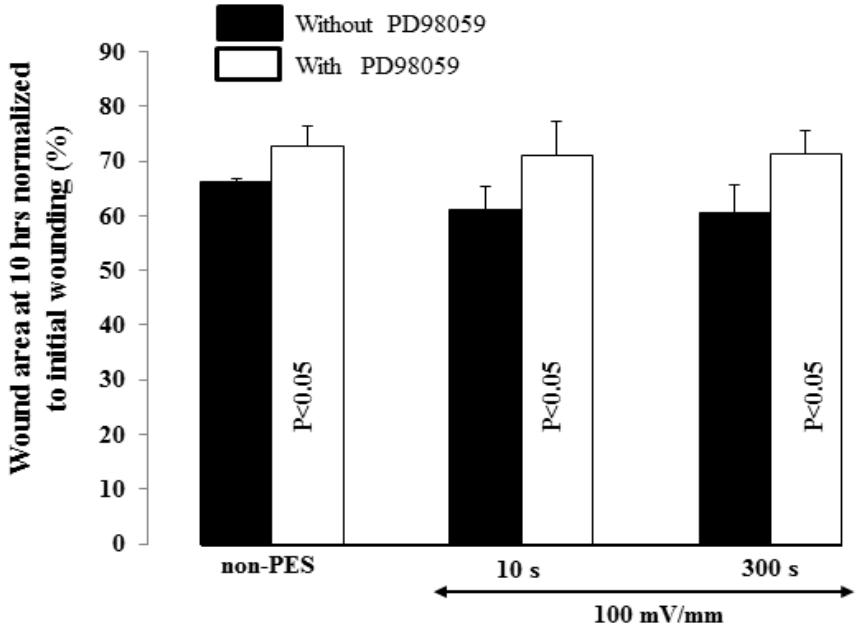

Fig. 34 ***In vitro*** **PES cell migration mediated by the ERK signalling pathway.** Following PES exposure, dermal fibroblasts were seeded in 6-well plates. A slower migration was observed in each ERK inhibition group corresponding to its own control group (n = 4).

4.4.5 Electrically stimulated fibroblasts maintained their myofibroblast phenotype even after subculture.

To clarify whether the PES-activated fibroblasts continued to express high levels of stress fibres after subculture, PES-activated cells were harvested and subcultured for 5 days prior to analysis. qRT-PCR results reveal that the level of α-SMA mRNA in the PES groups remained significantly higher than that in the controls (Fig. 35A). This finding is supported by the elevated number of α-SMA-positive cells observed in culture (3.1 ± 1.2%

at noES vs. 11.6 ± 4.4% at 10s 100mV mm^{-1}, 17.4 ± 3.1% at 300s 100mV mm^{-1}) (Figs. 35B, 35C).

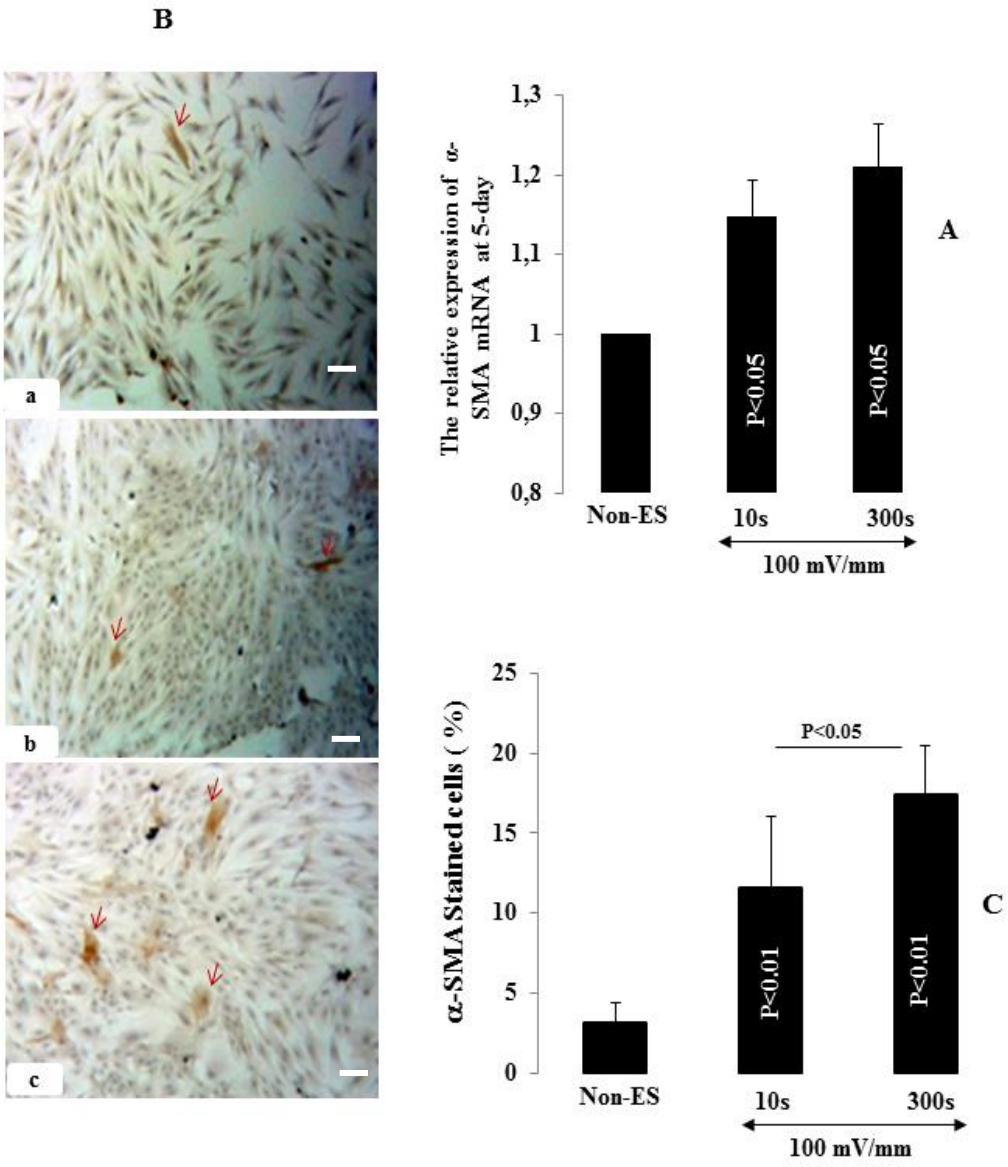

Fig. 35 **The effect of PES was maintained from mother to daughter cells.** Following PES, dermal fibroblasts were subcultured for 5 more days and were used either to extract total RNA for qRT-PCR (A), or to be reseeded on glass slides for α-SMA immunocytochemistry staining (B). α-SMA-positive cells were counted and are presented against the total number of cells (C). (a) non-ES; (b) 10 s 100mV mm^{-1}; (c) 300 s 100mV mm^{-1}. Scale bar = 100 μm.

4.4.6 Electrically stimulated fibroblast phenotyping following in vivo implementation

Fifteen days post-graft, histological analysis identified a cell-populated collagen scaffold (Fig. 36A). IHC staining revealed that most of the cells present in the implant were HLA-ABC-positive, confirming their human origin (Fig. 36B: a-c). The red fluorescence-labelled elongated fibroblasts were not only found in the collagen implants but had also migrated to the host tissue at the interface. Interestingly, many of the implanted fibroblasts remained, expressing stress fibres as labelled by anti-α-SMA antibody (Fig. 36A, d-f). Fig. 35B shows the merged images, showing the co-localization of human fibroblasts and α-SMA in either orange or yellow. To quantify these data, the HLA-ABC-positive cells and both the HLA-ABC- and α-SMA-positive cells were counted in all of the explants; this is summarized in Fig. 36C. A significant proportion of myofibroblasts were recorded in the PES groups, with 70 ± 9.6% and 65 ± 8.2% in the 300 s and 10 s groups, respectively, compared to 24 ± 5.8% in the control group.

A

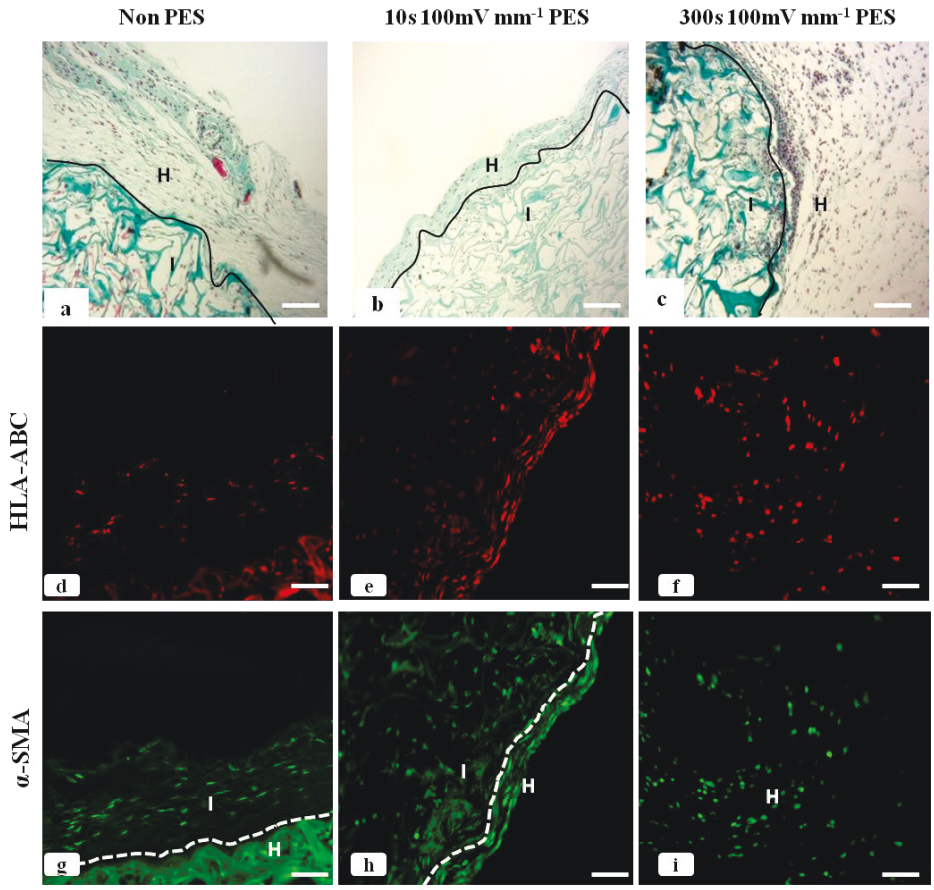
Non PES
10s 100mV mm-1 PES
300s 100mV mm-1 PES
HLA-ABC
α-SMA
H
I
a
b
c
d
e
f
g
h
i

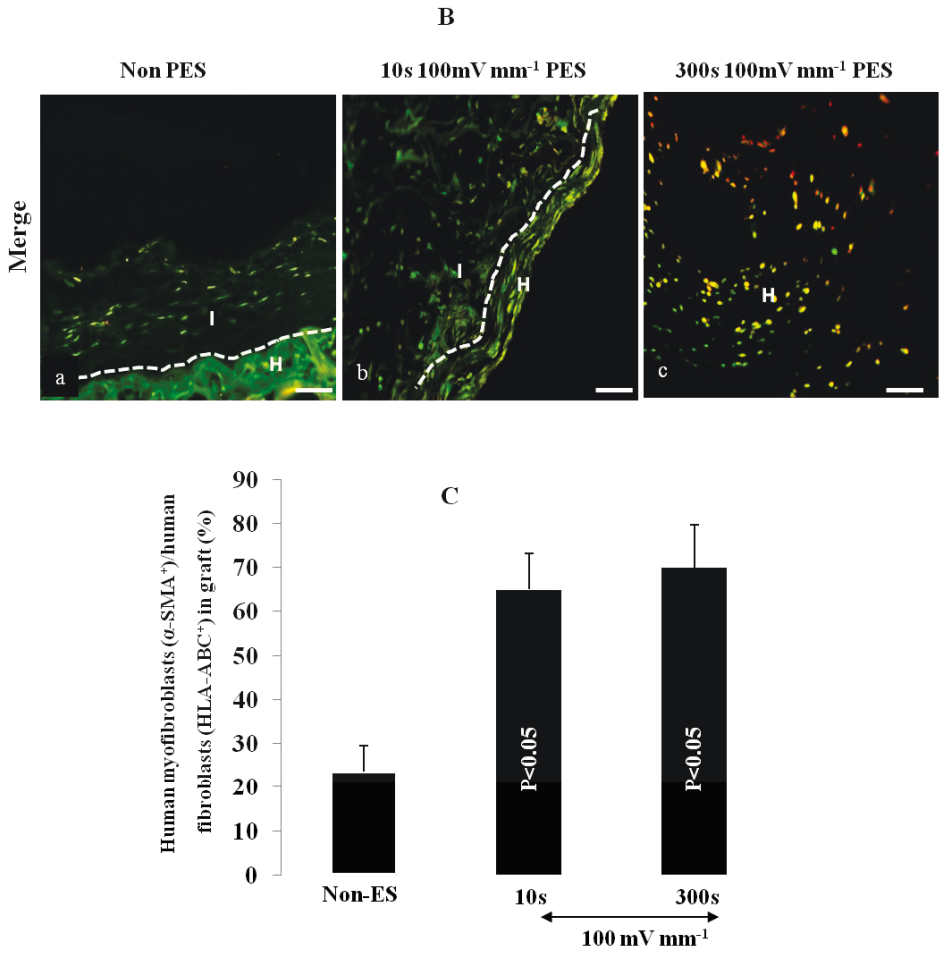

Fig. 36 **Tissue analyses following *in vivo* implantation of PES-cell-populated collagen scaffolds.** Following PES, dermal fibroblasts were cultured for 2 days on a porous collagen scaffold then subcutaneously implanted in nude mice for 15 days. Mason's trichrome stain shows cell distribution and the implant (I) in host tissue (H) (A; a, b, and c). HLA-ABC staining was performed to ascertain the presence of human dermal fibroblasts in the implant 15 days post-grafting (A; d, e, and f). Cells expressing α-SMA in the implant are identified by immunostaining (A; g, h, and i). Overlaying the HLA-ABC and α-SMA-positive cells enabled us to determine the grafted human fibroblasts expressing myofibroblast phenotype (B; a, b, and c, bright yellow). This is confirmed by the double stained cell counting (C) (n = 4). Scale bar = 100 μm.

4.5 Discussion

TGFβ1 has a variety of regulatory functions in cellular physiology and influences such important processes as wound repair and development. This study provides insight

regarding the involvement of TGFβ1/ERK/NF-κB in the fibroblast-to-myofibroblast transition under ES conditions as well as describes the potential use of ES-activated fibroblasts for wound care strategies.

4.5.1 PES, the physical cue, activated TGFβ1 expression

TGFβ1 plays several important roles in wound healing by regulating cell proliferation [30] and differentiation [31], and affecting inflammation response [32], granulation tissue generation [33], keratinocyte migration [34], remodeling, and ECM production [35]. TGFβ1 was suggested as improving wound healing in diabetic mice [36]. While EF or ES has been known to accelerate wound healing [37-40], studies on EF and TGFβ1 expression in human cells remain very limited, particularly mechanistic studies. Our previous work unveiled the activation of α-SMA and the Smad pathway in human dermal fibroblasts exposed to PES [41] and thus prompted us to explore the relationship between EF and TGFβ1 expression. The present study shows that PES increased TGFβ1 expression, which may further explain fibroblast-to-myofibroblast transition. Myofibroblasts may in fact contract wound surfaces and potentially shorten the migration distance for keratinocytes. However, the presence of myofibroblasts in the wound must be regulated to prevent their over-activation which leads to fibrotic disease (e.g. keloid). Further investigations are warranted to acquire confidence in terms of electric safety when used for wound healing purposes.

4.5.2 TGFβ1-ERK-NF-κB axis: Electrically stimulated myofibroblast differentiation and cell memory

Studies on signaling pathways under ES are rare. Zhao et al. reported that phosphatidylinositol-3-OH kinase-γ and phosphatase and tensin homolog (PTEN) controlled electrotaxis [42]. In our previous work, conductive polymer-mediated ES activated fibroblast proliferation [43], migration [44], ECM gene activation [45], and transdifferentiation [44]. This wide range of effects may thus involve TGFβ1 in fibroblast activity and wound healing. Within the complex signaling network, we investigated the TGFβ1-ERK-NF-κB axis and suggest that intracellular transduction may occur through the typical Smad signaling pathway as well as the ERK1/2 signaling branch [46-49]. As the major focus of this study regarded cellular survival and proliferation [50, 51] and because so

many nuclear factors can be phosphorylated and translocated into the nucleus to interfere with gene expression via different signaling pathways including NF-κB, Smad4, etc [23, 52-54]. ,We chose NF-κB as the downstream target. While this axis has been confirmed in other studies [55, 56] , none of these are associated with EF. The present study is the first to demonstrate that PES activated human fibroblasts through TGFβ1 expression and that this activation involved P-ERK and NF-κB, although NF- κB seems not clearly affirmative at 10s 100mV mm^{-1} group. The ES effect was maintained even after cell subculture by showing a higher number of myofibroblast phenotype, which suggests that ES is indeed capable of modulating cell beheavior over a long period of time. This finding is of importance in exploring the potential of ES-activated cells for use in wound healing applications. Further studies are required at longer periods to confirm the efficacy of ES in promoting wound healing.

4.5.3 In the view of tissue engineering and regenerative medicine: Potential of transplanting electrically activated cells

During the wound healing process, fibroblasts/myofibroblasts in granulation tissue interact with keratinocytes for better healing [57]. Maintaining a myofibroblast phenotype after as long as 15 days post-grafting of ES-differentiated fibroblasts may thus be significant in wound closure. Indeed, through their capacity to express α-SMA proteins, ES-differentiated fibroblasts may interact better with keratinocytes to promote greater wound healing. The fact that ES-activated cells are capable of memorizing certain acquired properties may have wider implications. For example, ES-activated autologous cells may be transplanted back to the patient as a temporary source of growth factors and cytokines to support the wound healing process. Safety issues such as phenotype stability through the gene activation and protein production of ES-stimulated cells will obviously require further study.

To sum up, the PES induced TGFβ1-ERK-NF-κB axis activation and relevant physiological outcomes. PES triggered the cells into producing more TGFβ1 which propagated the message from the extracellular matrix into the cytoplasm and activated ERK1/2. Activated NF-κB then migrated into the nucleus to target gene replication related to a wide spectrum of growth factors and cytokines such as FGF [43, 45], α-SMA, TGFβ1, among others. These biomolecules further contributed to cell proliferation, phenotype change, and angiogenesis, which are all important to wound healing. ES-

induced Ca^{2+} channel opening [58] and specific receptor activation [59] are documented. However, the influence of such voltage-gated ion channels on TGFβ1 expression remain unknown and thus additional mechanistic investigations should be performed to gain further knowledge in this regard.

4.6 Conclusion

Human dermal fibroblasts respond to PES in a 3-dimensional scaffoldded and conductive fabric. This study shows that PES upregulated the production of TGFβ1 in human dermal fibroblasts and that the transdifferentiation of dermal fibroblasts to myofibroblast phenotype was regulated by TGFβ1 through the TGFβ1-ERK-NF-κB signalling pathway. This study further demonstrates, for the first time, that this PES-induced phenotype change was maintained after 5 days of *in vitro* cell expansion and 15 days post-grafting. These findings thus highlight the feasibility of using electrically activated cells in wound healing.

4.7 Conflict of interest

The authors declare no conflicts of interest.

4.8 Acknowledgements

This study was financed by the operating grant of the Canadian Institutes of Health Research (CIHR, grant 106555). The support of the CHU Research Centre of Québec and the CREPEC is greatly appreciated. The authors are also grateful to the technical assistance and useful discussions of Hyun Jin Park, Zhiyong Du, and Dingkun Wang.

References

1 Reinke JM, Sorg H. Wound repair and regeneration. *Eur Surg Res*. 2012;49: 35-43.

2 Vozenin MC, Lefaix JL, Ridi R, Biard DSF, Daburon F, Martin M. The myofibroblast markers α-SM actin and β-actin are differentially expressed in 2 and 3-D culture models of fibrotic and normal skin. *Cytotechnology*. 1998;26: 29-38.

3 Hinz B. Formation and function of the myofibroblast during tissue repair. *J Invest Dermatol*. 2007;127(3): 526-537.

4 McCaig CD, Rajnicek AM, Song B, Zhao M. Controlling cell behavior electrically: current views and future potential. *Physiol Rev*. 2005;85(3): 943-978.

5 Chiang M, Robinson KR, Vanable JW Jr. Electrical fields in the vicinity of epithelial wounds in the isolated bovine eye. *Exp Eye Res*. 1992;54(6): 999-1003.

6 Thawer HA1, Houghton PE. Effects of electrical stimulation on the histological properties of wounds in diabetic mice. *Wound Repair Regen.* 2001;9(2): 107-15.

7 Kloth LC1. Electrical stimulation for wound healing: a review of evidence from in vitro studies, animal experiments, and clinical trials. *Int J Low Extrem Wounds*. 2005;4(1): 23-44.

8 Zhao M, Agius-Fernandez A, Forrester J V, McCaig CD. Orientation and directed migration of cultured corneal epithelial cells in small electric fields are serum dependent. *J Cell Sci*. 1996;109 (Pt 6): 1405-1414.

9 Chang KA, Kim JW, Kim JA, Lee SE, Kim S, Suh WH, et al. Biphasic electrical currents stimulation promotes both proliferation and differentiation of fetal neural stem cells. *PLoS One*. 2011;6(4): e18738.

10 Stewart E, Kobayashi NR, Higgins MJ, Quigley AF, Jamali S, Moulton SE, et al. Electrical Stimulation Using Conductive Polymer Polypyrrole Promotes Differentiation of Human Neural Stem Cells: A Biocompatible Platform for Translational Neural Tissue Engineering. *Tissue Eng Part C Methods*. 2015;21(4): 385-93.

11 Koppes AN, Nordberg AL, Paolillo G, Goodsell NM, Darwish HA, Zhang L, et al. Electrical Stimulation of Schwann Cells Promotes Sustained Increases in Neurite Outgrowth. *Tissue Eng Part A*. 2014;20(3-4): 494-506.

12 Luo B, Huang J, Lu L, Hu X, Luo Z, Li M. Electrically induced brain-derived neurotrophic factor release from schwann cells. *J Neurosci Res*. 2014;92(7): 893-903.

13 Hu WW, Hsu YT, Cheng YC, Li C, Ruaan RC, Chien CC, et al. Electrical stimulation to promote osteogenesis using conductive polypyrrole films. *Mater Sci Eng C Mater Biol Appl*. 2014;37: 28-36.

14 Sheikh AQ, Taghian T, Hemingway B, Cho H, Kogan AB, Narmoneva DA. Regulation of endothelial MAPK/ERK signalling and capillary morphogenesis by low-amplitude electric field. *J R Soc Interface*. 2013;10(78): 20120548.

15 Wu Y, Collier L, Qin W, Creasey G, Bauman WA, Jarvis J et al. Electrical stimulation modulates Wnt signaling and regulates genes for the motor endplate

and calcium binding in muscle of rats with spinal cord transection. *BMC Neurosci*. 2013;14(1): 81.

16 Matsuyama S, Moriuchi M, Suico MA , Yano S, Morino-Koga S, Shuto T, et al. Mild electrical stimulation increases stress resistance and suppresses fat accumulation via activation of LKB1-AMPK signaling pathway in C.elegans. *PLoS One.* 2014;9(12): e114690.

17 Ugarte G, Brandan E. Transforming growth factor beta (TGF-beta) signaling is regulated by electrical activity in skeletal muscle cells. TGF-beta type I receptor is transcriptionally regulated by myotube excitability. *J Biol Chem*. 2006;281(27): 18473-18481.

18 Todd I, Clothier RH, Huggins ML, Patel N, Searle KC, Jeyarajah S, et al. Electrical stimulation of transforming growth factor-beta 1 secretion by human dermal fibroblasts and the U937 human monocytic cell line. *Altern Lab Anim*. 2001;29(6): 693-701.

19 Zhuang H, Wang W, Seldes RM, Tahernia AD, Fan H, Brighton CT. Electrical stimulation induces the level of TGF-beta1 mRNA in osteoblastic cells by a mechanism involving calcium/calmodulin pathway. *Biochem Biophys Res Commun*. 1997;237(2): 225-229.

20 Strutz F, Zeisberg M, Renziehausen A, Raschke B, Becker V, van Kooten C, et al. TGF-beta 1 induces proliferation in human renal fibroblasts via induction of basic fibroblast growth factor (FGF-2). *Kidney Int*. 2001;59: 579-592.

21 Zhou F, Li GY, Gao ZZ, Liu J, Liu T, Li WR, et al. The TGF- 1/Smad/CTGF Pathway and Corpus Cavernosum Fibrous-Muscular Alterations in Rats With Streptozotocin-Induced Diabetes. *J Androl*. 2012;33(4): 651-659.

22 Pardali E, Goumans MJ, ten Dijke P. Signaling by members of the TGF beta family in vascular morphogenesis and disease. *Trends Cell Biol.* 2010;20(9): 556-67.

23 Roskoski R. ERK1/2 MAP kinases: Structure, function, and regulation. *Pharmacol Res*. 2012;66(2): 105-143.

24 Chang L, Karin M. Mammalian MAP kinase signalling cascades. *Nature*. 2001;410:37-40.

25 Wada T, Penninger JM. Mitogen-activated protein kinases in apoptosis regulation. *Oncogene*. 2004;23(16):2838-49.

26 Cuadrado A, Nebreda AR. Mechanisms and functions of p38 MAPK signalling. *Biochem J*. 2010;429(3): 403-17.

27 Roux PP, Blenis J. ERK and p38 MAPK-activated protein kinases: a family of protein kinases with diverse biological functions.*Microbiol Mol Biol Rev*. 2004;68(2): 320-44.

28 Wang Y, Rouabhia M, Zhang Z. PPy-coated PET fabrics and electric pulse-stimulated fibroblasts. *J Mater Chem B*. 2013;1: 3789-96.

29 Meng S, Zhang Z, Rouabhia M. Accelerated osteoblast mineralization on a conductive substrate by multiple electrical stimulation. Journal of bone and mineral metabolism. *J Bone Miner Metab.* 2011;29: 535-44.

30 Clark RA, McCoy GA, Folkvord JM, McPherson JM. TGF-beta 1 stimulates cultured human fibroblasts to proliferate and produce tissue-like fibroplasia: a fibronectin matrix-dependent event. *J Cell Physiol.* 1997;170: 69–80.

31 Thannickal VJ, Lee DY, White ES, Cui Z, Larios JM, Chacon R, et al. Myofibroblast differentiation by transforming growth factor-beta1 is dependent on cell adhesion and integrin signaling via focal adhesion kinase. *J Biol Chem.* 2003;278: 12384–12389 .

32 Han G, Li F, Singh TP, Wolf P, Wang XJ. The pro-inflammatory role of TGFbeta1: a paradox? *Int. J Biol Sci.* 2012;8: 228–235.

33 Blumbach K, Zweers MC, Brunner G, Peters AS, Schmitz M, Schulz JN, et al. Defective granulation tissue formation in mice with specific ablation of integrin-linked kinase in fibroblasts - role of TGFbeta1 levels and RhoA activity. *J Cell Sci.* 2010;123: 3872–3883.

34 Gailit J, Welch MP, Clark RA. TGF-beta1 stimulates expression of keratinocyte integrins during re-epithelialization of cutaneous wounds. *J Investig Dermatol.* 1994;103: 221–227.

35 Cyniak-Magierska A, Januszkiewicz-Caulier J, Brzezianska E, Lewinski A. Analysis of correlation between the process of thyroid fibrosis and TGFβ1 gene expression level in fine-needle aspiration biopsy (FNAB) thyroid specimens collected from patients with Hashimoto's thyroiditis and non-toxic goitre. *Exp Clin Endocrinol Diabetes*. 2010:118: 420–426.

36 El Gazaerly H, Elbardisey DM, Eltokhy H M, Teaama D. Effect of transforming growth factor beta 1 on wound healing in induced diabetic rats. *Int J Health Sci(Qassim)*. 2013;7: 160–172 .

37 Kloth LC, Feedar JA. Acceleration of wound healing with high voltage, monophasic, pulsed current. *Phys Ther.* 1988;68: 503-508.

38 Feedar JA, Kloth LC, Gentzkow GD. Chronic dermal ulcer healing enhanced with monophasic pulsed electrical stimulation. *Phys Ther.* 1991;71: 639-649.

39 Ud-Din S, Bayat A. Electrical stimulation and cutaneous wound healing: a review of clinical evidence. *Healthcare.* 2014;2: 445-467.

40 Balakatounis KC, Angoules AG. Low-intensity electrical stimulation in wound healing: review of the efficacy of externally applied currents resembling the current of injury. *Eplasty.* 2008;8(Lic): e28.

41 Wang Y, Rouabhia M, Lavertu D, Zhang Z. Pulsed electrical stimulation modulates fibroblasts' behaviour through the Smad signalling pathway. *J Tissue Eng Regen Med*. 2015; DOI: 10.1002/term.2014.

42 Zhao M, Song B, Pu J, Wada T, Reid B, Tai G, et al. Electrical signals control wound healing through phosphatidylinositol-3-OH kinase-gamma and PTEN. *Nature*. 2006;442: 457-60.

43 WangY L, Rouabhia M, Zhang Z. PPy-coated PET fabrics and electric pulse-stimulated fibroblasts. *J Mater Chem B.* 2013;1: 3789–3796.

44 Rouabhia M, Park H, Meng S, Derbali H, Zhang Z. Electrical stimulation promotes wound healing by enhancing dermal fibroblast activity and promoting myofibroblast transdifferentiation. *PLoS One*. 2013;8: e71660.

45 Park HJ, Rouabhia M, Lavertu D, Zhang Z. Electrical stimulation modulates the expression of multiple wound healing genes in primary human dermal fibroblasts. *Tissue Eng. Part A*. 2015; doi:10.1089/ten.TEA.2014.0687

46 Lu Z, Xu S. ERK1/2 MAP kinases in cell survival and apoptosis. *IUBMB Life.* 2006;58: 621-31.

47 Cargnello M, Roux PP. Activation and function of the MAPKs and their substrates, the MAPK-activated protein kinases. *Microbiol Mol Biol Rev*. 2011;75: 50-83.

48 Roberts PJ, Der CJ. Targeting the Raf-MEK-ERK mitogen-activated protein kinase cascade for the treatment of cancer. *Oncogene.* 2007;26: 3291-310.

49 McCubrey JA, Steelman LS, Chappell WH, Abrams SL, Wong EW, Chang F, et al. Roles of the Raf/MEK/ERK pathway in cell growth, malignant transformation and drug resistance. *Biochim Biophys Acta*. 2007;1773: 1263-84.

50 Li X, Gao L, Cui Q, Gary BD, Dyess DL, Taylor W, et al. Sulindac inhibits tumor cell invasion by suppressing NF-kappaB-mediated transcription of microRNAs. *Oncogene.* 2012;31: 4979-86.

51 Tornatore L, Sandomenico A, Raimondo D, Low C, Rocci A, Tralau-Stewart C, et al. Cancer-selective targeting of the NF-kappaB survival pathway with GADD45beta/MKK7 inhibitors. *Cancer Cell.* 2014;26: 495-508.

52 Runge MB, Dadsetan M, Baltrusaitis J, Knight AM, Ruesink T, Lazcano EA, et al. The development of electrically conductive polycaprolactone fumarate-

polypyrrole composite materials for nerve regeneration. *Biomaterials*. 2010;31: 5916-26.

53 Kim SI, Kim HJ, Han DC, Lee HB. Effect of lovastatin on small GTP binding proteins and on TGF-bold beta1 and fibronectin expression. *Kidney Int.* 2000;58: S88-S92.

54 Imamichi Y, Waidmann O, Hein R, Eleftheriou P, Giehl K, Menke A. TGF beta-induced focal complex formation in epithelial cells is mediated by activated ERK and JNK MAP kinases and is independent of Smad4. *Biol Chem.* 2005;386: 225-36.

55 Gingery A, Bradley EW, Pederson L et al. TGF-β coordinately activatesTAK1/MEK/AKT/NFkB and Smad pathways to promote osteoclast survival. *Exp Cell Res.* 2008;314: 2725-38.

56 Armstrong L, Huges O, Yung S, Ruan M, Horwood NJ, Oursler MJ. The role of PI3K/AKT, MAPK/ERK and NFκb signalling in the maintenance of human embryonic stem cell pluripotency and viability highlighted by transcriptional profiling and functional analysis. *Hum Mol Genet.* 2006;15: 1894-913.

57 Werner S, Krieg T, Smola H. Keratinocyte-fibroblast interactions in wound healing. *J Invest Dermatol*. 2007;127:998-1008

58 Artzy-Schnirman A, Blat D, Talmon Y, Fishler R, Gertman D, Oren R, et al. Electrically controlled molecular recognition harnessed to activate a cellular response. *Nano Letters.* 2011;11: 4997–5001.

59 Vernier P T, Sun Y, Marcu L, Craft CM, Gundersen MA. Nanosecond pulsed electric fields trigger intracellular signals in human lymphocytes. *NSTI-Nanotech.* 2004;1: 7–10.

CHAPTER V

GENERAL DISCUSSION

5.1 General discussion

This thesis studied the mechanistic basis of the celluar response under PES by focussing on human dermal fibroblasts in the context of skin wound healing. The author synthesized a conductive fabric scaffold and established an electrical stimulation protocol specifically optimized for this type of conductive substrate. In biological study, the author tried to explain how PES improved cell proliferation and accelerated myofibroblast transdifferentiation by investigating the key growth factors and signaling pathways. The methodologies used in this thesis encompass material chemsitry, engineering, and cellular and molecular biology, emphasizing the multidisciplinary characteristics of this thesis.

5.1.1 PPy-coated PET fabrics for electricity delivery

With the progresse, conductive polymeric materials have been continuously designed and manufactured in such applications as energy, bioengineering, etc. For instance, flexible conductive polymers may be used in future batteries [296]. Conductive microelectrodes modified with conductive polymer have been studied for brain signal recording [297]. In biomedical research, ES can be delivered as an EF either between electrodes or on the surface of a current-carrying conductor. Electrodes in direct contact with culture medium may have electrochemical reactions that produce cytotoxic products [298]. As a result, some labs performed the ES relevant experiments through salt bridge system. With the discovery of organic conductive polymers, the methodologies for exposing cells to EF were also expanded. The intrinsic fragile and britle property can be overcomed by forming composites such as the PPy-PLLA composite. Also, surface grafting provides another alternative to utilize materials of a variety of mechanical propterties as coating substrates. By surface modification, conductive woven fabrics, nonwoven fabrics and electronspun patches were manufactured. Previously, the conductive PLLA/PPy composite membranes were produced in our lab and used for continuous DC exposures. However, the rigidity of this type of membrane limits its application. In this study, coating PPy on the surface of soft PET fabrics is a good idea because of easy processing, the porous structure serving as cell growth scaffold, as well as the absence of electrode reactions. In order to firmly coat PPy onto the surface of PET fabrics, the substrate surface normally must be pre-treated by means of chemical activation or ionization, such as phosphorylation or plasma treatment [299, 300]. The simple two-step method developed in this thesis permits the formation of a thin layer of PPy on the surface of PET fibres without any pre-treatment, and allows a firm attachment of PPy with sufficient

conductivity. Should it be used in vivo, the thin layer may enable less inflammatory and immune reaction while maintaining electrical property, because PPy is considered non-biodegradable and is difficult to be removed from human body.

The conductivity of PPy decreases in an aqueous solution, which is particularly true when the PPy coating layer is thin and conducting electricity. Dedoping takes place much faster in a thin layer than in a thick composite membrane. In order to take the advantages of fabrics such as flexibility, a new ES protocol must be established to avoid significant dedoping. Taking advantage of the fast redoping phenomenon in thin layer of PPy, the discontinuousES protocol has been designed to allow the redoping or recovery time for conductivity. As found in this thesis, the two PES protocols (10s ES in a period of 1200s, and 300s ES in a period of 600s) are the successful examples of using discontinuous ES regimes. The PES regimes allow the conductivity lost during the active stimulation period be recovered during the non-ES period due to redopping. As showed in our study, the PPy-PET material was able to retain 80% of its initial conductivity after 24 h of PES in culture medium, which means that the cells on surface of the PPy-PET fabric can receive a relatively stable ES despite the vulnerable nature of PPy in aqueous environment (see Chapter II).

5.1.2 PES modulated dermal fibroblast behaviours

In the process of wound healing, wound EF has an unique role on cell migration, the initiation of wound repair. This phyical cue in the biological and physiological regulation has been investigated for decades, or centruries. EF and EMF have already been applied in the clinic, such as for bone non-union treatment [301]. In the field of biophysics, ion current has been known and investigated for decades, especially in the electrical conduction system of heart and neuron. The interpretation to electrophysiological processesneeds more contributions from structural biology and post-functional verification. To mimic physiological phenomena and to unveil the hidden secrets continuously generate curiosity in life science research.

Cell behaviours, including migration, growth, differentiation and apoptosis, determine the functions of tissues and organs, which are subtly regulated by microenvironment according to the needs of tissues and organs. ES is reportedly capable of influencing cell behaviours *in vitro*, e.g., osteoblast mineralization, nerve stem cell differentiation, and

keratinocyte migration [28, 54-55]. In order to translate bioelectricity for wound care purpose, the beneficial outcomes are essential to be proved prior to clinical application, which could be achieved by precisely controlling ES parameters such as intensity and exposure time. In the context of wound healing, fibroblasts play very important roles in ECM deposition and the contraction of wound edge to close the wound [131]. That ES is able to promote fibroblast growth has been proved previously using continuous ES. Chapter II extended that work to PES and conductive textile. In addition, PES was also showed to increase the collective cell migration/monolayer wound healing (Chapter III), and to mediate the transdifferentiation of fibroblasts to myofibroblasts (Chapter III, IV), as presented in the followings.

5.1.2.1 PES enhanced collective cell migration

Cell migration *in vitro* may be interpreted as the proliferative potential or to dominate the unoccupied region. It naturally reflects cell viability and needs energy support. In a well-organized tissue, cell migration enables the tissue formation, maitenance, and regeneration, which is spatio-temporally controlled by the cell communication system. To verify the contribution from ES exposure, in the context of wound repair, fast cell migration shortens time of granulation tissue formation and promotes wound closure. A study of the collective epithelial migration on a microdesigned scaffold demonstrated the formation of epithelial bridges within the migrating keratinocytes monolayers [302]. Zhao et al. reported the PI3Kγ and PTEN signalling invovlement in cellular electrotaxis [18]. In wound repair or tissue regneration process, cell migration is a very common process prior to granulation tissue formation. ES or EF has been reported to introduce cell orientation and to accelerate cell migration [58, 303]. As shown in this thesis, the PES-exposed fibroblasts re-seeded on a standard culture plate recorded a higher cell migration speed; this may involve growth factor secretion such as FGF [304, 305]. This study acquired some preliminary data about growth factors and TGFβ1 relevant signals. It was found that the PES-exposed fibroblasts secreted high concentration of FGF2 and TGFβ1. To verify the participation of ERK signalling in monolayer cell migration, ERK inhibition was found to decrease cell migration speed. Besides, It is likely that the high amount of α-SMA in the PES-exposed fibroblasts, or the high number of contractile phenotypic fibroblasts, contributed to the faster migration. Evidently, this remains a hypothesis and requires further investigation.

5.1.2.2 PES introduced differentiation

Dermal fibroblast transdifferentiates to myofibroblast to meet the needs of wound repair, because myofibroblast deposites more ECM and imposes stronger mechnical force to contract and close the wound. Normally this process is completed with the disappearance of myofibroblast. This transition is regulated by the biological signals in granulation tissue, such as TGFβ. Our new finding is that ES as a physical cue can activate or modify this transition. The fact that fibroblast to myofibroblast transition can be induced through PES may open a new door to modulate this process. PES of both 50 and 100 mV/mm in strength led to the upregulated production of α-SMA, proven at gene and protein levels. Furthermore, longer time (300s) and higher intensity (100mV/mm) appeared to be more effective. In addition, the greater expression of stress fibres was translated into higher contractile force to a membrane gel, which mimicked an accelerated wound closure process and implied the positive role of the ES activated fibroblasts in wound repair.

5.1.3 TGFβ1 signalling pathways were involved in cell response to PES

The studies about the signalling pathways of electrically stimulated cells are very limited, and the one dealing with ES-induced fibroblast-to-myofibroblast transition has not been reported. While some work focused on ion channels [306] and others on MAPK/ERK [42] and PKC [45], none of them investigated dermal fibroblasts. In cell development and linage tracing research, TGFs holds a key position. Consequently, TGFβ1 related signalling regulations may partially describ how fibroblasts respond to PES. It is widely acknowledged that TGFβ enables cell fate change as well as proliferation. TGFβ1, whose synthesis is stimulated by mechanical, physical, and biochemical factors [307], is widely involved in the regulation of cell differentiations ranging from embryonic development to tissue regeneration. Additionally, according to reports, TGFβ1 exerts a leading function in the healing of bone fracture by induction of ECM production and ossification [308]. In cartilage tissue, TGFβ1 promoted the proliferation of precusors or immature chondrocytes and increased ECM production. Also, TGFβ1 participated the recruitment and phenotypic regulation of macrophages [309]. In this study, a high concentration of TGFβ1 in extracellular environment was measured with ELISA assay and an upregulation of total TGFβ1 was revealed by Western blot in the PES-exposed (100mV/mm) fibroblasts. This upregulation could contribute not only to the ECM production but also to the inflammation enviroment at wound cavity. Because TGFβ1 can transduce differential

signal through Smad and non-Smad pathways, this work firstly revealed the involvement of TGFβ in the PES-induced fibroblast-to-myofibroblast differentiation, and then prompted our study of the downstream signalling pathways (Chapter III, IV).

5.1.3.1 Smad signalling pathway

TGFβ/Smad signalling pathway is a typical axis that regulates patterning, bone formation, and wound regeneration [310-315]. In the paradigm, TGFβ firstly binds to its receptor, and then its receptor phosphorylates Smad2, Smad3 in dermal fibroblast. Smad2/3 forms dimer with Smad4 and translocates into nucleus. However, the PES induced Smad involvement has not been reported before this work, not even mentionning the following outcomes. In this study, the TGFβ/Smad axis was found activated by PES and concerted with fibroblast-to-myofibroblast transdifferentiation, which has promoted phosph-Smad2, phosph-Smad3 and obviously Smad2/3 dimer nucleus translocation in concert with α-SMA expression. The outcome of this signalling pathway activation may explain the higher contractability of the PES-exposed fibroblasts and therefore is helpful in wound closure and may benefit wound healing. In clinic setting, although some practioners have already accepted ES or EMF as an alternative to treat chronic wounds, the statistic data were still difficult to convince the main stream community because of the sample size and the inconstant clinic outcomes probably caused by the diverse parameters such as ES equiment, exposed voltage and time, wound information, etc. In orde to verify the efficacy of ES in wound healing, a large sample size *in vivo* study should be performed, firstly on animal and then on patients, and neccessarily, a stadardized protocol must be adopted to ensure meaningful comparison among studies.

5.1.3.2 ERK signalling pathway

Non-canonical Smad pathways also play an important part in the regulation of TGFβ signal transduction. Among them, ERK signalling pathways are involved in cell survival, growth, apoptosis, motility, differentiation and adhesion, and thus are an important player in tissue regeneration, development, tumorgenesis, and wound healing [188, 196, 197, 316, 317]. This study revealed and quantified the higher activity of phosph-ERK1/2 and proved that longer time (300s) and higher EF intensity (100 mV/mm) resulted in more phosph-ERK1/2. The downstream executor was assigned to NF-κB that was found to migrate into nucleus and to initiate target gene transcription in collaboration with other transcription

factors. NF-κB usually participates in inflammation reaction and cellular stress response. In our study, the novel extenstion of NF-κB in fibroblast suggested that ES might be an external stress stimuli, which warrants appropriate investigation of ES in clinic treatment. The axis of TGFβ/ERK/NF-κB, herein, exerted regulatory functions for dermal fibroblasts in response to ES and channelled beneficial feedback to wound repair.

5.1.4 The memory of PES effect

How long the ES effect can last in cells is a critical issue that determines how such electrically stimulated cells will be used. In tissue engineering, cell-microenvironment interactions are known very important in determining the final fate and behaviours of transplanted cells. Researchers strive to figure out the factors influencing cell lineage, hoping to apply the findings to design better controlled product [318-320]. As documented, researches attempted to control stem cell fate by the stiffness of scaffold and the structure of substrates (i.e. photodegradable hydrogel) [321]. In this thesis, the simulated fibroblasts were found to retain their myofibroblast phenotype after 15 days implantation in nude mice. This finding may represent a new way to manipulate cell fate.

In addition, the interaction between fibroblasts/myofibroblasts and keratinocytes is of paramount importance to skin formation [135], which also referred to growth factors' paracrine effect and the maintenance of dermis and epidermis structure. Given the lasting effect of PES and the myofibroblast phenotype, the ES-activated autologous fibroblasts may be transplanted back to the patient as a temporary source of growth factors and cytokines to support skin wound healing, an approach that may be acceptable in biomedical engineering. One issue needs additional care is that the myofibroblast transdifferentiation should be well controlled because any uncontrolled fibrotic phenotype may lead to disease such as keloid [322]. Further studies are essential to guarantee the safety of using ES stimulated cells in wound treatment.

5.2 Limitations and perspectives

In this thesis, the author tried to elucidate how dermal fibroblast responds to PES and attempted to identify how such electrically activated cells may benefit wound repair. However, there are still a lot of limitations in this study. Above all, the mimicked physiological EF is not the same as that in human tissue that has 3 dimensional structure

and much complex architecture. A wound EF might be or has been acknowledged nowadays due to TEP that is generated by ionic potential, which might be different from the exogenous EF. In addition, to bring PES to bedside requires enormous efforts including large scale animal experiments and clinical trials. It should also mention that the observed cellular responses could be interpreted differently based on different context. The pathways studied in this thesis are limited considering the complexity of cell signalling. Consequently, in the future, the mechanistic studies should be continued, for example, about how calcium ions are involved in signalling pathways and in cell memory because calcium ion is a key second messenger in signaling transduction and free ions are affected by EF. Further *in vivo* experiment has to be accomplished for the accumulation of the first-hand data with the purpose of applying ES to help wound healing. It requires medical doctors to evaluate the effect of ES in terms of different forms, vectors and protocols, which would provide the most valuable feedback to basic research. In addition, a method of directly combing ES with woundcare may be realized via conductive wound dressing, a new battlefield for engineers and material scientists. Technically, in order to have precisely controllabe ES through conductive substrates or bandages, a new technology of nanodesigning or microfabrication may be introduced.

REFERENCES

1. Gadsby DC. Ion channels versus ion pumps: the principal difference, in principle. *Nat Rev Mol Cell Biol.* 2009; 10(5): 344–352.
2. Latorre R, Miller C. Conduction and selectivity in potassium channels. *J Membr Biol.* 1983;71(1-2): 11-30.
3. Zachariae U, Helms V, Engelhardt H. Multistep mechanism of chloride translocation in a strongly anion-selective porin channel. *Biophys J.* 2003;85(2): 954-962.
4. Catterall WA. From ionic currents to molecular mechanisms: the structure and function of voltage-gated sodium channels. *Neuron*. 2000;26(1): 13-25.
5. Payandeh J, Scheuer T, Zheng N et al. The crystal structure of a voltage-gated sodium channel. *Nature.* 2011;475(7356): 353-358.
6. Catterall WA. Molecular properties of voltage-sensitive sodium channels. Annu Rev Biochem. 1986;55:953-985.
7. Yu FH, Catterall WA. Overview of the voltage-gated sodium channel family. *Genome Biol.* 2003;4(3): 207.
8. Zhou W, Goldin AL. Use-dependent potentiation of the Nav1.6 sodium channel. *Biophys J.* 2004;87(6): 3862-3872.
9. Miller C. An overview of the potassium channel family. *Genome Biol.* 2000;1(4):REVIEWS0004.
10. Debanne D, Campanac E, Bialowas A et al. Axon physiology. *Physiol Rev.* 2011;91(2): 555-602.
11. Wang W, Hebert SC, Giebisch G. Renal K^+ channels: structure and function. *Annu Rev Physiol*. 1997;59: 413-436.
12. Hibino H, Inanobe A, Furutani K et al. Inwardly rectifying potassium channels : their structure, function, and physiological roles. *Physiol Rev*. 2010;90: 291-366.
13. Jentsch TJ, Introduction I, Stein V et al. Molecular structure and physiological function of chloride channels. *Physiol Rev*. 2002;82(2): 503-568.
14. Catterall WA. Voltage-gated calcium channels. *Cold Spring Harb Perspect Biol.* 2011;3(8): a003947.
15. Simms BA, Zamponi GW. Neuronal voltage-gated calcium channels: structure, function, and dysfunction. *Neuron*. 2014;82(1): 24-45.
16. Borgens RB. The role of ionic current in the regeneration and development of the amphibian limb. *Prog Clin Biol Res.* 1983;110 Pt A: 597-608.

17. Hotary KB, Robinson KR. Evidence of a role for endogenous electrical fields in chick embryo development. *Development.* 1992;114(4): 985-996.
18. Zhao M, Song B, Pu J et al. Electrical signals control wound healing through phosphatidylinositol-3-OH kinase-gamma and PTEN. *Nature.* 2006;442: 457-460.
19. Altizer AM, Moriarty LJ, Bell SM et al. Endogenous electric current is associated with normal development of the vertebrate limb. *Dev Dyn.* 2001;221(4): 391-401.
20. Adams DS, Robinson KR, Fukumoto T et al. Early, H^+-V-ATPase-dependent proton flux is necessary for consistent left-right patterning of non-mammalian vertebrates. *Development*. 2006;133(9): 1657-1671.
21. Aw S, Adams DS, Qiu D et al. H,K-ATPase protein localization and Kir4.1 function reveal concordance of three axes during early determination of left-right asymmetry. *Mech Dev.* 2008;125(3-4): 353-372.
22. Pietak AM. Endogenous electromagnetic fields in plant leaves: a new hypothesis for vascular pattern formation. *Electromagn Biol Med*. 2011;30(2): 93-107.
23. Lodish H, Berk A, Zipursky SL, Matsudaira P, Baltimore D, Darnell J. *Molecular cell biology.* 4th edition. New York: W. H. Freeman; 2000.
24. Anderson RH, Yanni J, Boyett MR, Chandler NJ, Dobrzynski H. The anatomy of the cardiac conduction system. *Clin Anat*. 2009;22(1):99-113.
25. Messerli MA, Graham DM. Extracellular electrical fields direct wound healing and regeneration. *Biol Bull.* 2011;221(1): 79-92.
26. Pilla AA. Nonthermal electromagnetic fields: from first messenger to therapeutic applications. *Electromagn Biol Med.* 2013;32(2): 123-136.
27. Chang KA, Kim JW, Kim JA et al. Biphasic electrical currents stimulation promotes both proliferation and differentiation of fetal neural stem cells. *PLoS One.* 2011;6(4): e18738.
28. Pires F, Ferreira Q, Rodrigues CA et al. Neural stem cell differentiation by electrical stimulation using a cross-linked PEDOT substrate: Expanding the use of biocompatible conjugated conductive polymers for neural tissue engineering. *Biochim Biophys Acta - Gen Subj*. 2015;1850(6): 1158-1168.
29. Ghasemi-Mobarakeh L, Prabhakaran MP, Morshed M et al. Electrical stimulation of nerve cells using conductive nanofibrous scaffolds for nerve tissue engineering. *Tissue Eng Part A.* 2009;15(11): 3605-3619.
30. Keuters MH, Aswendt M, Tennstaedt A et al. Transcranial direct current stimulation promotes the mobility of engrafted NSCs in the rat brain. *NMR Biomed.* 2015;28(2): 231-239.

31. Chan YC, Ting S, Lee YK et al. Electrical stimulation promotes maturation of cardiomyocytes derived from human embryonic stem cells. *J Cardiovasc Transl Res*. 2013;6(6): 989-999.
32. Luisa M, Luis HC, María P et al. Electric stimulation at 448 kHz promotes proliferation of human mesenchymal stem cells. *Cell Physiol Biochem*. 2014;34(5): 1741-55 .
33. Brust-Mascher I, Webb WW. Calcium waves induced by large voltage pulses in fish keratocytes. *Biophys J*. 1998;75(4): 1669-1678.
34. Hinsenkamp M, Jercinovic A, de Graef C et al. Effects of low frequency pulsed electrical current on keratinocytes in vitro. *Bioelectromagnetics.* 1997;18(3): 250-254.
35. Sebastian A, Iqbal S A, Colthurst J et al. Electrical stimulation enhances epidermal proliferation in human cutaneous wounds by modulating p53–SIVA1 interaction. *J Invest Dermatol.* 2014;135(4):1166-1174.
36. Nishimura KY, Isseroff RR, Nuccitelli R. Human keratinocytes migrate to the negative pole in direct current electric fields comparable to those measured in mammalian wounds. *J Cell Sci.* 1996;109 (Pt 1): 199-207.
37. Jennings JA, Chen D, Feldman DS. Upregulation of chemokine (C-C motif) ligand 20 in adult epidermal keratinocytes in direct current electric fields. *Arch Dermatol Res*. 2010;302(3): 211-220.
38. Arai KY, Nakamura Y, Hachiya Y et al. Pulsed electric current induces the differentiation of human keratinocytes. *Mol Cell Biochem.* 2013;379(1-2): 235-241.
39. Fukuda R, Suico MA, Koyama K et al. Mild electrical stimulation at 0.1-ms pulse width induces p53 protein phosphorylation and G2 arrest in human epithelial cells. *J Biol Chem.* 2013;288(22): 16117-16126.
40. Luther PW, Peng HB, Lin JJ. Changes in cell shape and actin distribution induced by constant electrical fields. *Nature*. 1983;303: 61-64.
41. Petrofsky J, Hinds CM, Batt J et al. The interrelationships between electrical stimulation, the environment surrounding the vascular endothelial cells of the skin, and the role of nitric oxide in mediating the blood flow response to electrical stimulation. *Med Sci Monit.* 2007;13(9): CR391-R397.
42. Sheikh AQ, Taghian T, Hemingway B et al. Regulation of endothelial MAPK/ERK signalling and capillary morphogenesis by low-amplitude electric field. *J R Soc Interface.* 2013;10(78): 20120548.

43. Bai H, Forrester J V, Zhao M. DC electric stimulation upregulates angiogenic factors in endothelial cells through activation of VEGF receptors. *Cytokine.* 2011;55(1): 110-115.
44. Houghton PE, Kincaid CB, Lovell M et al. Effect of electrical stimulation on chronic leg ulcer size and appearance. *Phys Ther.* 2003;83(1): 17-28.
45. Saigal R, Cimetta E, Tandon N et al. Electrical stimulation via a biocompatible conductive polymer directs retinal progenitor cell differentiation. *Proc Annu Int Conf IEEE Eng Med Biol Soc EMBS.* 2013: 1627-1631.
46. Kobelt LJ, Wilkinson AE, McCormick AM et al. Short duration electrical stimulation to enhance neurite outgrowth and maturation of adult neural stem progenitor cells. *Ann Biomed Eng.* 2014;40(10): 2164-2176.
47. Haastert-Talini K, Grothe C. Electrical stimulation for promoting peripheral nerve regeneration. *Int Rev Neurobiol*. 2013;109: 111-24.
48. Huang J, Zhang Y, Lu L et al. Electrical stimulation accelerates nerve regeneration and functional recovery in delayed peripheral nerve injury in rats. *Eur J Neurosci.* 2013;38(12): 3691-3701.
49. Koppes AN, Nordberg AL, Paolillo G et al. Electrical stimulation of schwann cells promotes sustained increases in neurite outgrowth. *Tissue Eng Part A*. 2014;20(3-4): 494-506..
50. Luo B, Huang J, Lu L et al. Electrically induced brain-derived neurotrophic factor release from schwann cells. *J Neurosci Res*. 2014;92(7): 893-903.
51. Schmidt CE, Shastri VR, Vacanti JP et al. Stimulation of neurite outgrowth using an electrically conducting polymer. *Proc Natl Acad Sci U S A.* 1997;94(17): 8948-8953.
52. Liu X, Gilmore KJ, Moulton SE et al. Electrical stimulation promotes nerve cell differentiation on polypyrrole/poly (2-methoxy-5 aniline sulfonic acid) composites. *J Neural Eng.* 2009;6(6): 065002.
53. Kotwal A, Schmidt CE. Electrical stimulation alters protein adsorption and nerve cell interactions with electrically conducting biomaterials. *Biomaterials.* 2001;22(10): 1055-1064.
54. Wiesmann H, Hartig M, Stratmann U et al. Electrical stimulation influences mineral formation of osteoblast-like cells in vitro. *Biochim Biophys Acta.* 2001;1538(1): 28-37.
55. Griffin M, Sebastian A, Colthurst J et al. Enhancement of differentiation and mineralisation of osteoblast-like cells by degenerate electrical waveform in an in vitro electrical stimulation model compared to capacitive coupling. *PLoS One*. 2013;8(9): e72978.

56. Clark CC, Wang W, Brighton CT. Up-regulation of expression of selected genes in human bone cells with specific capacitively coupled electric fields. *J Orthop Res.* 2014;32(7): 894-903.
57. Ercan B, Webster TJ. The effect of biphasic electrical stimulation on osteoblast function at anodized nanotubular titanium surfaces. *Biomaterials.* 2010;31(13): 3684-3693.
58. Gittens RA, Olivares-Navarrete R, Rettew R et al. Electrical polarization of titanium surfaces for the enhancement of osteoblast differentiation. *Bioelectromagnetics*. 2013;34(8): 599-612.
59. Meng S, Rouabhia M, Zhang Z. Electrical stimulation modulates osteoblast proliferation and bone protein production through heparin-bioactivated conductive scaffolds. *Bioelectromagnetics.* 2013;34(3): 189-199.
60. Zhang J, Neoh KG, Hu X et al. Combined effects of direct current stimulation and immobilized BMP-2 for enhancement of osteogenesis. *Biotechnol Bioeng.* 2013;110(5): 1466-1475.
61. Zhuang H, Wang W, Seldes RM et al. Electrical stimulation induces the level of TGF-beta1 mRNA in osteoblastic cells by a mechanism involving calcium/calmodulin pathway. *Biochem Biophys Res Commun*. 1997;237(2): 225-229.
62. Hu WW, Hsu YT, Cheng YC et al. Electrical stimulation to promote osteogenesis using conductive polypyrrole films. *Mater Sci Eng C Mater Biol Appl*. 2014;37: 28-36.
63. Bourguignon GJ, Jy W, Bourguignon LY. Electric stimulation of human fibroblasts causes an increase in Ca^{2+} influx and the exposure of additional insulin receptors. *J Cell Physiol.* 1989;140(2): 379-385.
64. Sebastian A, Syed F, McGrouther DA et al. A novel in vitro assay for electrophysiological research on human skin fibroblasts: degenerate electrical waves downregulate collagen I expression in keloid fibroblasts. *Exp Dermatol.* 2011;20(1): 64-68.
65. Todd I, Clothier RH, Huggins ML et al. Electrical stimulation of transforming growth factor-beta 1 secretion by human dermal fibroblasts and the U937 human monocytic cell line. *Altern Lab Anim.* 2001;29(6): 693-701.
66. Cho MR, Marler JP, Thatte HS et al. Control of calcium entry in human fibroblasts by frequency-dependent electrical stimulation. *Front Biosci.* 2002;7: a1-a8.
67. Soong HK, Parkinson WC, Sulik GL et al. Effects of electric fields on cytoskeleton of corneal stromal fibroblasts. *Curr Eye Res*. 1990;9(9): 893-901.

68. Chen QQ, Zhang W, Chen XF et al. Electrical field stimulation induces cardiac fibroblast proliferation through the calcineurin-NFAT pathway. *Can Physiol Pharmacol.* 2012;90(12): 1611-1622.
69. Harris AK, Pryer NK, Paydarfar D. Effects of electric fields on fibroblast contractility and cytoskeleton. *J Exp Zool*. 1990;253(2): 163-176.
70. Bourguignon GJ, Bourguignon LY. Electric stimulation of protein and DNA synthesis in human fibroblasts. *FASEB J.* 1987;1: 398-402.
71. Blume G, Müller-Wichards W, Goepfert C et al. Electrical stimulation of NIH-3T3 cells with platinum-PEDOT-electrodes integrated in a bioreactor. *Open Biomed Eng J*. 2013;7: 125-132.
72. Antov Y, Barbul A, Mantsur H et al. Electroendocytosis: exposure of cells to pulsed low electric fields enhances adsorption and uptake of macromolecules. *Biophys J*. 2005;88(3): 2206-2223.
73. Sun S, Cho M. Human fibroblast migration in three-dimensiional collagen gel in response to noninvasive electrical stimulation. *Tissue Eng*. 2004;10(9-10): 1558-1565
74. Onuma EK, Hui SW. Electric field-directed cell shape changes, displacement, and cytoskeletal reorganization are calcium dependent. *J Cell Biol*. 1988;106(6): 2067-2075.
75. Ugarte G, Brandan E. Transforming growth factor beta (TGF-beta) signalling is regulated by electrical activity in skeletal muscle cells. TGF-beta type I receptor is transcriptionally regulated by myotube excitability. *J Biol Chem.* 2006;281(27): 18473-18481.
76. Brighton CT, Wang W, Seldes R et al. Signal transduction in electrically stimulated bone cells. *J Bone Jt Surg Am.* 2001;83-A(10): 1514-1523.
77. Huang J, Ye Z, Hu X et al. Electrical stimulation induces calcium-dependent release of NGF from cultured Schwann cells. *Glia.* 2010;58(5): 622-631.
78. Xu J, Wang W, Clark CC et al. Signal transduction in electrically stimulated articular chondrocytes involves translocation of extracellular calcium through voltage-gated channels. *Osteoarthr Cartil.* 2009;17(3): 397-405.
79. Chang YJ, Hsu CM, Lin CH et al. Electrical stimulation promotes nerve growth factor-induced neurite outgrowth and signalling. *Biochim Biophys Acta - Gen Subj.* 2013;1830(8): 4130-4136.
80. Fukui T, Dai Y, Iwata K et al. Frequency-dependent ERK phosphorylation in spinal neurons by electric stimulation of the sciatic nerve and the role in electrophysiological activity. *Mol Pain.* 2007;3: 18.

81. Li F, Chen T, Hu S et al. Superoxide mediates direct current electric field-induced directional migration of glioma cells through the activation of AKT and ERK. *PLoS One.* 2013;8(4): e61195.
82. Wu Y, Collier L, Qin W et al. Electrical stimulation modulates Wnt signalling and regulates genes for the motor endplate and calcium binding in muscle of rats with spinal cord transection. *BMC Neurosci.* 2013;14(1): 81.
83. Morino-Koga S, Yano S, Kondo T et al. Insulin receptor activation through its accumulation in lipid rafts by mild electrical stress. *J Cell Physiol*. 2013;228(2): 439-446.
84. Koga T, Kai Y, Fukuda R et al. Mild electrical stimulation and heat shock ameliorates progressive proteinuria and renal inflammation in mouse model of alport syndrome. *PLoS One.* 2012;7(8): e43852.
85. Fukuda R, Suico MA, Koyama K et al. Mild electrical stimulation at 0.1-ms pulse width induces p53 protein phosphorylation and G2 arrest in human epithelial cells. *J Biol Chem*. 2013;288(22): 16117-16126.
86. Matsuyama S, Moriuchi M, Suico MA et al. Mild electrical stimulation increases stress resistance and suppresses fat accumulation via activation of LKB1-AMPK signalling pathway in C.elegans. *PLoS One*. 2014;9(12): e114690
87. Wang Y, Rouabhia M, Lavertu D et al. Pulsed electrical stimulation modulates fibroblasts' behaviour through the Smad signalling pathway. *J Tissue Eng Regen Med*. 2015; doi: 10.1002/term.2014.
88. Gurtner GC, Werner S, Barrandon Y et al. Wound repair and regeneration. *Nature.* 2008;453: 314-321.
89. Diegelmann RF, Evans MC. Wound healing: an overview of acute, fibrotic and delayed healing. *Front Biosci*. 2004;9(4):283-289.
90. Gill SE, Parks WC. Metalloproteinases and their inhibitors: regulators of wound healing. *Int J Biochem.* 2009;40(206): 1334-1347.
91. Grose R, Werner S. Wound-healing studies in transgenic and knockout mice. *Mol Biotechnol.* 2004;28: 147-166.
92. McCarty SM, Percival SL. Proteases and delayed wound healing. *Adv Wound Care.* 2013;2(8): 438-447.
93. Singer AJ, Clark RA. Cutaneous wound healing. *N Engl J Med.* 1999;341: 738-746.
94. Hsu YC, Li L, Fuchs E. Emerging interactions between skin stem cells and their niches. *Nat Med.* 2014;20(8): 847-856.

95. Ansell DM, Kloepper JE, Thomason HA et al. Exploring the "hair growth-wound healing connection": anagen phase promotes wound re-epithelialization. *J Invest Dermatol.* 2011;131: 518-528.

96. Ito M, Liu Y, Yang Z et al. Stem cells in the hair follicle bulge contribute to wound repair but not to homeostasis of the epidermis. *Nat Med.* 2005;11(12): 1351-1354.

97. Heldin CH, Eriksson U, Östman A. New members of the platelet-derived growth factor family of mitogens. *Arch Biochem Biophys*. 2002;398(2): 284-290.

98. Heldin CH, Westermark B. Mechanism of action and in vivo role of platelet-derived growth factor. *Physiol Rev.* 1999;79(4): 1283-1316.

99. Mandracchia VJ, Sanders SM, Frerichs JA. The use of becaplermin (rhPDGF-BB) gel for chronic nonhealing ulcers. A retrospective analysis. *Clin Podiatr Med Surg.* 2001;18(1): 189-209.

100. Kuoz M. Interleukin-6 Induced Basic Fibroblast Growth factor-dependent angiogenesis in aasal cell carcinoma Cell Line via JAK/STAT3 and PI3-Kinase/Akt Pathways. *J Biol Chem.* 2004: 1169-1175.

101. Xue H, McCauley RL, Zhang W. Elevated interleukin-6 expression in keloid fibroblasts. *J Surg Res.* 2000;89: 74-77.

102. Heinrich PC, Behrmann I, Haan S et al. Principles of interleukin (IL)-6-type cytokine signalling and its regulation. *Biochem J.* 2003;374: 1-20.

103. Finch PW, Rubin JS. Keratinocyte growth factor/fibroblast growth factor 7, a homeostatic factor with therapeutic potential for epithelial protection and repair. *Adv Cancer Res.* 2004;91:69-136.

104. Ferrara N, Davis-Smyth T. The biology of vascular endothelial growth factor. *Endocr Rev.* 1997;18(1): 4-25.

105. Wilgus TA, Ferreira AM, Oberyszyn TM et al. Regulation of scar formation by vascular endothelial growth factor. *Lab Invest*. 2008;88(6): 579-590.

106. Frazier K, Williams S, Kothapalli D et al. Stimulation of fibroblast cell growth, matrix production, and granulation tissue formation by connective tissue growth factor. *J Invest Dermatol*. 1996;107(3): 404-411.

107. Kubota S, Takigawa M. The role of CCN2 in cartilage and bone development. *J Cell Commun Signal.* 2011;5: 209-217.

108. Chen CC, Lau LF. Functions and mechanisms of action of CCN matricellular proteins. *Int J Biochem Cell Biol.* 2009;41(4): 771-783.

109. Wang Q, Usinger W, Nichols B et al. Cooperative interaction of CTGF and TGF-beta in animal models of fibrotic disease. *Fibrogenesis Tissue Repair*. 2011;4(1): 4.

110. Inoki I, Shiomi T, Hashimoto G et al. Connective tissue growth factor binds vascular endothelial growth factor (VEGF) and inhibits VEGF-induced angiogenesis. *FASEB J.* 2002;16(2): 219-221.

111. Turner N, Grose R. Fibroblast growth factor signalling: from development to cancer. *Nat Rev Cancer.* 2010;10(2): 116-129.

112. Traversa B, Sussman G. The role of growth factors , cytokines and proteases in wound management. *Prim Intent.* 2001;9(4): 161-167.

113 Cross MJ, Claesson-Welsh L. FGF and VEGF function in angiogenesis: signalling pathways, biological responses and therapeutic inhibition. *Trends Pharmacol Sci*. 2001;22(4): 201-207.

114. Pastar I, Stojadinovic O, Yin NC et al. Epithelialization in Wound Healing: A Comprehensive Review. *Adv Wound Care.* 2014;3(7): 445-464.

115. Lawrence DA. Transforming growth factor-beta: a general review. *Eur Cytokine Netw.* 1996;7(3): 363-374.

116. Walshe TE, Saint-Geniez M, Maharaj AS et al. TGF-β Is required for vascular barrier function, endothelial survival and homeostasis of the adult microvasculature. *PLoS One.* 2009;4(4): e5149.

117. Shigematsu S, Yamauchi K, Nakajima K et al. IGF-1 regulates migration and angiogenesis of human endothelial cells. *Endocr J.* 1999;46 Suppl: S59-S62.

118. Iwabu A, Smith K, Allen FD et al. Epidermal growth factor induces fibroblast contractility and motility via a protein kinase C delta-dependent pathway. *J Biol Chem.* 2004;279(15): 14551-14560.

119. Maretzky T, Evers A, Zhou W et al. Migration of growth factor-stimulated epithelial and endothelial cells depends on EGFR transactivation by ADAM17. *Nat Commun*. 2011;2: 229.

120. Sandberg T, Ehinger A, Casslen B. Paracrine stimulation of capillary endothelial cell migration by endometrial tissue involves epidermal growth factor and is mediated via up-regulation of the urokinase plasminogen activator receptor. *J Clin Endocrinol Metab*. 2001;86(4): 1724-1730.

121. Mehta VB, Besner GE. HB-EGF promotes angiogenesis in endothelial cells via PI3-kinase and MAPK signalling pathways. *Growth Factors*. 2007;25(4): 253-263.

122. King A, Balaji S, Le LD et al. Regenerative wound healing: The Role of Interleukin-10. *Adv wound care.* 2014;3(4): 315-323.

123. Gabay C, Lamacchia C, Palmer G. IL-1 pathways in inflammation and human diseases. *Nat Rev Rheumatol*. 2010;6(4): 232-241.

124. Rapala K. The effect of tumor necrosis factor-alpha on wound healing. An experimental study. *Ann Chir Gynaecol Suppl.* 1996;211: 1-53.

125. Werner S, Grose R. Regulation of wound healing by growth factors and cytokines. Physiol Rev. 2003;83:835-870.

126. Kawamoto K, Matsuda H. Nerve growth factor and wound healing. *Prog Brain Res*. 2004;146: 369-384.

127. Fang Y, Gong SJ, Xu YH et al. Impaired cutaneous wound healing in granulocyte/macrophage colony-stimulating factor knockout mice. *Br J Dermatol.* 2007;157(3): 458-465.

128. Jyung RW, Wu L, Pierce GF et al. Granulocyte-macrophage colony-stimulating factor and granulocyte colony-stimulating factor: differential action on incisional wound healing. *Surgery*. 1994;115(3): 325-334.

129. Sappino AP, Schurch W, Gabbiani G. Differentiation repertoire of fibroblastic cells: expression of cytoskeletal proteins as marker of phenotypic modulations. *Lab Invest.* 1990;63(2): 144-161.

130. Darby IA, Hewitson TD. Fibroblast differentiation in wound healing and fibrosis. *Int Rev Cytol*. 2007;257(07): 143-179.

131. Porter S. The role of the fibroblast in wound contraction and healing. *Wounds UK*. 2007;3(1): 33-40.

132. Visse R, Nagase H. Matrix metalloproteinases and tissue inhibitors of metalloproteinases: Structure, function, and biochemistry. *Circ Res.* 2003;92: 827-839.

133. Hinz B, Phan SH, Thannickal VJ et al. The myofibroblast: one function, multiple origins. *Am J Pathol.* 2007;170: 1807-1816.

134. Abe R, Donnelly SC, Peng T et al. Peripheral blood fibrocytes: differentiation pathway and migration to wound sites. *J Immunol.* 2001;166(12): 7556-7562.

135. Hinz B, Celetta G, Tomasek JJ et al. Alpha-smooth muscle actin expression upregulates fibroblast contractile activity. *Mol Biol Cell*. 2001;12(9): 2730-2741.

136. Hinz B. Formation and function of the myofibroblast during tissue repair. *J Invest Dermatol.* 2007;127: 526-537.

137. Werner S, Krieg T, Smola H. Keratinocyte-fibroblast interactions in wound healing. *J Invest Dermatol.* 2007;127: 998-1008.

138. Villaschi S, Nicosia RF. Paracrine interactions between fibroblasts and endothelial cells in a serum-free coculture model. Modulation of angiogenesis and collagen gel contraction. *Lab Invest.* 1994;71(2): 291-299.

139. Steinhauser ML, Kunkel SL, Hogaboam CM et al. Macrophage/fibroblast coculture induces macrophage inflammatory protein-1alpha production mediated by intercellular adhesion molecule-1 and oxygen radicals. *J Leukoc Biol*. 1998;64: 636-641.

140. McGee HM, Schmidt B, Booth CJ et al. Interleukin-22 promotes fibroblast-mediated wound repair in the skin. *J Invest Dermatol.* 2013;133(5): 1321-1329.
141. Ornitz DM, Itoh N. Fibroblast growth factors. *Genome Biol.* 2001;2(3): REVIEWS3005.
142. Turner N, Grose R. Fibroblast growth factor signalling: from development to cancer. *Nat Rev Cancer*. 2010;10: 116-129.
143. Eswarakumar VP, Lax I, Schlessinger J. Cellular signalling by fibroblast growth factor receptors. *Cytokine Growth Factor Rev*. 2005;16(2): 139-149.
144. Hart KC, Robertson SC, Kanemitsu MY et al. Transformation and Stat activation by derivatives of FGFR1, FGFR3, and FGFR4. *Oncogene*. 2000;19: 3309-3320.
145. Cao Y, Ekstrom M, Pettersson RF. Characterization of the nuclear translocation of acidic fibroblast growth factor. *J Cell Sci.* 1993;104 (Pt 1): 77-87.
146. Zhan X, Hu X, Friedman S et al. Analysis of endogenous and exogenous nuclear translocation of fibroblast growth factor-1 in NIH 3T3 cells. *Biochem Biophys Res Commun*. 1992;188(3): 982-991.
147. Mori S, Wu CY, Yamaji S et al. Direct binding of integrin αvβ3 to FGF1 plays a role in FGF1 signalling. *J Biol Chem.* 2008;283(26): 18066-18075.
148. Mellin TN, Mennie RJ, Cashen DE et al. Acidic fibroblast growth factor accelerates dermal wound healing. *Growth Factors.* 1992;7(1): 1-14
149. MacFarlane LA, Murphy P. FGF2 (fibroblast growth factor 2 (basic)). Atlas Genet Cytogenet Oncol Haematol. 2011;15(2).
150. Okada-Ban M, Thiery JP, Jouanneau J. Fibroblast growth factor-2. *Int J Biochem Cell Biol.* 2000;32(3): 263-267.
151. Woodbury ME, Ikezu T. Fibroblast growth factor-2 signalling in neurogenesis and neurodegeneration. *J Neuroimmune Pharmacol.* 2014;9(2): 92-101.
152. Gressner AM, Weiskirchen R, Breitkopf K et al. Roles of TGF-beta in hepatic fibrosis. *Front Biosci.* 2002;7: d793-d807.
153. Brown PD, Wakefield LM, Levinson AD et al. Physicochemical activation of recombinant latent transforming growth factor-beta's 1, 2, and 3. *Growth Factors*. 1990;3(1): 35-43.
154. Fortunel NO, Hatzfeld A, Hatzfeld JA. Transforming growth factor- beta: pleiotropic role in the regulation of hematopoiesis. *Blood.* 2000;96(6): 2022-2036.
155. Lyons RM, Gentry LE, Purchio AF et al. Mechanism of activation of latent recombinant transforming growth factor beta 1 by plasmin. *J Cell Biol.* 1990;110(4): 1361-1367.

156. Verderio E, Gaudry C, Gross S et al. Regulation of cell surface tissue transglutaminase: effects on matrix storage of latent transforming growth factor-beta binding protein-1. *J Histochem Cytochem*. 1999;47(11): 1417-1432.

157. Schultz-Cherry S, Lawler J, Murphy-Ullrich JE. The type 1 repeats of thrombospondin 1 activate latent transforming growth factor-beta. *J Biol Chem.* 1994;269(43): 26783-26788.

158 Wipff PJ, Hinz B. Integrins and the activation of latent transforming growth factor beta1 - an intimate relationship. *Eur J Cell Biol.* 2008;87(8-9): 601-615.

159. Moustakas A, Heldin CH. The regulation of TGFbeta signal transduction. *Development.* 2009;136(22): 3699-3714.

160. Helm CA, Knoll W, Israelachvili JN. Measurement of ligand receptor interactions. *Proc Natl Acad Sci U S A*. 1991;88: 8169-8173.

161. Petukh M, Stefl S, Alexov E. The role of protonation states in ligand-receptor recognition and binding. *Curr Pharm Des*. 2013;19(23): 4182-4190.

162. Nielsen JE. Analysing the pH-dependent properties of proteins using pKa calculations. *J Mol Graph Model.* 2007;25(5): 691-699.

163. Zacharias N, Dougherty DA. Cation-π interactions in ligand recognition and catalysis. *Trends Pharmacol Sci*. 2002;23(6): 281-287.

164. Meszaros B, Simon I, Dosztanyi Z. The expanding view of protein-protein interactions: complexes involving intrinsically disordered proteins. *Phys Biol.* 2011;8(3): 35003.

165. Vijayakumar M, Wong KY, Schreiber G et al. Electrostatic enhancement of diffusion-controlled protein-protein association: comparison of theory and experiment on barnase and barstar. *J Mol Biol*. 1998;278(5): 1015-1024.

166. Gao M, Skolnick J. The distribution of ligand-binding pockets around protein-protein interfaces suggests a general mechanism for pocket formation. *Proc Natl Acad Sci USA*. 2012;109(10): 3784-3789.

167. Fredriksson R, Lagerstrom MC, Lundin LG et al. The G-protein-coupled receptors in the human genome form five main families. Phylogenetic analysis, paralogon groups, and fingerprints. *Mol Pharmacol.* 2003;63(6): 1256-1272.

168. Alberts B, Johnson A, Lewis J et al. Molecular Biology of the Cell. 4th edition. New York: Garland Science; 2002. Signalling through G-Protein-Linked Cell-Surface Receptors.

169. Paravicini TM, Chubanov V, Gudermann T. TRPM7: a unique channel involved in magnesium homeostasis. *Int J Biochem Cell Biol*. 2012;44(8): 1381-1384.

170. Shi M, Zhu J, Wang R et al. Latent TGF-β structure and activation. *Nature.* 2011;474(7351): 343-349.

171. Poniatowski LA, Wojdasiewicz P, Gasik R et al. Transforming growth factor beta family: insight into the role of growth factors in regulation of fracture healing biology and potential clinical applications. *Mediators Inflamm*. 2015;2015:137823.
172. Shi Y, Massagué J. Mechanisms of TGF-beta signalling from cell membrane to the nucleus. *Cell.* 2003;113(6): 685-700.
173. Ten Dijke P, Hill CS. New insights into TGF-beta-Smad signalling. *Trends Biochem Sci.* 2004;29(5): 265-273.
174. Moustakas A, Heldin C-H. The regulation of TGFbeta signal transduction. *Development*. 2009;136: 3699-3714.
175. Wu JW, Fairman R, Penry J et al. Formation of a Stable Heterodimer between Smad2 and Smad4. *J Biol Chem.* 2001;276: 20688-20694.
176. Hariharan R, Pillai MR. Structure-function relationship of inhibitory Smads: Structural flexibility contributes to functional divergence. *Proteins Struct Funct Genet.* 2008;71: 1853-1862.
177. Kavsak P, Rasmussen RK, Causing CG et al. Smad7 binds to Smurf2 to form an E3 ubiquitin ligase that targets the TGF beta receptor for degradation. *Mol Cell.* 2000;6(6): 1365-1375.
178. Hata A, Lagna G, Massague J et al. Smad6 inhibits BMP/Smad1 signalling by specifically competing with the Smad4 tumor suppressor. *Genes Dev*. 1998;12(2): 186-197.
179. Aragón E, Goerner N, Xi Q et al. Structural basis for the versatile interactions of Smad7 with regulator WW domains in TGF-β pathways. *Structure*. 2012;20: 1726-1736.
180. Wu JW, Krawitz AR, Chai J et al. Structural mechanism of Smad4 recognition by the nuclear oncoprotein Ski: Insights on Ski-mediated repression of TGF-β signalling. *Cell.* 2002;111: 357-367.
181. Baburajendran N, Jauch R, Tan CY et al. Structural basis for the cooperative DNA recognition by Smad4 MH1 dimers. *Nucleic Acids Res*. 2011;39(18): 8213-8222.
182. BabuRajendran N, Palasingam P, Narasimhan K et al. Structure of Smad1 MH1/DNA complex reveals distinctive rearrangements of BMP and TGF-β effectors. *Nucleic Acids Res.* 2010;38: 3477-3488.
183. Schmierer B, Hill CS. TGFbeta-SMAD signal transduction: molecular specificity and functional flexibility. *Nat Rev Mol Cell Biol.* 2007;8(12): 970-982.
184. Chen W, Fu X, Sheng Z. Review of current progress in the structure and function of Smad proteins. *Chin Med J (Engl)*. 2002;115(3): 446-450.
185. Miyazono K, ten Dijke P, Heldin CH. TGF-beta signaling by Smad proteins. *Adv Immunol.* 2000;75: 115-157.

186. Wu JW, Hu M, Chai J et al. Crystal structure of a phosphorylated Smad2: Recognition of phosphoserine by the MH2 domain and insights on Smad function in TGF-β signalling. *Mol Cell.* 2001;8: 1277-1289.
187. Zhang YE. Non-Smad pathways in TGF-beta signalling. *Cell Res.* 2009;19(1):128-139.
188. Lu Z, Xu S. ERK1/2 MAP kinases in cell survival and apoptosis. *IUBMB Life*. 2006;58: 621-631.
189. Farooq A, Zhou MM. Structure and regulation of MAPK phosphatases. *Cell Signal*. 2004;16(7): 769-779.
190. MacGillivray MK, Cruz TF, McCulloch CA. The recruitment of the interleukin-1 (IL-1) receptor-associated kinase (IRAK) into focal adhesion complexes is required for IL-1beta -induced ERK activation. *J Biol Chem.* 2000;275(31): 23509-23515.
191. Gotoh I, Adachi M, Nishida E. Identification and characterization of a novel MAP kinase kinase kinase, MLTK. *J Biol Chem.* 2001;276(6): 4276-4286.
192. Salmeron A, Ahmad TB, Carlile GW et al. Activation of MEK-1 and SEK-1 by Tpl-2 proto-oncoprotein, a novel MAP kinase kinase kinase. *EMBO J*. 1996;15(4): 817-826.
193. Anjum R, Blenis J. The RSK family of kinases: emerging roles in cellular signalling. *Nat Rev Mol Cell Biol.* 2008;9(10): 747-758.
194. Roskoski R. ERK1/2 MAP kinases: Structure, function, and regulation. *Pharmacol Res.* 2012;66(2): 105-143.
195. Peti W, Page R. Molecular basis of MAP kinase regulation. *Protein Sci.* 2013;22(1):1698-1710.
196. McCubrey JA, Steelman LS, Chappell WH et al. Roles of the Raf/MEK/ERK pathway in cell growth, malignant transformation and drug resistance. *Biochim Biophys Acta - Mol Cell Res.* 2007;1773: 1263-1284.
197. Meloche S, Pouysségur J. The ERK1/2 mitogen-activated protein kinase pathway as a master regulator of the G1- to S-phase transition. *Oncogene*. 2007;26: 3227-3239.
198. Mooz J, Oberoi-Khanuja TK, Harms GS et al. Dimerization of the kinase ARAF promotes MAPK pathway activation and cell migration. *Sci Signal.* 2014;7: ra73-ra73.
199. Hayden MS, Ghosh S. Shared principles in NF-κB Signalling. *Cell.* 2008;132: 344-362.
200. Gilmore TD. Introduction to NF-kappaB: players, pathways, perspectives. *Oncogene.* 2006;25: 6680-6684.

201. Hoesel B, Schmid JA. The complexity of NF-κB signalling in inflammation and cancer. *Mol Cancer.* 2013;12(1):86.
202. Hayden MS, Ghosh S. Signalling to NF-kB. *Genes Dev*. 2004;18: 2195-2224.
203. Scollay R. Control of T-cell development. *Nature.* 1985;314(6006):16.
204. Khandelwal N, Simpson J, Taylor G et al. Nucleolar NF-κB/RelA mediates apoptosis by causing cytoplasmic relocalization of nucleophosmin. *Cell Death Differ*. 2011;18(12): 1889-1903.
205. Barré B, Perkins ND. A cell cycle regulatory network controlling NF-κB subunit activity and function. *EMBO J*. 2007;26(23): 4841-4855.
206. Guttridge DC, Albanese C, Reuther JY et al. NF-kappaB controls cell growth and differentiation through transcriptional regulation of cyclin D1. *Mol Cell Biol.* 1999;19(8): 5785-5799.
207. McCaig CD. Controlling cell behavior electrically: current views and future potential. *Physiol Rev.* 2005;85: 943-978.
208. Song B, Zhao M, Forrester J V et al. Electrical cues regulate the orientation and frequency of cell division and the rate of wound healing in vivo. *Proc Natl Acad Sci U S A*. 2002;99(21): 13577-13582.
209. Sta Iglesia DD, Vanable JW Jr. Endogenous lateral electric fields around bovine corneal lesions are necessary for and can enhance normal rates of wound healing. *Wound Repair Regen.* 1998;6(6): 531-542.
210. Cotsarelis G, Cheng SZ, Dong G et al. Existence of slow-cycling limbal epithelial basal cells that can be preferentially stimulated to proliferate: implications on epithelial stem cells. *Cell.* 1989;57(2): 201-209.
211. Shi G, Zhang Z, Rouabhia M. The regulation of cell functions electrically using biodegradable polypyrrole-polylactide conductors. *Biomaterials.* 2008;29(28): 3792-3798.
212. Zhao M. Electrical fields in wound healing—An overriding signal that directs cell migration *Semin Cell Dev Biol*. 2009;20(6): 674-682.
213. Chiang M., Robinson KR, Vanable JW Jr. Electrical fields in the vicinity of epithelial wounds in the isolated bovine eye. *Exp. Eye Res.* 1992;54(6): 999-1003.
214. Mehmandoust FG, Torkaman G, Firoozabadi M et al. Anodal and cathodal pulsed electrical stimulation on skin wound healing in guinea pigs. *J Rehabil Res Dev.* 2007;44(4): 611-618.
215. Thawer HA, Houghton PE. Effects of electrical stimulation on the histological properties of wounds in diabetic mice. *Wound Repair Regen*. 2001;9: 107-115.

216. Kloth LC. Electrical stimulation for wound healing: a review of evidence from in vitro studies, animal experiments, and clinical trials. *Int J Low Extrem Wounds*. 2005;4: 23-44.
217. Sumano H, Goiz G, Clifford V. Use of electrical stimulation for wound healing in dogs. *Isr J Vet Med.* 2002: 57(2).
218. Thakral G, LaFontaine J, Najafi B et al. Electrical stimulation to accelerate wound healing. *Diabet Foot Ankle*. 2013;4: 1-9.
219. Kloth LC, Feedar JA. Acceleration of wound healing with high voltage, monophasic, pulsed current. *Phys Ther.* 1988;68: 503-508.
220. Feedar JA, Kloth LC, Gentzkow GD. Chronic dermal ulcer healing enhanced with monophasic pulsed electrical stimulation. *Phys Ther.* 1991;71: 639-649.
221. Lundeberg TC, Eriksson SV, Malm M. Electrical nerve stimulation improves healing of diabetic ulcers. *Ann Plast Surg*. 1992;29: 328-331.
222. Baker L, Chambers R, DeMuth S et al. Effects of electrical stimulation on wound healing in patients with diabetic ulcers. *Diabetes Care*. 1997;20(3): 405-412.
223. Margara A, Boriani F, Obbialero FD et al. Frequency rhythmic electrical modulation system in the treatment of diabetic ulcers. Preliminary encouraging report. *Chirurgia (Bucur).* 2008;21: 311-314.
224. Ud-Din S, Bayat A. Electrical stimulation and cutaneous wound healing: a review of clinical evidence. *Healthcare.* 2014;2(4): 445-467.
225. Balakatounis KC, Angoules AG. Low-intensity electrical stimulation in wound healing: review of the efficacy of externally applied currents resembling the current of injury. *Eplasty.* 2008;8(Lic): e28.
226. Xu F, Zhang C, Graves DT. Abnormal cell responses and role of TNF-α in impaired diabetic wound healing. *Biomed Res Int.* 2013;2013: 754802.
227. Zanetti M, Weishaupt D. MR imaging of the forefoot: morton neuroma and differential diagnoses. *Semin Musculoskelet Radiol.* 2005;9(3): 175-186.
228. Gurtner GC. Chapter 2: Wound healing: normal and abnormal. *Grabb Smith's Plast Surgery,* Sixth Ed by Charles H Thorne. 2007.
229. Weller R, Hunter JA, Savin J et al. *Clinical Dermatology (4th Ed)*. Wiley; 2009.
230. Sakai N, Tager AM. Fibrosis of two: Epithelial cell-fibroblast interactions in pulmonary fibrosis. *Biochim Biophys Acta - Mol Basis Dis.* 2013;1832(7): 911-921.
231. Robles DT, Berg D. Abnormal wound healing: keloids. *Clin Dermatol*. 2007;25: 26-32.

232. Chronakis IS, Grapenson S, Jakob A. Conductive polypyrrole nanofibres via electrospinning: Electrical and morphological properties. *Polymer (Guildf)*. 2006;47: 1597-1603.
233. Li M, Guo Y, Wei Y et al. Electrospinning polyaniline-contained gelatin nanofibres for tissue engineering applications. *Biomaterials.* 2006;27: 2705-2715.
234. Cui X, Wiler J, Dzaman M et al. In vivo studies of polypyrrole / peptide coated neural probes. *Mater Sci.* 2003;24: 777-787.
235. Bidez PR, Li S, Macdiarmid AG et al. Polyaniline, an electroactive polymer, supports adhesion and proliferation of cardiac myoblasts. *J Biomater Sci Polym Ed.* 2006;17: 199-212.
236. Wang YL, Rouabhia M, Zhang Z. PPy-coated PET fabrics and electric pulse-stimulated fibroblasts. *J Mater Chem B.* 2013;1: 3789-3796.
237. Oh JS, Kim KN, Yeom GY. Graphene doping methods and device applications. *J Nanosci Nanotechnol.* 2014;14: 1120-1133.
238. Huang X, Zeng Z, Fan Z et al. Graphene-based electrodes. *Adv Mater*. 2012;24: 5979-6004.
239. Shi Z, Phillips GO, Yang G. Nanocellulose electroconductive composites. *Nanoscale*. 2013;5: 3194-3201.
240. Kai D, Prabhakaran MP, Jin G et al. Polypyrrole-contained electrospun conductive nanofibrous membranes for cardiac tissue engineering. *J Biomed Mater Res - Part A.* 2011;99 A: 376-385.
241. Shi G, Rouabhia M, Meng S et al. Electrical stimulation enhances viability of human cutaneous fibroblasts on conductive biodegradable substrates. *J Biomed Mater Res - Part A*. 2008;84: 1026-1037.
242. Jiang X, Marois Y, Traoré A et al. Tissue reaction to polypyrrole-coated polyester fabrics: an in vivo study in rats. *Tissue Eng.* 2002;8(4): 635-647.
243. Rouabhia M, Park H, Meng S et al. Electrical stimulation promotes wound healing by enhancing dermal fibroblast activity and promoting myofibroblast transdifferentiation. *PLoS One.* 2013;8(8): e71660.
244. Guiseppi-Elie A. Electroconductive hydrogels: synthesis, characterization and biomedical applications. *Biomaterials.* 2010;31(10): 2701-2716.
245. Balint R, Cassidy NJ, Cartmell SH. Conductive polymers: towards a smart biomaterial for tissue engineering. *Acta Biomater.* 2014;10(6): 2341-2353.
246. Jin G, Li K. The electrically conductive scaffold as the skeleton of stem cell niche in regenerative medicine. *Mater Sci Eng C.* 2014;45: 671-681.
247. Kong L, Chen W. Carbon nanotube and graphene-based bioinspired electrochemical actuators. *Adv Mater.* 2014;26: 1025-1043.

248. Hadjizadeh A, Doillon CJ. Directional migration of endothelial cells towards angiogenesis using polymer fibres in a 3D co-culture system. *J Tissue Eng Regen Med*. 2010;4: 524-531.
249. Alvares D, Wieczorek L, Raguse B et al. Development of nanoparticle film-based multi-axial tactile sensors for biomedical applications. *Sensor Actuat A-Phys*. 2013;196: 38-47.
250. Green RA, Lovell NH, Wallace GG et al. Conducting polymers for neural interfaces: Challenges in developing an effective long-term implant. *Biomaterials.* 2008;29: 3393-3399.
251. Aregueta-Robles UA, Woolley AJ, Poole-Warren LA et al. Organic electrode coatings for next-generation neural interfaces. *Front Neuroeng.* 2014;7: 15.
252. Zhang Z, Rouabhia M, Wang Z et al. Electrically conductive biodegradable polymer composite for nerve regeneration: electricity-stimulated neurite outgrowth and axon regeneration. *Artif Organs*. 2007;31(1): 13-22.
253. Meng S, Rouabhia M, Shi G et al. Heparin dopant increases the electrical stability, cell adhesion, and growth of conducting polypyrrole/poly(L,L-lactide) composites. *J Biomed Mater Res Part A*. 2008;87: 332-344.
254. Jakubiec B, Marois Y, Zhang Z et al. In vitro cellular response to polypyrrole-coated woven polyester fabrics: Potential benefits of electrical conductivity. *J Biomed Mater Res.* 1998;41: 519-526.
255. Shi G, Zhang Z, Rouabhia M. The regulation of cell functions electrically using biodegradable polypyrrole-polylactide conductors. *Biomaterials.* 2008;29: 3792-3798.
256. Sirivisoot S, Pareta R, Harrison BS. Protocol and cell responses in three-dimensional conductive collagen gel scaffolds with conductive polymer nanofibres for tissue regeneration. *Interface Focus*. 2014;4: 20130050.
257. Shi Z, Li Y, Chen X et al. Double network bacterial cellulose hydrogel to build a biology-device interface. *Nanoscale*. 2014;6(2): 970-977.
258. Wheeldon IR, Gallaway JW, Barton SC. Bioelectrocatalytic hydrogels from electron-conducting metallopolypeptides coassembled with bifunctional enzymatic building blocks. *Proc Natl Acad Sci U S A*. 2008;105: 15275-15280.
259. Green RA, Lovell NH, Poole-Warren LA. Cell attachment functionality of bioactive conducting polymers for neural interfaces. *Biomaterials.* 2009;30(22): 3637-3644.
260. Ley C, Holtmann D, Mangold KM et al. Immobilization of histidine-tagged proteins on electrodes. *Colloids Surf B Biointerfaces.* 2011;88(2): 539-551.

261. Bhattacharya P, Du D, Lin Y. Bioinspired nanoscale materials for biomedical and energy applications Bioinspired nanoscale materials for biomedical and energy applications. *J R Soc Interface.* 2014; 11(95): 20131067.

262. Shen H, Guo J, Wang H et al. Bioinspired modification of h-BN for high thermal conductive composite films with aligned structure. *ACS Appl Mater Interfaces*. 2015; 7(10): 5701-5708.

263. Akkouch A, Shi G, Zhang Z et al. Bioactivating electrically conducting polypyrrole with fibronectin and bovine serum albumin. *J Biomed Mater Res Part A*. 2010;92: 221-231.

264. Green RA, Lovell NH, Poole-Warren LA. Impact of co-incorporating laminin peptide dopants and neurotrophic growth factors on conducting polymer properties. *Acta Biomater.* 2010;6(1): 63-71.

265. Merrill DR, Bikson M, Jefferys JG. Electrical stimulation of excitable tissue: design of efficacious and safe protocols. *J Neurosci Methods.* 2005;141(2):171-198.

266. Cogan SF. Neural stimulation and recording electrodes. *Annu Rev Biomed Eng.* 2008;10: 275-309.

267. Brighton CT, Adler S, Black J et al. Cathodic oxygen consumption and electrically induced osteogenesis. *Clin Orthop Relat Res.* 1975;(107): 277-282.

268. Curtze S, Dembo M, Miron M et al. Dynamic changes in traction forces with DC electric field in osteoblast-like cells. *J Cell Sci*. 2004;117: 2721-2729.

269. Kuzyk PR, Schemitsch EH.The science of electrical stimulation therapy for fracture healing. *Indian J Orthop*. 2009; 43(2): 127–131

270. Wong JY, Langer R, Ingber DE. Electrically conducting polymers can noninvasively control the shape and growth of mammalian cells. *Proc Natl Acad Sci U S A*. 1994;91: 3201-3204.

271. Tessier D, Dao LH, Zhang Z et al. Polymerization and surface analysis of electrically-conductive polypyrrole on surface-activated polyester fabrics for biomedical applications. *J Biomater Sci Polym Ed*. 2000;11: 87-99.

272. Engin M, Demirel A, Engin EZ et al. Recent developments and trends in biomedical sensors. *Meas J Int Meas Confed.* 2005;37: 173-188.

273. Lee JY. Electrically conducting polymer-based nanofibrous scaffolds for tissue engineering applications. *Polym Rev.* 2013;53: 443-459.

274. Hsiao CW, Bai MY, Chang Y et al. Electrical coupling of isolated cardiomyocyte clusters grown on aligned conductive nanofibrous meshes for their synchronized beating. *Biomaterials.* 2013;34(4): 1063-1072.

275. Runge MB, Dadsetan M, Baltrusaitis J et al. The development of electrically conductive polycaprolactone fumarate-polypyrrole composite materials for nerve regeneration. *Biomaterials.* 2010;31(23): 5916-5926.

276. Kloth LC, McCulloch JM. Promotion of wound healing with electrical stimulation. *Adv Wound Care*. 1996;9(5): 42-45.

277. Su WP, Schrieffer JR. Soliton dynamics in polyacetylene. *Proc Natl Acad Sci U S A*. 1980;77(10): 5626-5629.

278. Bredas J, Street G. Polarons, bipolarons, and solitons in conducting polymers. *Acc Chem Res*. 1985;1305(4): 309-315.

279. G.Wegner. Contemporary topics in polymer science, Plenum Press. 1984;5: 281-319.

280. Kotwal A, Schmidt CE. Electrical stimulation alters proteinadsorption and nerve cell interactions with electrically conducting biomaterials. *Biomaterials*. 2001; 2: 1055–1064.

281. Zhang Z, Roy R, Dugre FJ et al. In vitro biocompatibility study of electrically conductive polypyr-role-coated polyester fabrics. *J Biomed Mater Res*. 2001; 57: 63–71.

282. Wang X, Gu X, Yuan C et al. Evaluation of biocompatibility of polypyr-role in vitro and in vivo. *J Biomed Mater Res A.* 2004; 68: 411–422.

283. Wang Z, Roberge C, Dao LH et al. In vivo evaluation of a novel electrically conductive polypyrrole/poly(D, L-lactide) composite and polypyrrole-coated poly(D, L-lactide-co-glycolide) membranes. *J Biomed Mater Res A.* 2004; 70: 28–38.

284. Waghuley SA, Yenorkar SM, Yawale SS et al. Application of chemically synthesized conducting polymer-polypyrrole as a carbon dioxide gas sensor. *Sensor Actuat B-Chem*. 2008;128: 366-373.

285. Sadrolhosseini AR, Noor AS, Bahrami A et al. Application of polypyrrole multi-walled carbon nanotube composite layer for detection of mercury, lead and iron ions using surface plasmon resonance technique. *PLoS One.* 2014;9(4): e93962.

286. Xia J, Chen L, Yanagida S. Application of polypyrrole as a counter electrode for a dye-sensitized solar cell. *J Mater Chem.* 2011;21: 4644.

287. Ramanaviciene A, Ramanavicius A. Application of polypyrrole for the creation of immuosensors. immunosensors. *Crit Rev Anal Chem*. 2002;32(3): 245-252.

288. Li Y, Cheng XY, Leung MY et al. A flexible strain sensor from polypyrrole-coated fabrics. *Synth Met.* 2005;155: 89-94.

289. Winther-Jensen B, Clark N, Subramanian P et al. Application of polypyrrole to flexible substrates. *J Appl Polym Sci*. 2007;104(6): 3938-3947.

290. Castano H, O'Rear EA, McFetridge PS et al. Polypyrrole thin films formed by admicellar polymerization support the osteogenic differentiation of mesenchymal stem cells. *Macromol Biosci*. 2004;4(8): 785-794.

291. Garner B, Georgevich A, Hodgson AJ et al. Polypyrrole-heparin composites as stimulus-responsive substrates for endothelial cell growth. *J Biomed Mater Res*. 1999;44(2): 121-129.

292. Song HK, Toste B, Ahmann K et al. Micropatterns of positive guidance cues anchored to polypyrrole doped with polyglutamic acid: a new platform for characterizing neurite extension in complex environments. *Biomaterials.* 2006;27(3): 473-484.

293. Sanghvi AB, Miller KP, Belcher AM et al. Biomaterials functionalization using a novel peptide that selectively binds to a conducting polymer. *Nat Mater.* 2005;4(6): 496-502.

294. Nickels JD, Schmidt CE. Surface modification of the conducting polymer, polypyrrole, via affinity peptide. *J Biomed Mater Res A.* 2013;101(5): 1464-1471.

295. De Giglio E, Sabbatini L, Colucci S et al. Synthesis, analytical characterization, and osteoblast adhesion properties on RGD-grafted polypyrrole coatings on titanium substrates. *J Biomater Sci Polym Ed.* 2000;11(10): 1073-1083.

296. Chen J, Liu Y, Minett AI, Lynam C, Wang J, Wallace GG. Flexible, aligned carbon nanotube/conducting polymer electrodes for a lithium-ion battery. *Chem. Mater*., 2007; 19 (15), 3595–3597.

297. Abidian MR, Ludwig KA, Marzullo TC, Martin DC, Kipke DR. Interfacing conducting polymer nanotubes with the central nervous system: chronic neural recording using poly(3-4-ethylenedioxythiophene) nanotubes. *Adv. Mat*. 2009; 1(17): 3764-3770.

298. Gittens RA, Olivares-Navarrete R, Tannenbaum R et al. Electrical implications of corrosion for osseointegration of titanium implants. *J Dent Res.* 2011; 90(12): 1389–1397.

299. Jiang X, Marois Y, Traoré A, et al. Tissue reaction to polypyrrole-coated polyester fabrics: an in vivo study in rats. *Tissue Engineering*. 2002; 8(4): 635-647.

300. Mehmood T, Kaynak A, Dai X et al. Study of oxygen plasma pre-treatment of polyester fabric for improved polypyrrole adhesion. *Mater Chem Phys.* 2014;143(2): 668-675.

301. Islam MS, Rabbani KS, Talukder MS. Pulsed electromagnetic fields for the treatment of bone fractures. *Bangladesh Med Res Counc Bull.* 1999;25(1):6-10

302. Vedula SR, Hirata H, Nai MH, Brugués A, Toyama Y, Trepat X, Lim CT, Ladoux B. Epithelial bridges maintain tissue integrity during collective cell migration. *Nat Mater*. 2014;13(1):87-96.

303. Yuan X, Arkonac DE, Chao PH et al. Electrical stimulation enhances cell migration and integrative repair in the meniscus**.** *Sci Rep*. 2014; 4: 3674.

304. Kottakis F, Polytarchou C, Foltopoulou P et al. FGF-2 Regulates Cell Proliferation, Migration, and Angiogenesis through an NDY1/KDM2B-miR-101-EZH2 Pathway. *Mol Cell*. 2011;43(2): 285-298.

305. Pintucci G, Moscatelli D, Saponara F et al. Lack of ERK activation and cell migration in FGF-2-deficient endothelial cells. *FASEB J Off Publ Fed Am Soc Exp Biol*. 2002;16(6): 598-600.

306. Barat E, Boisseau S, Bouyssières C et al. Subthalamic nucleus electrical stimulation modulates calcium activity of nigral astrocytes. *PLoS One*. 2012;7(7): e41793.

307. Bolanowski M, Bednarczuk T, Bobek-Billewicz B et al. Neuroendocrine neoplasms of the small intestine and the appendix-management guidelines (recommended by the Polish Network of Neuroendocrine Tumours). *Endokrynol Pol*. 2013;64(6): 480-493.

308. Poniatowski ŁA, Wojdasiewicz P, Gasik R, Szukiewicz D. Transforming growth factor beta family: insight into the role of growth factors in regulation of fracture healing biology and potential clinical application. *Mediators Inflamm*. 2015;2015:137823.

309. SunX, Robertson SA, Ingman WV. Regulation of epithelial cell turnover and macrophage phenotype by epithelial cell-derived transforming growth factor beta1 in the mammary gland. *Cytokine.* 2013;61(2):377-388.

310. Yoshida K, Murata M, Yamaguchi T et al. TGF-β/Smad signalling during hepatic fibro-carcinogenesis. *Int J Oncol*. 2014: 2-3.

311. Kim BS, Kang HJ, Park JY et al. Fucoidan promotes osteoblast differentiation via JNK- and ERK-dependent BMP2-Smad 1/5/8 signalling in human mesenchymal stem cells. *Exp Mol Med*. 2015;47: e128.

312. Lu N, Liu Y, Tang A, Chen L et al. Hepatocyte-specific ablation of PP2A catalytic subunit alpha attenuates liver fibrosis progression via TGF-beta1/Smad signalling. *Biomed Res Int*. 2015;2015: 794862.

313. Xu J, Acharya S, Sahin O et al. 14-3-3zeta turns TGF-beta's function from tumor suppressor to metastasis promoter in breast cancer by contextual changes of Smad partners from p53 to Gli2. *Cancer Cell*. 2015;27(2): 177-192.

314. Tong KK, Ma TC, Kwan KM. BMP/Smad signalling and embryonic cerebellum development: Stem cell specification and heterogeneity of anterior rhombic lip. *Dev Growth Differ*. 2015;57(2): 121-134.

315. Wang D-T, Huang RH, Cheng X et al. Tanshinone IIA attenuates renal fibrosis and inflammation via altering expression of TGF-beta/Smad and NF-kappaB signalling pathway in 5/6 nephrectomized rats. *Int Immunopharmacol*. 2015; 26(1): 4-12.

316. Roberts PJ, Der CJ. Targeting the Raf-MEK-ERK mitogen-activated protein kinase cascade for the treatment of cancer. *Oncogene*. 2007;26: 3291-3310.

317. Robinson MJ, Stippec SA, Goldsmith E et al. A constitutively active and nuclear form of the MAP kinase ERK2 is sufficient for neurite outgrowth and cell transformation. *Curr Biol*. 1998;8: 1141-1150.

318. Keung AJ, Healy KE, Kumar S et al. Biophysics and dynamics of natural and engineered stem cell microenvironments. *Wiley Interdiscip Rev Syst Biol Med*. 2010;2(1): 49-64.

319. Brafman DA. Constructing stem cell microenvironments using bioengineering approaches. *Physiol Genomics*. 2013;45(23): 1123-1135.

320. Barthes J, Ozcelik H, Hindie M et al. Cell microenvironment engineering and monitoring for tissue engineering and regenerative medicine: the recent advances. *Biomed Res Int*. 2014;2014: 921905.

321. Yang C, Tibbitt MW, Basta L, Anseth KS. Mechanical memory and dosing influence stem cell fate. *Nat Mater*. 2014;13(6):645-652.

322. Chipev CC, Simman R, Hatch G, et al. Myofibroblast phenotype and apoptosis in keloid and palmar fibroblasts in vitro. *Cell Death Differ*. 2000;7(2): 166-176.

Publication list

- **Yongliang Wang**, Mahmoud Rouabhia, Ze Zhang, "Conductive polymer-mediated pulsed-electrical stimulation benefits wound healing by activating skin fibroblasts through the TGFβ1/ERK/NF-κB axis" (2015) (submitted)
- **Yongliang Wang**, Mahmoud Rouabhia, Denis Lavertu, Ze Zhang, "Pulsed electrical stimulation modulates fibroblasts' behaviour through the Smad signalling pathway", *Journal of Tissue Engineering and Regenerative Medicine* (2015), DOI: 10.1002/term.2014
- **Yongliang Wang**, Mahmound Rouabhia, Ze Zhang, "PPy-Coated PET Fabrics and Electric Pulse-Stimulated Fibroblasts", *Journal of Materials Chemistry B,* 2013: 1(31), 3789-3796.